Characterization of WT1-Expressing Interneurons and Investigation of Their Role in Locomotion

by

Farhia Haque

A thesis submitted in partial fulfillment of the requirements for the degree of

Doctor of Philosophy

Neuroscience

University of Alberta

ABSTRACT

Mammalian locomotion is controlled by a specialized neural network, known as the locomotor central pattern generator (CPG), which is situated entirely within the ventral spinal cord. A number of studies completed over the past two decades have indicated that this neural network is comprised of interneurons that can be categorized into populations based on the combinatorial expression of transcription factors throughout development. This thesis focuses on one such genetically defined population, the WT1-expressing cells, which are located in the ventral spinal cord postnatally. Here I characterize these neurons and investigate their role during fictive locomotion in the neonatal mouse spinal cord. In the first part of the thesis, I describe an upright *in vitro* spinal cord preparation that we developed which enables recordings to be made from WT1-expressing interneurons while keeping the core components of the locomotor CPG intact. In the second part of the thesis, I use this preparation to record from WT1+ cells and demonstrate that they are an inhibitory interneuronal population, which primarily project commissural axons, and are involved in regulating left-right alternation during fictive locomotion. In the final part of the thesis, I use a viral tracing approach to identify upstream synaptic partners of these neurons in order to provide insight into the network structure of the locomotor CPG. Taken together the data presented in this thesis provides key information regarding the development and function of this neural network.

This thesis is an original work by Farhia Haque. The research project, of which this thesis is a part, received research ethics approval from the University of Alberta Research Ethics Board, Project Name "Analysis of the role of genetically-defined interneurons in the development and operation of the locomotor CPG", No. AUP00000258, November 19 2014.

TABLE OF CONTENTS

LIST OF TABLES

LIST OF FIGURES

LIST OF ABBREVIATIONS

5-HT	5-hydroxytrptamine
AMPA	α-amino-3-hydroxy-5-methyl-4-isoxazolepropionic acid
CNO	Clozapine N-oxide dihydrochloride
CPG	Central pattern generator
daCSF	Dissecting artificial cerebrospinal fluid
Dbx1	Developing brain homeobox protein 1
Dmrt3	Doublesex and Mab3 related transcription factor 3
DOPA	Dihydroxyphenylalanine
DREADD	Designer receptor exclusively activated by designer drug
EMG	Electromyography
En1	Engrailed 1
ENG	Electroneurography
Evx1	Even-skipped homeobox 1
FRA	Flexor reflex afferents
GATA2/3	GATA binding protein 2/3
GC	Gastrocnemius muscle
MNX1	Motor neuron and pancreas homeobox protein 1
NeuN	Neuronal nuclei
NMDA	N-methyl-D-aspartate
raCSF	Recording artificial cerebrospinal fluid
Sim1	Single-minded homolog 1

TA	Tibialis anterior muscle
TMRD	Tetramethyl rhodamine dextran
TTX	Tetrodotoxin
UBG	Unit burst generator
VR	Ventral root
WT1	Wilms Tumor 1

Chapter 1 -
General introduction

1.1 Introduction.

Locomotion, the seemingly effortless act of moving from one place to another, is a complex motor behavior that is executed by coordinated contractions of multiple joint-specific flexor and extensor muscles. While supraspinal regions such as the cortex, basal ganglia, midbrain, and hindbrain are involved in locomotor initiation and adaptation, the rhythm and pattern are generated by a specialized neural circuit located entirely within the spinal cord. Once this neural circuit, referred to as the locomotor central pattern generator (CPG) is activated, it is capable of generating ongoing rhythmic locomotor bouts in the absence of descending supraspinal control or peripheral sensory inputs. The experiments that comprise this thesis involve a characterization of a group of spinal interneurons that express the transcription factor WT1, and an investigation of their role during locomotion. Prior to describing and interpreting the results of my experimental work I will provide a brief historical overview of the studies that were integral in establishing the current level of understanding regarding the neural mechanisms underlying locomotor generation and control.

1.2 Early evidence supporting the existence of a locomotor CPG.

The first experimental evidence indicating that higher centres are not required for the generation of locomotor activity came from studies demonstrating that spontaneous stepping-like movements could be seen in spinalized and decerebrate animals lifted off the ground (Philippson 1905, Sherrington 1910). Initially it was postulated that this rhythmic motor output results from a chain of reflexes in which sensory afferents activate excitatory interneurons which in turn activate motor neurons that lead out to hindlimb muscles, and these same afferents disynaptically inhibit motoneurons that activate antagonistic muscles (Sherrington 1910).

Based on the observation that continuous afferent stimulation in the spinalized cat results

in stepping with a different frequency than that of the stimulus, Charles Sherrington's student, Thomas Graham Brown, hypothesized that intrinsic neural networks, rather than reflexes, are responsible for generating the locomotor rhythm (Brown 1914). Initial support for this hypothesis came from experiments in which he demonstrated that anesthetized animals in the lateral recumbent position display spontaneous stepping movements in the hindlimbs following transection of the spinal cord at the lower thoracic level, and that these stepping movements persist after deafferentation (Brown 1911). Furthermore, he demonstrated that the midline transected spinal cord is capable of generating stepping movements in one limb (Brown 1913). These observations led to the development of the "half-center" model (Figure 1.1A) in which Brown proposed that each limb is controlled by a separate CPG, and these CPGs mutually inhibit each other. Within each CPG there are two groups of excitatory neurons (i.e. "half-centres"), one controls the activity of ipsilateral extensor motoneurons while the other controls the activity of ipsilateral flexor motoneurons. Activity in the extensor half-center will excite extensor muscles and simultaneously inhibit the flexor half-center, thus silencing antagonistic (i.e. flexor) muscles. Despite this compelling data, the dominant view through the first half of the 20th century was that locomotion occurs due to rhythmic sensory input (reviewed in Clarac 2005). The rhythmic limb movement observed when spinalized animals were lifted off the ground was attributed to muscle proprioceptors that were excited when a limb was extended, thus activating a flexion reflex in the limb (Sherrington 1910).

The first cellular evidence in support of the existence of a neural network responsible for locomotor activity was provided by Anders Lundberg. In the 1960's, Lundberg's group showed that intravenous injection of DOPA in the adult spinalized cat depresses the flexion reflex and evokes long lasting alternating activity of the hindlimb flexor and extensor muscles (Anden et al.

1963; Anden et al. 1964). They then leveraged intracellular recording techniques to show that this long-lasting activity is reciprocally inhibitory in nature as activity in the extensor motoneurons evoked by contralateral FRA (i.e. afferents that, when stimulated, evoke the flexor reflex) can be inhibited by stimulating the ipsilateral FRA (Jankowska et al. 1965), and that this reciprocal inhibition is facilitated via interneurons in lamina VII of the lumbar spinal cord (Jankowska et al. 1967a; Jankowska et al. 1967b; Fu et al. 1975). Based on their response to FRA stimulation, the interneurons were placed into three categories: those activated by ipsilateral FRA stimulation; those activated by contralateral FRA stimulation; and those activated by both ipsi- and contralateral FRA stimulation. The first and the second group of interneurons were reciprocally inhibitory, a finding consistent with Graham Brown's theory that mutually inhibiting "half-centers" are responsible for the alternating activity in the flexor and extensor motor neurons.

Further evidence for the half-centre hypothesis comes from experiments demonstrating that, during locomotion, the onset of EMG activity in extensor muscles (active during "stance" phase of locomotion, silent during "swing phase") begins prior to the point at which the paw hits the ground marking the onset of the stance phase (Engberg and Lundberg, 1969). This provided evidence that reflexes were likely not responsible for generating locomotor activity since the reflex would not be evoked until the paw struck the ground and the sensory afferents were activated.

A plethora of experimental evidence generated largely from the 1960s onwards showed that, across species, stereotyped rhythmic movements persist in the spinal cord when isolated from all descending and afferent input (Grillner & Zangger 1975; Wallén & Williams 1984; Robertson & Pearson 1985). Collectively these studies provide clear evidence that, while sensory

input is almost certainly involved in modulating locomotor output, the basic left/right and flexor/extensor movements that are the hallmarks of mammalian locomotion are produced by central networks located entirely within the spinal cord.

1.3 Location of the locomotor CPG.

Once it was generally accepted that a neural network was responsible for generating basic locomotor movements work began to focus on identifying the region of the spinal cord in which it resides. Initial experiments in which rhythmic hindlimb movements were generated in low spinalized cats indicated that rhythmically active neurons, presumably belonging to this network, were situated caudally – in the thoracic, lumbar, and/or sacral segments (Jankowska et al., 1967). In the cat, it was shown that rhythmic alternation of the hindlimbs can be generated if the spinal cord is transected rostral to the L4 segment in chronic preparations (Afelt 1970) and rostral to the L5 segment in acute preparations (Grillner and Zangger 1979).

More specific information regarding the location of the locomotor CPG emerged after the development of a novel in vitro animal model that could be used to study mammalian locomotor activity. In the late 1980's two groups published work demonstrating that the brainstem/spinal cord isolated from a neonatal rodent contained all of the functional circuitry required for locomotor rhythm generation (Kudo and Yamada 1987; Smith and Feldman 1987). This experimental preparation was shown to be capable of producing alternating electroneurogram (ENG) activity in lumbar ventral roots that innervate flexor muscles on either side of the body. The evoked activity called 'fictive locomotion' can be generated by stimulating descending pathways from the brainstem or by application of a pharmacological cocktail.

Using this isolated spinal cord preparation, systemic lesion studies was carried out to localize the specific region(s) of the spinal cord that contains the primary elements of locomotor

CPG. Spinal cords were isolated from neonatal rats and fictive locomotion was evoked by bath application of 5-HT and/or NMDA, and recorded from the related ventral roots or electroneurogram activity from nerves (Kjaerulff and Kiehn 1996; Cowley and Schmidt 1997). Lesions were made to various aspects of the spinal cord to assess the functional relevance of each of these sites. Results from these studies indicated that the rhythm-generating network is situated ventral to the central canal and is distributed throughout the caudal thoracic and lumbar spinal cord (T12 to L6) with a rostro-caudal gradient such that the rostral segments have a higher rhythmogenic potential compared to caudal segments (Kjaerullf and Kiehn 1996; Cowley and Schmidt 1997). This rostrocaudal gradient was verified in intact animals where ablation of interneurons in the L1-L2 segments was shown to impair overground locomotion whereas disrupting the caudal segments had little effect (Magnuson et al. 2005). The cause of disparity in rhythmogenic potential between rostral and caudal lumbar segments is unknown, although, differences in receptor expression (for example 5HT receptor gradient) have been implicated (Liu and Jordan 2005).

1.4 How activity is initiated in the locomotor CPG.

Pharmacologically induced locomotor activity in spinalized animals or in the isolated spinal cord preparation occurs due to the activation of component interneurons of this neural network by the pharmacological cocktail used (Jankowska et al. 1967a; Kudo and Yamada 1987; Smith and Feldman 1987; Barbeau and Rossignol 1990; Barbeau and Rossignol 1991). The possibility that the monoaminergic system may be involved in the activation of the locomotor CPG was first suggested in the 1960s when it was shown that electrical stimulation of the descending tracts caused the release of 5-HT and noradrenaline in the spinal cord (Anden et al. 1964 & 1965). Interestingly, while 5-HT can initiate robust fictive locomotor activity in neonatal rodent spinal

cord (Kudo and Yamada 1987; Smith and Feldman 1987), only L-DOPA (a precursor of noradrenaline) can initiate stepping in acute spinalized cats (Barbeau and Rossignol 1990; Barbeau and Rossignol 1991). In the intact animal, the source of these neurotransmitters is typically from supraspinal structures such as: medullary raphe pallidus, raphe obscuris, the raphe magnus, and part of the reticular formation surrounding the pyramidal tract (Dhalstrom and Fuxe 1964). Tracing these descending fibers leads us to a functionally defined region located in the midbrain called the mesencephalic locomotor region (MLR) that is capable of initiating full body locomotion (Shik et al. 1966; Sirota and Shik 1973). This region has been shown to be present in all species studied from lamprey to primates (Eidelberg et al. 1981; Skinner and Garcia-Rill, 1984; Bernau et al. 1991; Dubuc et al. 2008) and it controls the spinal CPG via reticulospinal neurons of the medullary reticular formation (Shik et al. 1966; Grillner et al. 1968).

The identity of the spinal neurons that receive input from these descending tracts and initiate activity in the locomotor CPG is unknown. However, recently it was shown that selective activation of excitatory neurons in the lumbar spinal cord is sufficient to generate rhythm (Hägglund et al. 2010 & 2013). It is likely that the aforementioned descending tracts synapse directly on the excitatory rhythm generating neurons and once the rhythm is initiated, exert a modulatory effect on the network. However, this is mere speculation at this point.

1.5 Network properties.

In order to understand how the nervous system generates a behaviour such as locomotion we need to be able to identify the neuronal components that participate in this behaviour, and then identify their intrinsic membrane properties, as well as the manner in which they are interconnected (Getting 1989). Due to the complexity of the mammalian CNS, and the limited anatomical and electrophysiological tools available, many of the central tenets of neural circuit

structure and function were first worked out in simpler vertebrates such as the lamprey (Grillner 2003).

1.5a Network organization - Insight from Lampreys

Unlike mammals, the spinal cord of lampreys is relatively transparent due to the lack of myelin. This has enabled spinal neurons to be visualized and targeted for recording following minimal surgical intervention. Another advantage of using the lamprey as an experimental model is that the in vitro brainstem-spinal cord preparations can be maintained for several days (McClellan 1984). Based on visual cues, neurotransmitter expression and axonal projection pattern, interneurons in the spinal cord of the lamprey can be divided into four distinct classes (Rovainen 1974; Rovainen and Dill, 1984; Buchanan and Grillner 1987; Buchanan and Grillner 1988). These spinal interneurons receive tonic excitatory drive from descending reticulospinal neurons. Rhythmic activity in the spinal cord of the lamprey has been shown to be generated by ipsilaterally projecting neurons which provide phasic excitation to ipsilateral motoneurons, and large commissural inhibitory neurons which inhibit the contralateral CPG interneurons and motoneurons (Buchanan and Grillner 1987), while intersegmental coordination is achieved by a lag in the onset of burst in each segment (Wallen and Williams 1984).

The ion channels and receptors that play a major role in the burst initiation and termination are as follows: NMDA, AMPA, various subtypes of Ca^{2+} channels, Ca^{2+} and Na^{+} dependent K^{+} channels (reviewed in Grillner et al. 2001). At the onset of the burst, NMDA receptors are activated by synaptic input from reticulospinal neurons as well as the interconnected excitatory spinal interneurons. This phase can be boosted by activation of low voltage activated Ca^{2+} channels and the action of both results in a plateau potential. The entry of Ca^{2+} leads to the

activation of Ca^{2+} dependent K^+ channels which results in a slow hyperpolarization (Wallen and Grillner 1987; El Manira et al. 1994; Cangiano et al. 2002; Wallen et al. 2002). Burst termination and spike frequency adaption is determined by this slow afterhyperpolarization – a long lasting slow afterhyperpolarization results in shorter locomotor burst and vice versa.

Compared to the lamprey much less is known regarding the specific properties involved in generating the mammalian locomotor rhythm. This is largely due to an inability to identify neurons that are components of the locomotor CPG and target them for electrophysiological and anatomical characterization. In chapter 2 of this thesis we describe a new spinal cord preparation that we have developed which addresses many of these issues and has the potential to enable a comprehensive characterization of locomotor-related neurons. We are optimistic that this preparation will allow us to determine whether the intrinsic and network properties that are responsible for locomotor activity in the lamprey are shared with limbed mammals.

1.5b The Unit Burst Generator- a conceptual model of the locomotor CPG in limbed mammals.

Although Brown's half-centre model can explain the generation of rhythmic alternation on either half of the spinal cord, it cannot account for the existence of bifunctional motor pools and their involvement in locomotor activity. Bifunctional motor pools are active during both the stance and swing phase of walking and intracellular recording experiments have indicated that a number of interneurons and motoneurons are active in this manner during stepping. This activity pattern was originally argued to be the result of proprioceptive afferent input, however was later demonstrated that this pattern persisted even after deafferentiation of the hindlimb in decerebrate cats (Grillner and Zangger 1975). Since reciprocal inhibition is key for rhythmogenesis in the

half-centre organization of the CPG, additional evidence in disagreement with this model is that rhythmic flexor- extensor alternation persists after all inhibitory synaptic transmission is blocked (Cowley and Schmidt 1995; Cangiano and Grillner 2003; 2005).

To account for several of these phenomenons, a new model called the unit burst generator (UBG) was proposed (Grillner 1981). In this model, the generation of rhythmicity occurs due to tightly coupled smaller half centre modules which enable the activity of subsets of motor pools to be controlled discretely, with each module regulated by a combination of excitatory and inhibitory synaptic connectivity (see Figure 1.1B). Experimental support for this model comes from studies in the lamprey and rodent which demonstrated that swimming or alternating motor output (in the case of rodents) is generated by a chain of oscillators located in each spinal segment/myotome and that each oscillator is sufficient to produce rhythmic activity in each segment/ myotome in which it is situated (Grillner et al. 1988; Cowley and Schmidt, 1997). The individual oscillators are coupled to neighboring oscillators and thus generate a wave of rhythmic activity in synergistic muscles. The UBG framework offers a degree of flexibility and can also account for rhythmic movements that do not follow the stereotypical locomotor pattern, such as scratching, swimming or backwards stepping. Contemporary models of the mammalian locomotor network have incorporated many central tenets of the unit burst generator, and have developed it further to formulate a two-level CPG model (McCrea & Rybak 2008- see General Discussion).

1.6 Using molecular genetics to identify interneuronal components of the mammalian locomotor CPG.

Regardless of its specific configuration, if we hope to understand how locomotor activity is produced, we must be able to identify functional connectivity of interneurons that make up the

locomotor CPG. Traditionally, the search for component interneurons has involved making electrophysiological recordings from interneurons in the ventromedial aspect of the lumbar spinal cord during fictive locomotion, and investigating the properties of those that are rhythmically active and related to locomotor activity (see Angel et al. 1996). This experimental approach has been complicated by the fact that the locomotor CPG is distributed over a number of spinal segments (see section 1.3), and thus the spinal cord must remain largely intact for locomotor activity to be generated. This has dictated that "blind" recordings must be made from spinal interneurons, and based on the vast number of neurons in the mammalian spinal cord, together with the fact that neurons with different functions are intermingled with one another, this approach has proven to be tedious and extremely low yield.

An enormous amount of progress has been made in this regard since the turn of the century and we have seen the identification of a number of populations of interneurons that are involved in locomotion, as well as their specific function during stepping. The key to this work was the implementation of a molecular approach to demonstrate that all interneurons in the developing spinal cord of mammals can be divided up into 10 genetically distinct populations (dI1-dI6, V0-V3) based on the specific transcription factors they express during embryonic development (Tanabe and Jessell 1996; Goulding 2009, see Figure 1.2). A number of subsequent studies have used transgenic mouse lines, in which a specific interneuronal population is labeled (with a reporter protein) or ablated, to characterize and/or assess the function of many of these populations during locomotor activity. Broadly speaking, these studies have demonstrated that cells with an identical genetic origin share intrinsic properties and, in many cases, play a specific role during locomotor activity (reviewed in Goulding 2009; Kiehn 2016). The findings related to each of the interneuronal populations shown to be involved in locomotor activity are described

briefly in the sections below and are summarized in table 1.

1.6a Ventrally-derived interneurons with commissural axons: the V0 and V3 populations.

The V0 interneurons express the transcription factor Dbx1 and are located in lamina VII and VIII of the postnatal spinal cord (Pierani et al. 2001). This cell population can be further subdivided into a glutamatergic ventral subset ($V0_v$) that expresses Evx1, and a GABAergic dorsal subset ($V0_D$) that is negative for Evx1 (Moran-Rivard et al. 2001; Talpalar et al. 2013). The V0 interneurons were the first population of genetically defined interneurons to have their function studied during locomotion and they were initially shown to regulate left-right alternation during stepping (Lanuza et al. 2004). Subsequent work has suggested that they do so in a speed dependent manner with the $V0_D$ cells responsible for this function at slow locomotor speeds and $V0_v$ neurons responsible as the speed of stepping increases (Talpalar et al. 2013).

The V3 interneurons express the transcription factor Sim1, are excitatory, and were initially shown to be involved in maintaining a stable, symmetrical locomotor rhythm (Zhang et al. 2008). While the manner in which they carry out this function remains unclear, recent work has further characterized this population and found that V3 cells form a layered microcircuit, in which those located ventromedially synapse onto other V3 cells located ventrolaterally (Chopek et al. 2018). The ventrolaterally located V3 cells in turn make synaptic contact onto ipsilateral motoneurons. Both ventrolaterally and ventromedially located V3 neurons have bifurcating axons and send ascending and descending projections along the spinal cord (Chopek et al. 2018).

1.6b Ventrally-derived interneurons with ipsilateral axons: the V1 and V2 populations.

The V1 interneurons express the transcription factor En1 and give rise to Renshaw cells, Ia inhibitory interneurons, as well as a host of undefined inhibitory interneurons (Bikoff et al.

2016). This population has been shown to control the duration of the locomotor step cycle and play a role in regulating locomotor speed (Gosgnach et al. 2006). More recent work has shown that V1 neurons also work together with the GATA2/3 expressing inhibitory V2b interneurons to coordinate flexor-extensor alternation on the ipsilateral side of the spinal cord during locomotion (Zhang et al. 2014; Britz et al. 2015).

The Chx10 expressing V2a cells are the second subset of the V2 population (Briscoe et al. 2000; Al-Mosawie et al. 2007). These cells are excitatory, project to ipsilaterally located $V0_v$ interneurons, and are involved in regulating left/right alternation at high locomotor speeds (Lundfald et al. 2007; Crone et al. 2009).

1.6c Ventrally-derived interneuronal populations capable of locomotor rhythmogenesis.

Lesion experiments indicate that rhythmic, alternating activity can be generated in the midline hemisected spinal cord (Kjaerulff and Kiehn 1996; Cowley and Schmidt 1997). This finding indicates that, in addition to being excitatory, the rhythm generating neurons of the locomotor CPG must be ipsilaterally projecting. Outside of V2a neurons (described in the previous section), two additional interneuronal populations fit this description. The first of these expresses the transcription factor Shox2. Suppressing the activity of this subset of neurons during locomotor activity results in the persistence of flexor-extensor and left-right alternation however the locomotor frequency is reduced. Based on this ability to modulate the frequency of the locomotor rhythm together with their intrinsic electrophysiological properties the Shox2-expressing neurons have been postulated to be involved in rhythm generation (Dougherty et al. 2013).

The second population of ipsilaterally-projecting, excitatory interneurons express the

transcription factor Hb9 and is located in the ventromedial spinal cord, close to the central canal (Hinckley et al. 2005; Wilson et al. 2005; Caldeira et al. 2017). Recordings in the spinal cord slice preparation indicate that these interneurons possess many intrinsic electrophysiological properties of rhythm generating neurons (Wilson et al. 2005) however, in the intact spinal cord, rhythmic bursting in motoneurons was shown to precede that in ipsilaterally located Hb9 interneurons during fictive locomotion (Kwan et al. 2009) ruling out a role in rhythm generation. This confounding data can now be explained in light of new evidence that shows that the Hb9 subset is a heterogenous population with only one third being glutamatergic (Caldeira et al. 2017). Similar to the locomotor phenotype in the absence of the Shox2-expressing population, selective silencing of glutamatergic Hb9 neurons resulted in the reduction of locomotor frequency without affecting coordination, suggesting that these neurons may also be involved in locomotor rhythm generation.

While the aforementioned populations display some properties of rhythm generating neurons we cannot lose sight of the fact that to this point, a single genetically-defined interneuronal population is yet to be identified as the sole rhythm generator. The fact that locomotor-like rhythms persist after selectively silencing or removing each the V0, V1, V2, V3 (Lanuza et al., 2004; Gosgnach et al., 2006; Crone et al., 2008; Zhang et al., 2008) populations raises the possibility that rhythm generation could be a shared function amongst small subsets of a number of interneuronal populations.

1.6d Dorsally derived interneurons involved in locomotor activity.

In addition to the V0-V3 cells, there are six populations of interneurons located in the dorsal spinal cord (dI1- dI6), some of which migrate ventrally during development. The dI6

interneurons fit this description and are generated between embryonic day 11 (i.e. E11) and E13, and migrate to laminae VII/VIII of the postnatal spinal cord just before birth. Interestingly, dI6 interneurons are closely related to the Dbx1- expressing V0 interneurons. In mice that lack Dbx1, ~25% of the neural progenitor cells that would normally differentiate to V0 neurons instead generate dI6 interneurons (Lanuza et al. 2004). Additionally, dI6 and $V0_D$ interneurons migrate along a similar ventromedial pathway and develop from Pax7+, Dbx2+ progenitors. Due to these similarities, it was initially suggested that dI6 interneurons are involved in the regulation of left/right during locomotion (Lanuza et al. 2004; Goulding 2009). Until recently however, the lack of a unique marker for the dI6 population, has precluded a functional study of these cells.

Postmitotically, the dI6 interneurons were originally shown to express the transcription factor WT1 (Goulding 2009). More recent work has shown that a second subpopulation of dI6 neurons exists and expresses the transcription factor DMRT3 (Andersson et al. 2012). Based on the expression of either WT1 or DMRT3 or both WT1 and DMRT3, the dI6 interneurons can be subdivided into three subpopulations. Characterization of the DMRT3+ interneurons revealed that they are inhibitory, extend projections both ipsi- and contralaterally, and synapse onto motoneurons on either side of the spinal cord (Andersson et al. 2012). DMRT3 mutant mice display deficits in their locomotion pattern with difficulties running at higher velocities, and frequent twitching of the limbs. Additionally, fictive locomotor activity in spinal cords isolated from DMRT3 mutant mice displayed an uncoordinated and irregular rhythm. Work characterizing the WT1-expressing neurons and exploring their role during locomotion forms the skeleton of this PhD project and will be discussed in the succeeding chapters.

1.7 Aims and hypotheses.

Based largely on their settling position in the ventromedial aspect of the spinal cord the WT1-expressing neurons have been predicted to be involved in locomotor activity (Goulding 2009). My PhD thesis involves a comprehensive characterization of the WT1-expressing neurons and an investigation into their function during locomotor activity. In project 1 (Chapter 2) I describe an upright spinal cord preparation that we devised which enables visualization and recording from this population of cells (which is located in the ventromedial spinal cord) during fictive locomotion. In project 2 (Chapter 3), I used this upright spinal cord preparation to study the activity of WT1-expressing neurons during fictive locomotion, determine their specific function during locomotion, and identify their downstream synaptic partners. Based on their similarity to the V0 population I hypothesize that WT1-expressing neurons work together with the V0 population to coordinate left-right alternation during locomotion via monosynaptic and disynaptic contacts onto contralateral motoneurons. In project 3 (Chapter 4), I used a viral tracing approach to identify the source of synaptic input onto WT1 neurons and test the hypothesis that they receive monosynaptic input from neurons involved in locomotor rhythm generation.

We found that WT1 neurons are inhibitory with commissural axons projecting onto DMRT3 and $V0_V$ neurons. The WT1 neurons in turn receive synaptic input from DMRT3 neurons and from caudal brainstem nuclei - GiV and MdV. We utilized our upright preparation to record from WT1 neurons and showed that they are all rhythmically active. Inhibiting the activity of WT1 neurons affect proper left-right alternation in the *in vitro* isolated rodent spinal cord.

REFERENCES

Afelt, Z. (1970) Reflex activity in chronic spinal cats. Acta Neurobiol. 30:129-144.

Al-Mosawie, A., Wilson, J.M. and Brownstone, R.M., (2007) Heterogeneity of V2-derived interneurons in the adult mouse spinal cord. European Journal of Neuroscience. 26(11):3003-15.

Alvarez FJ, Jonas PC, Sapir T, Hartley R, Berrocal MC, Geiman EJ, Todd AJ, Goulding M. (2005) Postnatal phenotype and localization of spinal cord V1 derived interneurons. J Comp Neurol. 493(2):177-92.

Anden NE, Lundberg A, E Rosengren LV. 1963. The effect of DOPA on spinal reflexes from the FRA (flexor reflex afferents). 229, pp.654–655.

Anden, N.E., Carlsson, A., Hillarp, N.A., and Magnusson T. (1964) 5-Hydroxytryptamine release by nerve stimulation of the spinal cord. Life Sci. 3: 473-478.

Anden, N.E., Carlsson, A., Hillarp, N.A., and Magnusson T. (1965) Noradrenaline release by nerve stimulation of the spinal cord. Life Sci. 4: 129-132.

Andersson LS, Larhammar M, Memic F, Wootz H, Schwochow D, Rubin CJ, Patra K, Arnason T, Wellbring L, Hjälm G, Imsland F, Petersen JL, McCue ME, Mickelson JR, Cothran G, Ahituv N, Roepstorff L, Mikko S, Vallstedt A, Lindgren G, Andersson L, Kullander K. (2012) Mutations in DMRT3 affect locomotion in horses and spinal circuit function in mice. *Nature*. 488(7413):642-6.

Barbeau, H. and Rossignol, S. (1991) Initiation and modulation of the locomotor pattern in the adult chronic spinal cat by noradrenergic, serotonergic and dopaminergic drugs. Brain Research. 546(2):250-60.

Barbeau, H. and Rossignol, S. (1990) The effects of serotonergic drugs on the locomotor pattern and on cutaneous reflexes of the adult chronic spinal cat. Brain Research.

Bikoff JB, Gabitto MI, Rivard AF, Drobac E, Machado TA, Miri A, Brenner-Morton S, Famojure E, Diaz C, Alvarez FJ, Mentis GZ, Jessell TM. (2016). Spinal Inhibitory Interneuron Diversity Delineates Variant Motor Microcircuits. Cell. 165:207-219.

Bernau NA, Puzdrowski RL, Leonard RB (1991) Identification of the midbrain locomotor region and its relation to descending locomotor pathways in the Atlantic stingray, Dasyatis sabina. Brain Res 557:83–94.

Briscoe J, Pierani A, Jessell TM, and Ericson J. (2000) A homeodomain protein code specifies progenitor cell identity and neuronal fate in the ventral neural tube. Cell. 101(4):435-45.

Britz, O. Zhang J, Grossmann KS, Dyck J, Kim JC, Dymecki S, Gosgnach S, Goulding M. (2015) A genetically defined asymmetry underlies the inhibitory control of flexor-extensor locomotor movements. eLife, pp.1–22.

Brown, T.G. (1911) The intrinsic factors in the act of progression in mammals. Proc. R. Soc. B, 84, pp. 308-319

Brown, T.G. (1912) The Factors in Rhythmic Activity of the Nervous System. Royal Society Publishing.

Brown, TG. (1913) The phenomenon of "narcosis progression" in mammals. Proc. R. Soc. B 86, 140–164.

Brown, T.G. (1914) On the nature of the fundamental activity of the nervous centres; together with an analysis of the conditioning of rhythmic activity in progression, and a theory of the evolution of function in the nervous system. Physiology, 48(1), pp.18–46.

Buchanan JT, Grillner S. (1987) Newly identified 'glutamate interneurons' and their role in

locomotion in the lamprey spinal cord. Science, 236, pp. 312-314

Buchanan JT, Grillner, S. (1988) A new class of small inhibitory interneurones in the lamprey

spinal cord. Brain Res., 438, pp. 404-407

Caldeira V, Dougherty KJ, Borgius L, Kiehn O. (2017) Spinal Hb9::Cre-derived excitatory

interneurons contribute to rhythm generation in the mouse. Scientific Reports. 7:41369.

Cangiano, L., Wallen, P. and Grillner, S. (2002) Role of apamin-sensitive KCa channels for

reticulospinal synaptic transmission to motoneuron and for the afterhyperpolarization. J.

Neurophysiol. 88, 289–299.

Cangiano L, Grillner S. (2003) Fast and slow locomotor burst generation in the hemi-spinal cord

of the lamprey. J. Neurophysiol. 89(6):2931–42.

Cangiano L, Grillner S. (2005) Mechanisms of rhythm generation in a spinal locomotor network

deprived of crossed connections: the lamprey hemicord. J. Neurosci. 25(4):923–35

Chopek JW, Nascimento F, Beato M, Brownstone RM, Zhang Y. (2018) Sub-populations of

Spinal V3 Interneurons Form Focal Modules of Layered Pre-motor Microcircuits. Cell

Reports. 25(1):146-156

Clarac F, 2005. The history of reflexes. Part 2: from Sherrington to 2004. IBRO Neuro History

Cowley KC, Schmidt BJ. (1995) Effects of inhibitory amino acid antagonists on reciprocal

inhibitory interactions during rhythmic motor activity in the in vitro neonatal rat spinal cord.

J Neurophysiol. 74(3):1109-17.

Cowley KC and Schmidt BJ. (1997) Regional distribution of the locomotor pattern-generating

network in the neonatal rat spinal cord. Journal of neurophysiology. 77(1):247-59.

Crone SA, Quinlan KA, Zagoraiou L, Droho S, Restrepo CE, Lundfald L, Endo T, Setlak J, Jessell TM, Kiehn O, Sharma K. (2008). Genetic ablation of V2a ipsilateral interneurons disrupts left-right locomotor coordination in mammalian spinal cord. Neuron. 60:70-83.

Crone SA, Zhong G, Harris-Warrick R, Sharma K. (2009) In Mice Lacking V2a Interneurons, Gait Depends on Speed of Locomotion. Journal of Neuroscience. 29(21):7098-109.

Dhalstrom A. & Fuxe K. (1964) Evidence for the existence of monoamine neurons in the central nervous system - I. Demonstration of monoamines in the cell bodies of brainstem neurons. Acta physiologica Scandinavica. 232:1-55.

Dougherty KJ, Zagoraiou L, Satoh D, Rozani I, Doobar S, Arber S, Jessell TM, Kiehn O. (2013). Locomotor rhythm generation linked to the output of spinal shox2 excitatory interneurons. Neuron. 80:920-933.

Dubuc R, Brocard F, Antri M, Fénelon K, Gariépy JF, Smetana R, Ménard A, Le Ray D, Viana Di Prisco G, Pearlstein É, Sirota MG, Derjean D, St-Pierre M, Zielinski B, Auclair F, Veilleux D (2008) Initiation of locomotion in lampreys. Brain Res Rev 57:172–182.

Eidelberg E, Yu J (1981) Effects of corticospinal lesions upon treadmill locomotion by cats. Exp brain Res 43:101–103.

El Manira A, Tegner J, Grillner S. (1994) Calcium-dependent potassium channels play a critical role for burst termination in the locomotor network in lamprey. J. Neurophysiol. 72, 1852–1861.

Engberg I. & Lundberg A. (1969) An Electromyographic Analysis of Muscular Activity in the Hindlimb of the Cat during Unrestrained Locomotion. Acta Physiologica Scandinavica.

75(4):614-30.

Jankowska E, Fu TC, & Lundberg, A. (1975) Reciprocal Ia inhibition during the late reflexes
evoked from the flexor reflex affrents after DOPA. Brain Research. 85(1):99-102.

Getting PA. (1989). Emerging principles governing the operation of neural networks. Annu. Rev.
Neurosci. 12: 185–204.

Gosgnach S, Lanuza GM, Butt SJ, Saueressig H, Zhang Y, Velasquez T, Riethmacher D,
Callaway EM, Kiehn O, Goulding M. (2006) V1 spinal neurons regulate the speed of
vertebrate locomotor outputs. Nature. 440(7081):215-9.

Goulding, M., (2009) Circuits controlling vertebrate locomotion: Moving in a new direction.
Nature Reviews Neuroscience. 10(7):507-18

Grillner, S., (1981) Control of Locomotion in Bipeds, Tetrapods, and Fish. In M. V. In:
Brookhart JM, ed. Comprehensive Physiology. Bethesda.

Grillner, S., (2003) The motor infrastruction: from ion channels to neuronal networks. Nature
Review Neuroscience. 4(7): 573-86.

Grillner, S., Buchanan, J.T. & Lansner, A., (1988) Simulation of the segmental burst generating
network for locomotion in lamprey. Neuroscience Letters. 89(1):31-5.

Grillner, S., Hongo, T. & Lund, S., (1968) The origin of descending fibres monosynaptically
activating spinoreticular neurones. Brain Research. 10(2):259-62.

Grillner, S., Wallén, P., Hill, R., Cangiano, L., & El Manira, A. (2001). Ion channels of
importance for the locomotor pattern generation in the lamprey brainstem-spinal cord. The
Journal of physiology. 533(Pt 1), 23–30.

Grillner, S. and Zangger, P., (1975) How detailed is the central pattern generation for

locomotion? Brain Research.

Grillner, S. and Zangger, P., (1979) On the central generation of locomotion in the low spinal cat. Exp. Brain Res. 34: 241-261.

Hägglund, M., Borgius, L., Dougherty, K.J., Kiehn, O. (2010) Activation of groups of excitatory neurons in the mammalian spinal cord or hindbrain evokes locomotion. Nature Neuroscience. 13(2): 246-52.

Hagglund M, Dougherty K.J., Borgius L., Itohara S., Iwasato T. and Kiehn O. (2013) Optogenetic dissection reveals multiple rhythmogenic modules underlying locomotion. Proc. Natl Acad. Sci. 110:11589–11594.

Hinckley CA, Hartley R, Wu L, Todd A, Ziskind-Conhaim L. (2005) Locomotor-Like Rhythms in a Genetically Distinct Cluster of Interneurons in the Mammalian Spinal Cord. Journal of Neurophysiology.

Jankowska E, Jukes MG, Lund S, Lundberg A. (1967a) The Effect of DOPA on the Spinal Cord 5. Reciprocal organization of pathways transmitting excitatory action to alpha motoneurones of flexors and extensors. Acta Physiologica Scandinavica. 70(3):369-88.

Jankowska E, Jukes MG, Lund S, Lundberg A. (1967b) The Effect of DOPA on the Spinal Cord 6. Half- centre organization of interneurones transmitting effects from the flexor reflex afferents. Acta Physiologica Scandinavica. 70(3):389-402.

Kiehn, O., (2016) Decoding the organization of spinal circuits that control locomotion. Nature Reviews Neuroscience. 17(4):224-38.

Kjaerulff, O. & Kiehn, O., (1996) Distribution of networks generating and coordinating locomotor activity in the neonatal rat spinal cord in vitro: a lesion study. J Neurosci.

16(18):5777-94.

Kudo N, Yamada T. (1987). N-methyl-D,L-aspartate-induced locomotor activity in a spinal cord-hindlimb muscles preparation of the newborn rat studied in vitro. Neurosci Lett. 75(1):43-48.

Kwan AC, Dietz SB, Webb WW, Harris-Warrick RM. (2009). Activity of Hb9 interneurons during fictive locomotion in mouse spinal cord. J Neurosci. 29:11601-11613.

Lanuza GM, Gosgnach S, Pierani A, Jessell TM, Goulding M. (2004) Genetic identification of spinal interneurons that coordinate left-right locomotor activity necessary for walking movements. Neuron. 42(3):375-86.

Liu J., Jordan LM. (2005) Stimulation of the parapyramidal region of the neonatal rat brainstem produces locomotor-like activity involving spinal 5-HT7 and 5-HT2A receptors. J.Neurophysiol. 94:1392–404.

Lundfald L, Restrepo CE, Butt SJ, Peng CY, Droho S, Endo T, Zeilhofer HU, Sharma K, Kiehn O. (2007) Phenotype of V2-derived interneurons and their relationship to the axon guidance molecule EphA4 in the developing mouse spinal cord. European Journal of Neuroscience. 26(11):2989-3002.

Magnuson DS, Lovett R, Coffee C, Gray R, Han Y (2005) Functional consequences of lumbar spinal cord contusion injuries in the adult rat. J. Neurotrauma 22:529–43

McClellan A.D., (1984) Descending control and sensory gating of 'fictive' swimming and turning responses elicited in an in vitro preparation of the lamprey brainstem/spinal cord. 302(1): 151-162.

McCrea DA, & Rybak IA. (2008) Organization of mammalian locomotor rhythm and pattern generation. Brain Research Reviews. 57(1):134-46.

Moran-Rivard L., Kagawa T., Saueressig H., Gross MK., Burrill J., and Goulding M. (2001) Evx1 is a postmitotic determinant of v0 interneuron identity in the spinal cord. *Neuron.* 29(2):385-99.

Philipson, M. (1905) L'autonomie et la centralisation dans le systeme nerveux dex animaux. Trav. Lab. Physiol. Inst. Solvay, Bruxelles 7, Part 2: 1-208.

Pierani A, Moran-Rivard L, Sunshine MJ, Littman DR, Goulding M, Jessell TM. (2001) Control of interneuron fate in the developing spinal cord by the progenitor homeodomain protein Dbx1. Neuron. 29(2):367-84.

Robertson RM, & Pearson KG, (1985.) Neural circuits in the flight system of the locust. Journal of Neurophysiology. 53(1):110-28.

Rovainen, C.M., Dill, D.A. Counts of axons in electron microscopic sections of ventral roots in lampreys. J. Comp. Neurol., 225 (1984), pp. 433-440

Rovainen, C.M. Synaptic interactions of identified nerve cells in the spinal cord of the sea lamprey. J. Comp. Neurol., 154 (1974), pp. 189-206.

Sapir T, Geiman EJ, Wang Z, Velasquez T, Mitsui S, Yoshihara Y, Frank E, Alvarez FJ, Goulding M. (2004) Pax6 and Engrailed 1 regulate two distinct aspects of Renshaw cell development. J. Neurosci. 24:1255–1264.

Sherrington, CS. (1910) Flexion- reflex of the limb, crossed extension- reflex, and reflex stepping and standing. The Journal of Physiology, 40(1–2), pp.28–121.

Shik ML, Severin FV & Orlovskii GN, (1966) Control of walking and running by means of electric stimulation of the midbrain. Biofizika. 26(5):549.

Sirota MG, and Shik ML, (1973) The cat locomotion elicited through the electrode implanted in the midbrain. Sechenom Physiol. J. USSR 59: 1314-1321.

Skinner RD, Garcia-Rill E (1984) The mesencephalic locomotor region (MLR) in the rat. Brain Res 323:385–389.

Smith JC, Feldman JL. (1987). In vitro brainstem-spinal cord preparations for study of motor systems for mammalian respiration and locomotion. J Neurosci Methods. 1987 21:321-333.

Talpalar AE, Bouvier J, Borgius L, Fortin G, Pierani A, Kiehn O. (2013) Dual-mode operation of neuronal networks involved in left-right alternation. Nature. 500:85-88.

Tanabe Y, Jessell TM. (1996) Diversity and pattern in the developing spinal cord. Science. 274(5290):1115-23.

Wallén, P., Hess, D., El Manira, A. & Grillner, S. (2002) A slow non-Ca2+-dependent afterhyperpolarization in lamprey neurons. Soc. Neurosci. Abstr. 28, 46.9.

Wallén, P. & Grillner, S. (1987) N-methyl-D-aspartate receptor-induced, inherent oscillatory activity in neurons active during fictive locomotion in the lamprey. J. Neurosci. 7, 2745–2755.

Wallén P. & Williams TL. (1984) Fictive locomotion in the lamprey spinal cord in vitro compared with swimming in the intact and spinal animal. The Journal of Physiology. 347:225-39.

Wilson JM, Hartley R, Maxwell DJ, Todd AJ, Lieberam I, Kaltschmidt JA, Yoshida Y, Jessell

TM, Brownstone RM. (2005) Conditional Rhythmicity of Ventral Spinal Interneurons Defined by Expression of the Hb9 Homeodomain Protein. Journal of Neuroscience. 25(24):5710-9.

Zagoraiou, L. Akay T, Martin JF, Brownstone RM, Jessell TM, Miles GB. (2009) A Cluster of Cholinergic Premotor Interneurons Modulates Mouse Locomotor Activity. Neuron. 64(5):645-62.

Zhang J, Lanuza GM, Britz O, Wang Z, Siembab VC, Zhang Y, Velasquez T, Alvarez FJ, Frank E, Goulding M. (2014) V1 and v2b interneurons secure the alternating flexor-extensor motor activity mice require for limbed locomotion. Neuron. 82(1):138-50.

Zhang Y, Narayan S, Geiman E, Lanuza GM, Velasquez T, Shanks B, Akay T, Dyck J, Pearson K, Gosgnach S, Fan CM, Goulding M (2008). V3 spinal neurons establish a robust and balanced locomotor rhythm during walking. Neuron 60:84-96
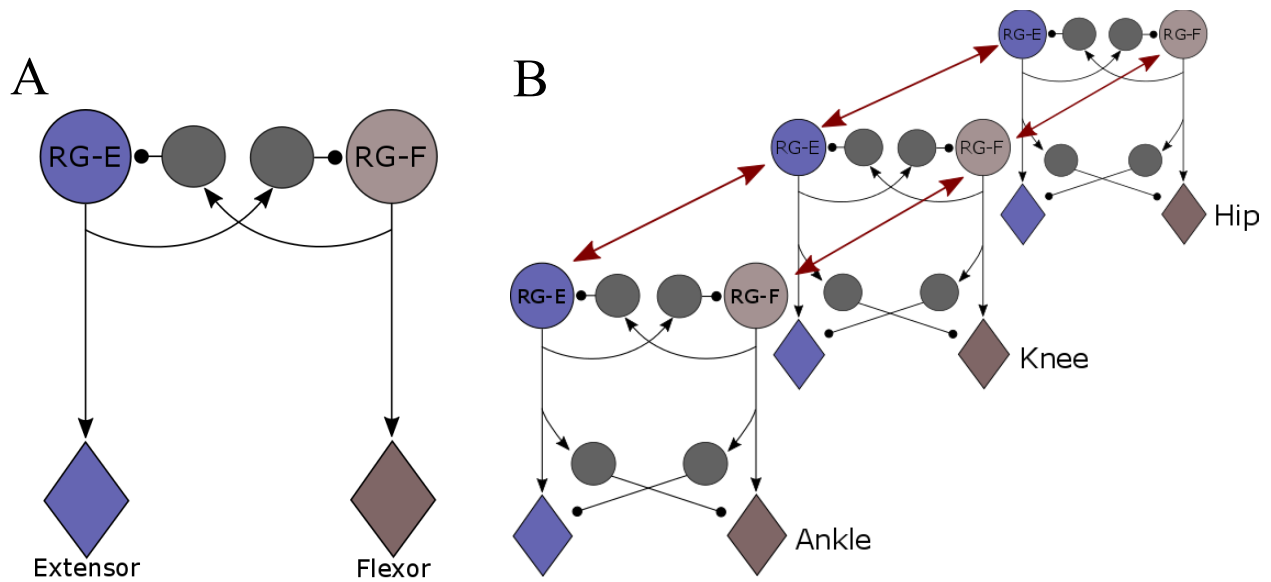
Figure 1.1. Conceptual models of the organization of locomotor CPG. (A) Classis half-centre model proposed by Thomas G Brown where the flexors and extensors on one side are controlled by their respective CPG (RG-E/RG-F). Individual CPGs excite their respective motor pool and are mutually inhibitory. (B) Unit burst generator proposed by Sten Grillner who hypothesised that there is an interconnected series of burst generators (CPGs) for each joint (hip, knee and ankle). Figure adapted from McCrea and Rybak 2008.

A

Dp1 Lhx2
Dp2 Foxd3
Dp3 lsl1
Dp4 Lbx1/Pax2
Dp5 Lbx1/Lmx1b
Dp6 Wt1/Dmrt3
Vp0 Dbx1/Evx1
Vp1 En1
Vp2 Gata2/3/Chx10
MN Hb9
Vp3 Sim1

E10-E12

B

E17-Postnatal
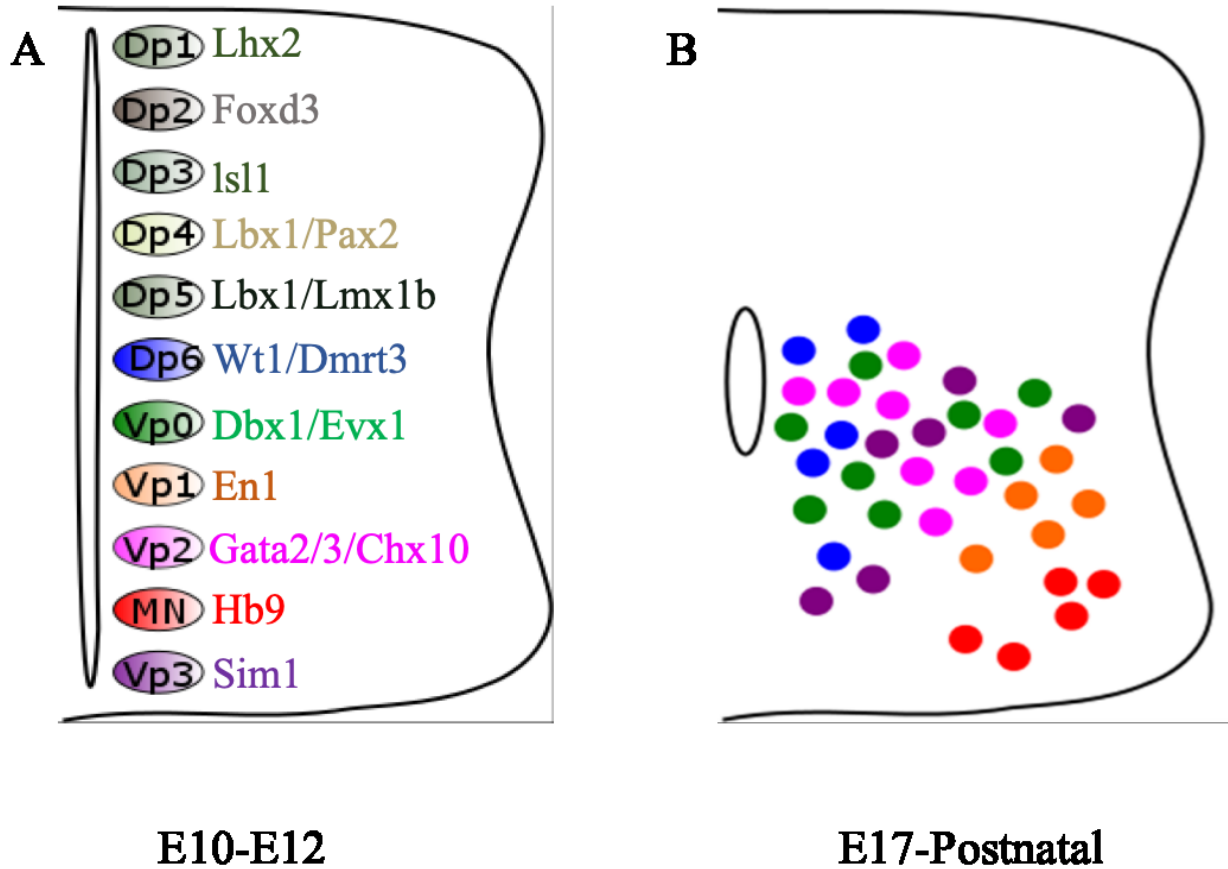
Figure 1.2. Genetically-defined neuronal populations in the developing spinal cord. Spinal interneurons are broadly divided into 11 parent populations, Dp1-Dp6, Vp0-Vp3, based on the combinatorial expression of transcription factors they express during embryogenesis. (A) Each parent population can be identified unique transcription factor expression during the post-mitotic phase (E= embryonic). The parent populations then migrate and settle in their final position in the spinal cord which they reach just before birth. The final settling position of the parent populations which give rise to neurons residing specifically in the ventral spinal cord is shown in (B).

28

opulation	Subset	Transmitter	Axonal projection	Synaptic targets	Proposed function during locomotion
V0	V0d	inhibitory	contralateral	contralateral motoneurons[1]	left-right alternation at slow speeds[1,10]
	V0v	excitatory	contralateral		left-right alternation at high speeds[1,10]
	V0c	excitatory	ipsi/contralateral	ipsi/contralateral motoneurons, unidentified lamina VIII and dorsal horn interneurons[2]	regulation of motoneuron activity[2]
V1	RC	inhibitory	ipsilateral	motoneurons, IaINs[3]	recurrent inhibition[3]
	IaIN	inhibitory	ipsilateral	motoneurons[4]	reciprocal inhibition[4]
	V1	inhibitory	ipsilateral	flexor motoneurons[5], unidentified ventral interneurons[5]	regulation of locomotor speed[11], flexor extensor alternation[5]
V2	V2a	excitatory	ipsilateral	V0v and unidentified commissural interneurons[6]	regulation of motoneuron activity[12], control of V0 neurons[6]
	V2b	inhibitory	ipsilateral	extensor motoneurons, V0c INs, unidentified neurons in lamina VII and VIII[5]	flexor-extensor alternation[5]
V3		excitatory	ipsi/contralateral	ipsi/contralateral motoneurons[7], IaINs[7], ipsilateral V3 interneurons as well as unidentified ipsilateral and contralateral targets.[8]	locomotor stability[7]
dI6	DMRT3	inhibitory	ipsi/contralateral	ipsilateral and contralateral motoneurons[9]	development of a robust locomotor rhythm[9]
	WT1	inhibitory		To be investigated in this thesis	

ɔle 1. Proposed function, axonal projection pattern and identified synaptic targets for each of the genetically-defined interneuronal ɔulations located in the ventral spinal cord postnatally that have been identified to participate in locomotor activity.

ˊerences- for full citations see reference list: [1]Lanuza et al. 2004 [2]Zagoraiou et al. 2009 [3]Sapir et al. 2004 [4]Alvarez et al. 2005 ang et al. 2014 [6]Crone et al. 2009 [7]Zhang et al. 2008 [8]Chopek et al. 2018 [9]Andersson et al. 2012 [10]Talpalar et al. 2012 [11]Gosgnach l. 2006 [12]Dougherty et al 2013

Chapter 2 -

Using an upright preparation to identify and characterize locomotor related neurons across the transverse plane of the neonatal mouse spinal cord.

Vladimir Rancic, Farhia Haque*, Klaus Ballanyi, Simon Gosgnach (2019)

Contributions

VR: experimental design, carried out experiments, data analysis

FH: experimental design, assisted with carrying out experiments, data analysis

KB: provided comments on manuscript

SG: experimental design, data analysis, wrote manuscript

2.1 Introduction.

A neural circuit, located in the spinal cord, known as the locomotor central pattern generator (CPG) is responsible for generating the basic rhythmicity which underlies stepping in mammals (reviewed in Kiehn 2016). A significant breakthrough for the study of this neural circuit was the development of an *in vitro* preparation in which rhythmic locomotor- like activity (i.e. fictive locomotion) could be generated in a spinal cord isolated from a newborn rodent (Kudo and Yamada 1987; Smith and Feldman 1987). This preparation enabled the pharmacological basis of locomotor rhythm generation and modulation to be identified (Cazalets et al. 1992; Cowley and Schmidt 1994; Gordon and Whelan 2006), and it was also used to demonstrate that the locomotor CPG is distributed throughout the ventral aspect of the caudal thoracic and lumbar segments of the spinal cord (Cowley and Schmidt 1997; Kjaerullf and Kiehn 1996).

One of the challenges that has historically hindered investigations into the network structure and mechanism of function of the locomotor CPG has been the identification and characterization of its component interneurons. Recent work incorporating a molecular approach to divide spinal neurons into a handful of populations based on their transcription factor expression has generated a substantial amount of new information regarding the interneuronal components of the locomotor CPG, as well as their specific function (Goulding 2009; Grillner and Jessell 2009). In spite of this, the distributed nature of the locomotor CPG, which dictates that several spinal segments must remain intact for locomotor activity to be generated, has made it extremely difficult to determine the specific proportion of each population that is active during locomotion, and to identify intrinsic properties and morphological features that are exhibited by these specific neurons. Although a number of attempts have been made to devise experimental

preparations which provide access to interneuronal components of the CPG during fictive locomotor activity (Antri et al. 2011; Dougherty et al. 2013; Dyck and Gosgnach 2009; Hinckley et al. 2005; Kiehn et al. 1996), each has only enabled the study of neurons residing within restricted regions of the spinal cord.

In this article we describe an in vitro preparation that we have developed in which the spinal cord is sectioned in the transverse plane and placed in an upright orientation under a 2-photon microscope. This preparation enables neurons spanning the transverse plane of the spinal cord at a given spinal segment to be visualized while robust fictive locomotor activity is recorded from the lumbar ventral roots. Ca^{2+} imaging can then be used to simultaneously identify neurons that are rhythmically active during fictive locomotion, and target these specific neurons for whole cell recording and application of intracellular tracers. This preparation enables the identification and comprehensive characterization of those specific spinal neurons that are rhythmically active during locomotion, and has the potential to provide new information on the cellular and network properties of this neural circuit. By altering the location of Ca^{2+} indicator application the upright spinal cord preparation can also be used to visually identify and characterize neurons involved in sensory processing.

2.2 Materials and methods.

Spinal cord dissection, sectioning, and mounting

All procedures were in accordance with the Canadian Council on Animal Care (CCAC) and approved by the Animal Welfare Committee at the University of Alberta. Experiments were performed on spinal cords isolated from 64 postnatal day 0-3 (P0-P3) mice. After anesthesia via inhalation of isoflurane (2-3% delivered with 95% O_2-5% CO_2) animals were decapitated and eviscerated with sharp scissors, and spinal cords (rostral cervical to caudal sacral segments) were dissected out in a bath containing oxygenated (95% O_2 and 5% CO_2) dissecting artificial cerebrospinal fluid (dACSF) containing in mM (111 NaCl, 3.08 KCl, 11 glucose, 25 $NaHCO_3$, 1.18 KH_2PO_4, 3.7 $MgSO_4$, and 0.25 $CaCl_2$, pH 7.4, osmolarity 280 –300 mosM). The spinal cord was then positioned, ventral side up, in 2-3 ml of dACSF in a separate dissection chamber. Two plastic supports (prepared in advance) were required to stabilize the spinal cord during sectioning and recording. The first, support A (Figure 2.1A), was prepared from a piece of plastic weigh boat 5 mm in width and 39 mm in length. A scalpel was used to cut the plastic 14mm from one end. The 14 mm and 25 mm pieces were placed next to one another (lengthwise) on top of a piece of double-sided tape coated with a small amount of acrylic glue in order to avoid tape detachment, and to create a bendable junction point. Support B was also cut (7 mm wide, 25 mm long) from a plastic weigh boat. A block of Sylgard (10 mm high x 7 mm wide x 7 mm long) was attached to one end of plastic support B using acrylic glue (Figure 2.1B). Support A was placed in front of the rostral end of the spinal cord such that the 14 mm segment faced the spinal cord (see Figure 2.1C for orientation). A small amount of vaseline was applied to the underside of support A to prevent movement, and a line of acrylic glue was applied to its center (Figure 2.1C). Fine forceps were then used to drag the spinal cord towards support A and place it on the

line of acrylic glue (Figure 2.1C, 2.1D) with the small pool of dACSF facilitating movement. When positioning the spinal cord on support A the spinal segments to be examined were placed at the end of support A (Figure 2.1D). Fictive locomotion can be evoked in spinal cords sectioned anywhere from the 1st to the 5th lumbar segments, however all spinal cords included in this study were sectioned at the L2 or L3 segment. After the glue had dried (approximately 10 s), the entire preparation was submerged in oxygenated dACSF, and the spinal segments caudal to those which were to be examined were trimmed with scissors and discarded.

In preparation for sectioning, support A (with the spinal cord attached) was removed from the solution with forceps and the underside was dried using filter paper. Acrylic glue was applied to the surface of plastic support B (Figure 2.1E) and forceps were used to apply pressure to support A at the cut line in order to obtain the upright configuration and attach support A to support B (Figure 2.1F). The entire preparation was then fixed to the vibratome (Leica VT1200, Leica Biosystems, Wetzler, Germany) plate using acrylic glue, immersed in oxygenated daCSF, and positioned so that the ventral aspect of the spinal cord was facing the blade (Figure 2.1F). During sectioning the blade speed was set at 0.5 mm/s and the frequency of vibration was set at maximum in order to avoid spinal cord compression. Sections were cut until the desired region of the spinal cord was visible. Following a 30 minute incubation period at room temperature in daCSF (to allow for recovery), the entire preparation (supports A, B, and the sectioned spinal cord) was transferred to a recording chamber (volume 10mL) under the objective lens of an upright two photon microscope and attached to the base of the chamber using Vaseline (Figure 2.1G). The entire preparation was immersed in room temperature recording solution (raCSF) which was identical to the daCSF except for the following (in mM): 1.25 $MgSO_4$, 2.52 $CaCl_2$.

For the remainder of the experiment the preparation was perfused with room temperature raCSF at a rate of 10 mL/minute.

Electrophysiological recording

Pharmacologically-induced fictive locomotor activity was evoked via bath application of 5-HT (5-15 μM) and NMDA (3-8 μM), or 5-HT (10 μM) and dopamine (50 μM) (Sigma, St Louis, MO), and recorded via extracellular electrodes (A-M Systems Inc., Carlsborg, WA) attached to the primarily flexor (L1, L2, L3) lumbar ventral roots (VRs) via suction (Figure 2.1G). Electroneurogram (ENG) signals from the VRs were acquired at 10,000 Hz, amplified (10,000x) and band-pass-filtered (0.3-3 kHz) using a Model-1700 differential amplifier (AM-Systems, Sequim, WA, USA) and integrated (time constant (τ): 50 ms) using a MA-821/RSP module (CWE Inc. Allentown, PA).

For whole cell patch clamp recordings, patch pipettes (5-7 MΩ) were pulled from borosilicate glass capillaries using a vertical puller (PC-10, Narishige International Inc, East Meadow, NY) and backfilled with intracellular solution containing (in mM): 140 K gluconate, 1 NaCl, 0.5 $CaCl_2$, 2$MgCl_2$, 1ATP-Na_2, 10 HEPES, pH adjusted to 7.30. In some cases the fluorescent dye Alexa Fluor 594 was included with the intracellular solution. A micromanipulator (MPC-385, Sutter Instruments, Novato, CA) was used to position the electrode over the sectioned surface of the spinal cord and lower it into the tissue. With a patch clamp amplifier (EPC-10, HEKA Lambrecht, Germany) in voltage- clamp mode, a 15 ms, 10 mV square pulse (50 Hz) was used to monitor tip resistance as the electrode was advanced toward the cell of interest. Once a gigaohm seal with a cell was formed, the command voltage was set to -60 mV and gentle suction was applied to break through the membrane and obtain whole-cell recording. Intracellular as well as extracellular (i.e. VR) signals were digitized with a Powerlab

8/35 and recorded using LabChart software (AD Instruments, Colorado Springs, CO, USA) running on a PC. Off-line analysis was performed with Clampfit software (Molecular Devices, San Jose, CA).

Ca^{2+} imaging

Throughout the periods of Ca^{2+} indicator loading and imaging the tissue was perfused (10 mL/minute) with raCSF. Membrane permeant Cal-520AM (AAT Bioquest, Sunnyvale, CA) was pressure-injected at 25-30 mmHg for 15 min into the ventral aspect of the sectioned surface of the spinal cord using a patch pipette (tip Ø 20 μm) containing 5 mM of the Ca^{2+} dye in 20% DMSO + pluronic acid, further diluted to 0.5 mM in rACSF containing no Ca^{2+}, Mg^{2+} or glucose. Cal-520AM was used as it has been shown to have a low dissociation constant (320 nM- Lock et al. 2015) indicating that it is a high-affinity chelator and efficiently binds Ca^{2+}. When compared to other commonly used synthetic and genetically encoded Ca^{2+} indicators, Cal520AM was shown to have a greatest dynamic range (ΔF/F0 0.05->0.6, Lock et al. 2015), and fast kinetics (Lock et al. 2015, Tada et al. 2014). Furthermore Cal-520AM was shown to be a reliable reporter of single action potentials (>95%, Li et al. 2017) and no significant evidence of sequestration or extrusion was observed over a period of several hours (Lock et al. 2015).

A MaiThai-BB Ti:sapphire femtosecond pulsed laser set to excite at 810 nm was used for fluorescence excitation, and a FV1000 MPE multiphoton scanning microscope (Olympus, Richmond Hill, ON, Canada) fitted with an XLUMPlan Olympus 20X immersion objective (1.0 NA) was used to image the neurons, and monitor the free cytosolic neuronal Ca^{2+} concentration. Loaded cells within a radius of approximately 400 μm and to a depth of approximately 100 μm below the sectioned surface of the spinal cord were imaged at a scan rate of 3-4 Hz. In order to

correlate cytosolic Ca^{2+} oscillations with electrophysiological signals, the two systems were synchronized (with a TTL pulse) and aligned before analysis.

Data analysis and statistics

All means are reported ± standard deviation (SD). Student's t-tests with a significance level of 0.05 were used to determine whether means differed significantly. As described previously (Haque et al. 2018), circular statistics (Zar 1974) were used to determine the coupling strength between ventral root pairs.

For analysis of Ca^{2+} imaging data, regions of interest (ROIs) were manually placed over each cell that was visible in a 20x image of the optical section being investigated. The average fluorescent intensity of the pixels within each ROI was calculated (Fluoview software, Olympus, Richmond Hill, ON, Canada) and plotted over time, with the average fluorescence intensity before each period of fictive locomotion acting as the baseline fluorescence for each cell. All optical signals were expressed as relative fluorescence changes with respect to initial fluorescence (ΔF/F), and plots were generated by extrapolating the values of the fluorescence intensity changes of each ROI into Clampfit 10 (Molecular Devices, San Jose, CA) for further analysis. Cross-correlation between ENG recordings and neuronal Ca^{2+} oscillations was performed using Clampfit after the electrophysiological sampling rate was reduced to match that of the Ca^{2+} imaging. In order to compare the frequency of oscillation of the Ca^{2+} signals to the frequency of oscillation of the VR activity the power spectrum function in Clampfit was used and plots were generated.

2.3 Results

In order to demonstrate that the upright spinal cord preparation is an effective tool for visually identifying and characterizing neurons that are involved in locomotor activity it was first necessary to establish that long lasting fictive locomotion could be generated in spinal cords prepared in this manner.

Initial experiments were performed on a preparation in which the spinal cord was bent at the caudal thoracic segments (Figure 2.2A). Preparing the spinal cord in this fashion generated unreliable results. In total, 17 preparations were bent between T8 and T11, and bath application of 5 μM NMDA and 10 μM 5-HT resulted in only one spinal cord exhibiting rhythmic, alternating ENG bursts in the contralateral ventral roots for greater than 30 minutes. In 5 preparations fictive locomotion could not be evoked at all, and in the remaining 11 preparations rhythmic activity was observed in one or both ventral roots, however it lasted for less than 30 minutes before becoming irregular and ultimately changing to either tonic activity, or completely vanishing (Figure 2.2B). Neither the quality nor the duration of rhythmic activity evoked from the 16 spinal cords which produced suboptimal fictive locomotor activity was improved by altering the concentrations of NMDA (3 μM -8 μM) and 5-HT (5 μM - 15 μM) or by perfusing the cord with 10 μM 5-HT and 50 μM dopamine, an alternative pharmacological cocktail shown to be effective at eliciting fictive locomotion in the neonatal mouse spinal cord (Madriaga et al. 2004).

The success rate for generating stable fictive locomotor activity increased substantially upon altering the preparation such that it was bent at the caudal cervical or rostral thoracic segments (Figure 2.2C). Application of either 5 μM NMDA and 10 μM 5-HT (n= 36) or 10 μM 5-HT and 50 μM dopamine (n= 7) to the perfusate of spinal cords prepared in this manner

typically evoked ENG activity in the VRs within the first 10 minutes. An initial tonic increase in VR activity was followed by rhythmicity and alternation between contralateral lumbar VR pairs (Figure 2.2D, 2.2E). Of the 43 spinal cords bent at the caudal cervical/rostral thoracic segments, 34 exhibited long lasting (> 30 min) rhythmic alternating VR activity (27/36 5-HT/NMDA, 7/7 5-HT/dopamine), 4 generated locomotor-like bursting that was maintained for less than 30 min, and in the remaining 5 rhythmic activity was absent. Analysis of the 34 preparations in which long-lasting fictive locomotor activity occurred indicated that the mean cycle period (CP) of fictive locomotor activity evoked by bath application of 10 μM 5-HT and 50 μM dopamine was significantly greater than that evoked by 5 μM NMDA and 10 μM 5-HT ($CP_{5HT/DOPA}$= 16.9 $\pm$ 2.6 SD s n=7, $CP_{NMDA/5HT}$= 5.6 $\pm$ 1.4 SD s n=27, t (32) = 19.9 p < 0.0001, Figure 2.2F).

Our next goal was to implement an imaging approach to simultaneously identify those neurons within the field of view of our objective lens that were locomotor- related. To this end the Ca^{2+} indicator Cal-520AM was pressure-injected unilaterally into the ventral aspect of the sectioned surface of 13 spinal cords bent at the caudal cervical/rostral thoracic segments in which long lasting fictive locomotion was evoked in response to bath application of 5 μM NMDA and 10 μM 5-HT or 10 μM 5-HT and 50 μM dopamine. Visual inspection with a GFP filter 30 minutes after Cal-520AM injection indicated that the majority of cells in the ventromedial spinal cord had taken up the Ca^{2+} indicator (Figure 2.3A, 2.3B). In addition to inducing rhythmic alternation between contralateral VRs (Figure 2.3C), bath application of the pharmacological cocktail induced rhythmic oscillations of cytosolic Ca^{2+} in cells (Figure 2.3D) in all 13 spinal cords. In each optical section we were also able to identify cells in which there were no observable Ca^{2+} oscillations (Figure 2.3E). Post hoc spectral analysis of the activity of rhythmically active cells as well as VRs confirmed that the primary frequencies of oscillation

were identical (Figure 2.3F), providing strong evidence that the cells were involved in fictive locomotor activity.

In order to quantify the number of cells that took up the Ca^{2+} indicator as well as the number that were rhythmically active during fictive locomotion we analyzed an additional 4 upright spinal cord preparations in which the application site of the Ca^{2+} indicator was standardized to the middle of the ventral aspect of the spinal cord isolated from a P0/P1 mouse (approximately 250 μm from both the midline and ventral extent of the spinal cord), 100 μm below the sectioned surface. In these preparations a mean of 182.5 ± 27.4 SD cells took up Cal-520AM with 96.0 ± 12.7 SD of these exhibiting oscillations of fluorescent intensity during fictive locomotion. Power spectrum analysis indicated that slightly more than half of these oscillatory neurons (52.8 ± 14.6 SD) displayed Ca^{2+} oscillations with a frequency identical to VR output while the remaining neurons oscillated at a frequency unrelated to fictive locomotor activity.

The final step was to determine whether neurons close to the sectioned surface of the upright spinal cords were healthy, and rhythmic oscillations of membrane potential could be recorded during pharmacologically-induced fictive locomotion. We restricted our study to cells located in the ventral region of the spinal cord, the location that has been shown to contain the core elements of the locomotor CPG (Kjaerullf and Kiehn 1996). In total, whole cell recordings were made from 38 neurons, located in the L2 and L3 segments, in 23 of the 43 spinal cords that were used for Ca^{2+} imaging. Fifteen of these cells were recorded in raCSF alone (i.e. without NMDA/5-HT or 5-HT/dopamine added to the bath) in order to assess their intrinsic electrophysiological properties. Mean membrane resistance (953.6 MΩ ± 225.4 SD) and resting membrane potential (-50.9 mV ± 8.8 SD) of these cells were in line with previous recordings

made from ventral interneurons in either spinal cord slices (Wilson et al 2005), or the midline hemisected spinal cord preparation (Hinckley et al. 2005). Whole cell recordings were made from an additional 18 neurons in the presence of either 5 μM NMDA and 10 μM 5-HT (n=12) or 10 μM 5-HT and 50 μM dopamine (n=6). All eighteen cells that exhibited rhythmic, locomotor-related Ca^{2+} oscillations also exhibited rhythmic oscillations of membrane potential during fictive locomotion that were either in phase (n= 11) or out of phase (n= 7) with ipsilateral VR activity in the same spinal segment in which they were located (i.e. the local VR). Typically, the cells fired one or more action potentials during their depolarized phase (Figure 2.4A), however in some cases the cells were depolarized during the active phase of the left or right VR without spiking (Figure 2.4B). By including the fluorescent tracer AlexaFluor 594 in the patch pipette the morphology of the cells from which we recorded was able to be assessed in real time. Five minutes after breaking through the membrane of a cells the soma was labeled, as were its primary processes (Figure 2.4C), and by 30 minutes much smaller processes could be identified (Figure 2.4D). Beyond this time point there was no noticeable change in the number, or projection, of labeled processes (Figure 2.4E).

2.4 Discussion.

This study describes an upright preparation which enables the visual identification and electrophysiological characterization of locomotor-related neurons spanning the transverse plane of the neonatal mouse spinal cord. The utility of this preparation is demonstrated by a) the long lasting fictive locomotor activity that can be recorded from contralateral ventral roots, b) the fact that more than 50 rhythmically active, locomotor- related cells can be identified per optical section, c) the health of spinal neurons as indicated by their spike height and membrane potential

values, and d) the ability to identify morphological features of cells in real time after application of an intracellular tracer.

In order to understand how locomotor activity is generated we need to be able to identify the interneuronal components of this neural circuit, determine how these components are interconnected, and identify their intrinsic electrophysiological properties that allow for the initiation and maintenance of rhythmic activity. The advent of molecular genetic techniques to label and ablate populations of spinal interneurons based on their transcription factor expression has generated a great deal of information regarding the identity of component interneurons of the locomotor CPG, and we are now able to identify populations of neurons that are responsible for a number of specific functions including left-right (Lanuza et al. 2004; Talpalar et al. 2012), and flexor-extensor (Britz et al. 2015; Zhang et al. 2014) alternation. Transgenic mouse strains have been developed, many of which are commercially available, in which these genetically- defined interneuronal populations express reporter proteins and can be visualized in live tissue.

Despite this progress it is essential not to lose sight of the fact that there is still a paucity of information regarding the intrinsic electrophysiological properties of these neurons, their morphology, or the manner in which they are connected to one another. This is primarily due to difficulty accessing these neurons for electrophysiological and morphological study given their location in the intermediate nucleus of the spinal cord, and the fact that the distributed nature of the locomotor CPG dictates that several spinal segments must remain intact in order for locomotor activity to be evoked. These issues have resulted in many experiments, which have investigated the intrinsic properties of these populations, being carried out in a spinal cord slice preparation (Dougherty et al. 2013; Ha and Dougherty 2018; Zhong et al. 2010; Zhang et al. 2008) in which locomotor activity cannot be evoked. This approach is problematic since we have

very little information regarding the proportion of each neuronal population that participate in locomotor activity. In fact, of the ventrally-located interneuronal populations in the lumbar spinal cord only two, the Chx10- expressing V2a, and the Shox2- expressing, neurons have had their activity assessed during stepping, with 44% of Chx10- expressing (Zhong et al. 2010), and 69% of Shox2- expressing (Dougherty et al. 2013), neurons shown to be rhythmically active during fictive locomotion. It is therefore essential to proceed with caution when interpreting electrophysiological or morphological data generated from the slice preparation and incorporating it into network models of the locomotor CPG, since a substantial proportion of the neurons analyzed in these slice studies likely do not participate in locomotor activity.

In an attempt to characterize only those neurons that are active during locomotion, several groups have devised experimental preparations which provide access to interneuronal populations located in the intermediate nucleus during fictive locomotion by removing specific regions of the dorsal spinal cord (Antri et al. 2011; Dougherty et al. 2013; Dyck et al. 2009) or by performing a midline hemisection (Kiehn et al. 1996; Hinckley et al. 2005). While useful for investigating the longitudinal distribution of the locomotor CPG, or characterizing specific neuronal populations of interest in each study, these preparations are limited in that they only allow access to neurons in discrete regions of the spinal cord. Another recently developed experimental approach has incorporated 2-photon (Kwan et al. 2009), or fluorescent (Jean-Francois et al. 2018), microscopy to image the activity of locomotor-related neurons through the intact, isolated spinal cord at optical sections along the anterior posterior plane. This approach provides an excellent means to identify locomotor-related neurons in the longitudinal plane, however given the current single cell recording techniques available, this approach would make it difficult to access rhythmically active neurons in the intermediate lamina of the spinal cord for

electrophysiological recording or tracing. Other experimental approaches, similar to the upright spinal cord preparation presented in this study, have been used to investigate connectivity between the brainstem and spinal cord (Szokol and Perreault 2009) or neuronal excitability (Christie and Whelan 2005; Lev-Tov and O'Donovan 1995). Since the analysis of locomotor-related neurons was not the goal of these studies we cannot be sure whether fictive locomotor activity could have been evoked with these modified brainstem spinal cord preparations. The fact that these preparations were bent at the caudal (lower thoracic/lumbar) segments may impact their ability to generate fictive locomotion as we found bending the spinal cord at these, more caudal, segments produced poor bursting, likely due to the physical damage to components of the locomotor CPG situated in these segments.

In contrast to these approaches, the upright spinal cord preparation described in this study provides a means to identify neurons across the transverse plane of the spinal cord that are rhythmically active during fictive locomotion. We have previously shown that this preparation can be used to record from rhythmically active neurons during fictive locomotion (Haque et al. 2018; discussed in Chapter 3 of this thesis), and here we demonstrate that rhythmic Ca^{2+} oscillations can also be recorded. This allows us to simultaneously identify locomotor related neurons spanning our field of view. By using Ca^{2+} indicators with different emission spectra (Cal-520, Cal-590) we can visualize rhythmic Ca^{2+} oscillations in neurons expressing various reporter proteins (i.e. GFP, YFP, tdTomato), and focus electrophysiological studies solely on oscillatory neurons, ignoring members of a population that do not participate in locomotor activity. Inclusion of intracellular tracers such as AlexaFluor in the patch pipette enables the basic morphological features of these select neurons of interest to be identified.

While it is possible some smaller axial motoneurons were included in our dataset we believe that the majority of the rhythmically-active cells were interneurons, as opposed to motoneurons, since our Ca^{2+} indicator did not spread to lamina IX. In this study approximately 29% of the total number of cells per optical section were locomotor-related. It is important to keep in mind that this likely under-represented the proportion of neurons involved in fictive locomotor activity since we have no way of distinguishing between neurons and glia cells. Furthermore, although our whole cell recording experiments indicate that cells in the superficial optical sections are generally in good health, there are undoubtably some neurons within the field of view that are dead or dying and, although locomotor-related, will not display Ca^{2+} oscillations. Under-representation of locomotor-related cells could also stem from sequestration of the Ca^{2+} indicator, or its leakage from rhythmically-active neurons, however we do not believe this is a major concern since previous work has demonstrated that there is no significant run down of Ca^{2+} responses in cells loaded with Cal-520AM after several hours of recording (Lock et al. 2016). Furthermore, in experiments in which we bath applied strychnine and GABAzine to the upright spinal cord preparation we saw no noticeable decrease of the baseline Ca^{2+} signal, or Ca^{2+} oscillations, in cells over a period of 4 hours.

In addition to facilitating the electrophysiological and morphological characterization of locomotor related neurons, the upright preparation has the capacity to provide information regarding the distribution of the component interneurons of the locomotor CPG in the transverse plane. Lesion studies have revealed the segmental distribution of the mammalian locomotor CPG as well as its location in the ventral spinal cord (Kjaerullf and Kiehn 1996; Cowley and Schmidt 1997), however we know little regarding the specific transverse distribution of its interneuronal components. Previous attempts to localize components have relied on activity dependent labeling

approaches (Dai et al. 1998; Kjaerullf et al. 1994; Jasmin et al. 1994) during fictive locomotion which are flawed as they do not differentiate between tonically active and rhythmically active neurons.

Information regarding the transverse distribution of the locomotor CPG is of particular interest given recent findings which indicate that locomotor activity at different speeds results in different muscle synergies (Bellardita and Kiehn 2015). This has been attributed to the recruitment of different neuronal populations at different locomotor speeds. Experimental evidence supporting this speed- dependent recruitment of interneuronal populations comes from analysis of the locomotor pattern in the absence of the $V0_D$ and $V0_V$ subpopulations (Talpalar et al. 2012) which indicates that the former is likely to be responsible for left-right alternation at slow locomotor speeds while the latter is likely to carry out this function during faster stepping. Imaging the sectioned surface of the upright spinal cord preparation while modulating the frequency of fictive locomotion in an animal model in which the two subsets of V0 neurons are labeled would enable identification of the specific speed at which each is activated. These experiments would also allow us to determine what happens to either subset when locomotor speed changes. Do they continue firing and serve a different role, or do they simply cease activity?

While the experiments presented in this study involve a single injection of Ca^{2+} indicator to reveal the activity of neurons in the ventromedial aspect of the spinal cord it is possible to make multiple injections in different regions, or simply bath apply the indicator, in order to monitor the activity of the entire transverse face of the spinal cord. In addition to enabling access to motoneurons and lateral interneurons, this would also reveal neurons in the dorsal spinal cord, and may allow the specific cells which receive input from sensory afferents to be identified.

The utility of the upright spinal cord preparation is not limited to investigations of the neuronal mechanisms underlying locomotion. Given the recent molecular dissection of the dorsal spinal cord and the identification of genetically-defined neurons that respond to various types of nociceptive and non-nociceptive input (reviewed in Gatto et al. 2019; Koch et al. 2018), this preparation can also be used to identify the proportion of each population involved in the sensory response, and characterize the anatomical and electrophysiological properties of these sensory related neurons. The upright spinal cord preparation thus provides an excellent approach to identify and characterize the spinal neurons which are involved in multiple facets of sensorimotor control.

REFERENCES

Antri M, Mellen N, Cazalets JR. (2011). Functional organization of locomotor interneurons in the ventral lumbar spinal cord of the newborn rat. PLoS One 6:e20529

Bellardita C, Kiehn O. (2015). Phenotypic characterization of speed-associated gait changes in mice reveals modular organization of locomotor networks. Curr Biol. 25:1426-1436.

Britz O, Zhang J, Grossmann KS, Dyck J, Kim JC, Dymecki S, Gosgnach S, Goulding M. (2015). A genetically defined asymmetry underlies the inhibitory control of flexor-extensor locomotor movements. Elife. 4. doi: 10.7554/eLife.04718.

Cazalets, J.R., Sqalli-Houssaini, Y. and Clarac, F., (1992). Activation of the central pattern generators for locomotion by serotonin and excitatory amino acids in neonatal rat. J. Physiol., 455:187-204.

Christie KJ, Whelan PJ. (2005). Monoaminergic establishment of rostrocaudal gradients of rhythmicity in the neonatal mouse spinal cord. J Neurophysiol. 94:1554-1564.

Cowley KC, Schmidt BJ. (1994). A comparison of motor patterns induced by N-methyl-D-aspartate, acetylcholine and serotonin in the in vitro neonatal rat spinal cord. Neurosci Lett. 171:147-150.

Cowley KC, Schmidt BJ. (1997). Regional distribution of the locomotor pattern-generating network in the neonatal rat spinal cord. J Neurophysiol. 77:247-259.

Dai X, Noga BR, Douglas JR, Jordan LM. (2005). Localization of spinal neurons activated during locomotion using the c-fos immunohistochemical method. J Neurophysiol. 93:3442-3452.

Dougherty KJ, Zagoraiou L, Satoh D, Rozani I, Doobar S, Arber S, Jessell TM, Kiehn O. (2013). Locomotor rhythm generation linked to the output of spinal shox2 excitatory interneurons. Neuron. 80:920-933.

Dyck J, Gosgnach S. (2009). Whole cell recordings from visualized neurons in the inner laminae of the functionally intact spinal cord. J Neurophysiol. 102:590-597.

Gatto G, Smith KM, Ross SE, Goulding M. (2019). Neuronal diversity in the somatosensory system: bridging the gap between cell type and function. Curr Opin Neurobiol. 56:167-174.

Gordon IT, Whelan PJ. (2006). Monoaminergic control of cauda-equina-evoked locomotion in the neonatal mouse spinal cord. J Neurophysiol. 96:3122-3129.

Goulding M (2009). Circuits controlling vertebrate locomotion: moving in a new direction. Nat. Rev. Neurosci. 10:507-518.

Grillner S, Jessell TM (2009). Measured motion: searching for simplicity in spinal locomotor networks. Curr. Opin. Neurobiol. 19:572-586.

Ha NT, Dougherty KJ. (2018). Spinal Shox2 interneuron interconnectivity related to function and development. Elife. 31 pii: e42519.

Haque F, Rancic V, Zhang W, Clugston R, Ballanyi K, Gosgnach S. (2018). WT1-Expressing Interneurons Regulate Left-Right Alternation during Mammalian Locomotor Activity. J Neurosci. 38:5666-5676.

Hinckley CA, Hartley R, Wu L, Todd A, Ziskind-Conhaim L. (2005). Locomotor-like rhythms in a genetically distinct cluster of interneurons in the mammalian spinal cord. J Neurophysiol. 93:1439-1449.

Jasmin L, Gogas KR, Ahlgren SC, Levine JD, Basbaum AI. (1994). Walking evokes a distinctive pattern of Fos-like immunoreactivity in the caudal brainstem and spinal cord of the rat. Neuroscience. 58:275-286.

Jean-Xavier C, Perreault MC. (2018). Influence of Brain Stem on Axial and Hindlimb Spinal Locomotor Rhythm Generating Circuits of the Neonatal Mouse. Front Neurosci. 12:53.

Kiehn O. (2016). Decoding the organization of spinal circuits that control locomotion. Nat Rev Neurosci. 17:224-238.

Kiehn O, Johnson BR, Raastad M. (1996). Plateau properties in mammalian spinal interneurons during transmitter-induced locomotor activity. Neuroscience. 75:263-273.

Kjaerulff O, Barajon I, Kiehn O. (1994). Sulphorhodamine-labelled cells in the neonatal rat spinal cord following chemically induced locomotor activity in vitro. J Physiol. 478 :265-273.

Kjaerulff O, Kiehn O. (1996). Distribution of networks generating and coordinating locomotor activity in the neonatal rat spinal cord in vitro: a lesion study. J Neurosci.16:5777-5794.

Koch SC, Acton D, Goulding M. (2018). Spinal circuits for touch, pain, and itch. Annu Rev Physiol. 80: 189-217.

Kudo N, Yamada T. (1987). N-methyl-D,L-aspartate-induced locomotor activity in a spinal cord-hindlimb muscles preparation of the newborn rat studied in vitro. Neurosci Lett. 75(1):43-48.

Kwan AC, Dietz SB, Webb WW, Harris-Warrick RM. (2009). Activity of Hb9 interneurons during fictive locomotion in mouse spinal cord. J Neurosci. 29:11601-11613.

Lanuza GM, Gosgnach S, Pierani A, Jessell TM, Goulding M (2004). Genetic identification of spinal interneurons that coordinate left-right locomotor activity necessary for walking movements. Neuron. 42:375-386.

Lev-Tov A, O'Donovan MJ. (1995). Calcium imaging of motoneuron activity in the en-bloc spinal cord preparation of the neonatal rat. J Neurophysiol. 74:1324-1334.

Li J, Zhang J, Wang M, Pan J, Chen X, Liao X. (2017). Functional imaging of neuronal activity of auditory cortex by using Cal-520 in anesthetized and awake mice. Biomed Opt Express. 8:2599-2610.

Lock JT, Parker I, Smith IF. (2015). A comparison of fluorescent Ca^{2+} indicators for imaging local Ca^{2+} signals in cultured cells. Cell Calcium. 58:638-648.

Madriaga MA, McPhee LC Chersa T, Christie KJ, Whelan PJ. (2004). Modulation of locomotor activity by multiple 5-HT and dopaminergic receptor subtypes in the neonatal mouse spinal cord. J. Neurophysiol. 92:1566-1576.

Smith JC, Feldman JL. (1987). In vitro brainstem-spinal cord preparations for study of motor systems for mammalian respiration and locomotion. J Neurosci Methods. 1987 21:321-333.

Szokol K, Perreault MC. (2009). Imaging synaptically mediated responses produced by brainstem inputs onto identified spinal neurons in the neonatal mouse. J Neurosci Methods. 180:1-8.

Tada M, Takeuchi A, Hashizume M, Kitamura K, Kano M. (2014). A highly sensitive fluorescent indicator dye for calcium imaging of neural activity in vitro and in vivo. Eur J Neurosci. 39:1720-1728.

Talpalar AE, Bouvier J, Borgius L, Fortin G, Pierani A, Kiehn O (2013). Dual-mode operation of neuronal networks involved in left-right alternation. Nature 500:85-88.

Zar, J.H. Circular Distribution. In "Biostatistical Analysis", p310-327. Prentice Hall, Engelwood Cliffs, NJ. 1974.

Zhang J, Lanuza GM, Britz O, Wang Z, Siembab VC, Zhang Y, Velasquez T, Alvarez FJ, Frank E, Goulding M. (2014). V1 and v2b interneurons secure the alternating flexor-extensor motor activity mice require for limbed locomotion. Neuron. 82:138-150.

Zhang Y, Narayan S, Geiman E, Lanuza GM, Velasquez T, Shanks B, Akay T, Dyck J, Pearson K, Gosgnach S, Fan CM, Goulding M (2008). V3 spinal neurons establish a robust and balanced locomotor rhythm during walking. Neuron 60:84-96

Zhong G, Droho S, Crone SA, Dietz S, Kwan AC, Webb WW, Sharma K, Harris-Warrick RM. (2010). Electrophysiological characterization of V2a interneurons and their locomotor-related activity in the neonatal mouse spinal cord. J Neurosci.30:170-182.
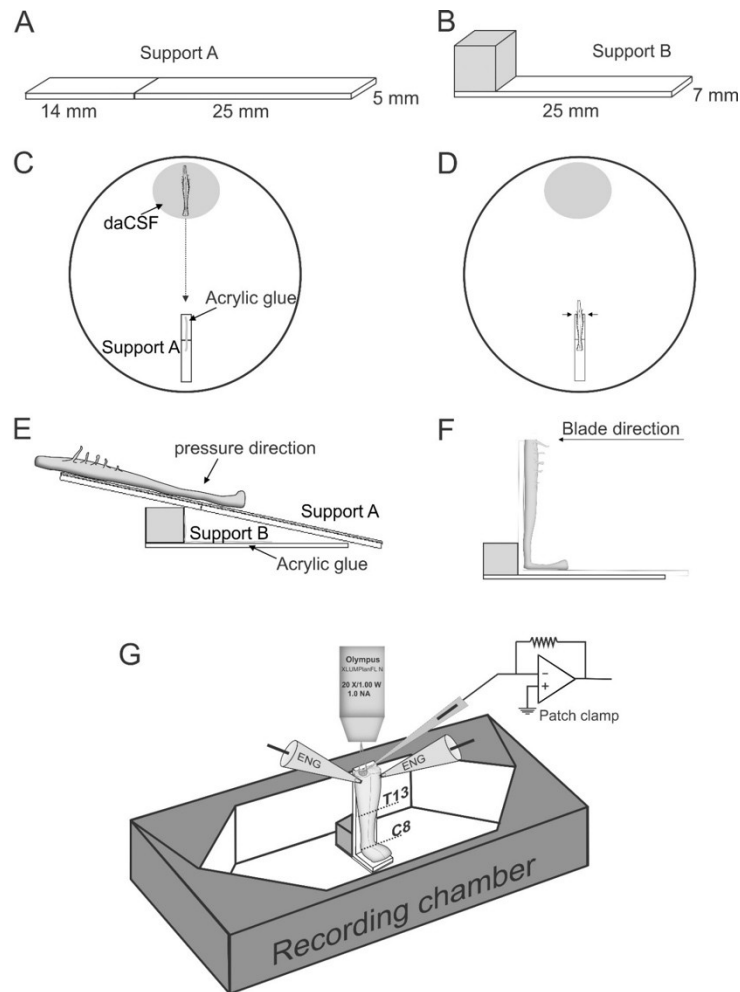
FIGURES

Figure 2.1. The upright spinal cord preparation. A, B. Supports A and B are cut to size from plastic weigh boats. A horizontal cut (to facilitate a 90º bend) is made 14 mm from one end of support A, and the resulting 2 segments are placed next to one another on a piece of double sided tape. The Sylgard block in support B is attached with acrylic glue. **C.** The spinal cord is placed in a pool of daCSF in a dish, ventral side up, with its rostral end towards the 14 mm segment of support A, and then pulled onto support A with fine forceps such that the spinal segment of interest (indicated by arrows) is located at the end of the support (**D**). **E.** Support A is placed on top of support B and pressure is applied at the junction between the 14 mm and 25 mm segments which results in the spinal cord being bent at a 90º angle. **F.** The region of the spinal cord caudal to the segment of interest is cut off and discarded, the remaining spinal cord is sectioned with a vibratome in the transverse plane resulting in a horizontal surface for imaging and recording. **G.** The preparation is placed in a recording chamber under the objective lens of an upright microscope which can be used for Ca^{2+} imaging, and visual identification of neurons for whole cell recordings. ENG electrodes are attached to ipsilateral and contralateral ventral roots to record fictive locomotor activity.
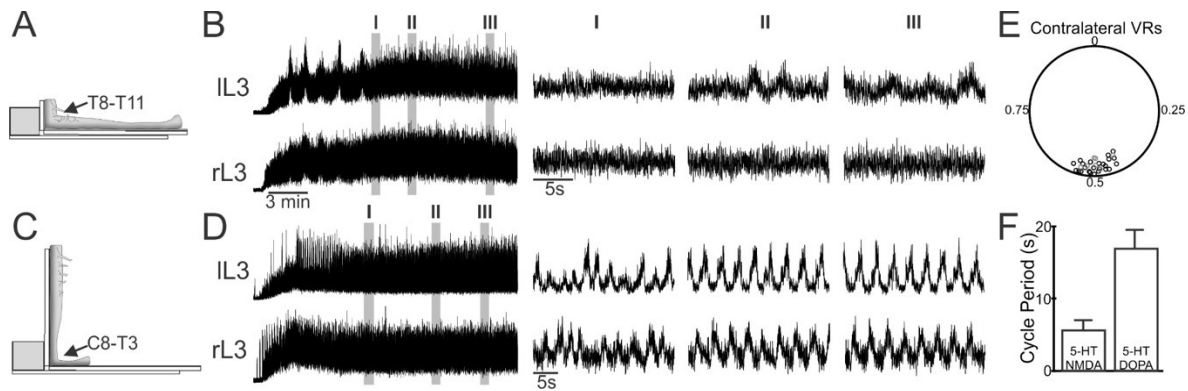
Figure 2.2. Fictive locomotor activity in the upright spinal cord preparation. A. Schematic of the upright preparation which was bent at the caudal thoracic segments and sectioned at L2. **B**. Typical bout of fictive locomotor activity evoked from spinal cords prepared in this manner in which weak rhythmic activity can be seen in the right and left L2 ventral roots (rL2, lL2) in response to bath application of 5 μM NMDA and 10 μM 5-HT. In panels B and D shaded portions (I, II, III) are expanded to the right. **C-D.** Fictive locomotor activity evoked by application of the same pharmacological cocktail to a spinal cord bent at the caudal cervical/rostral thoracic segments and sectioned at L2 (**C**) is marked by clear rhythmic alternation of contralateral VR activity (**D**). **E**. Alternation between contralateral VRs was consistent in all preparations in which long lasting ENG activity was generated as indicated by the points clustered around 0.5 in the polar plot. Each point indicates the mean vector value for one experiment. Black circles indicate experiments in which fictive locomotion was evoked by 5-HT/NMDA, grey circles indicate experiments in which 5-HT/dopamine was applied **F.** Bar chart illustrating that mean cycle period of fictive locomotor evoked by either pharmacological cocktail.
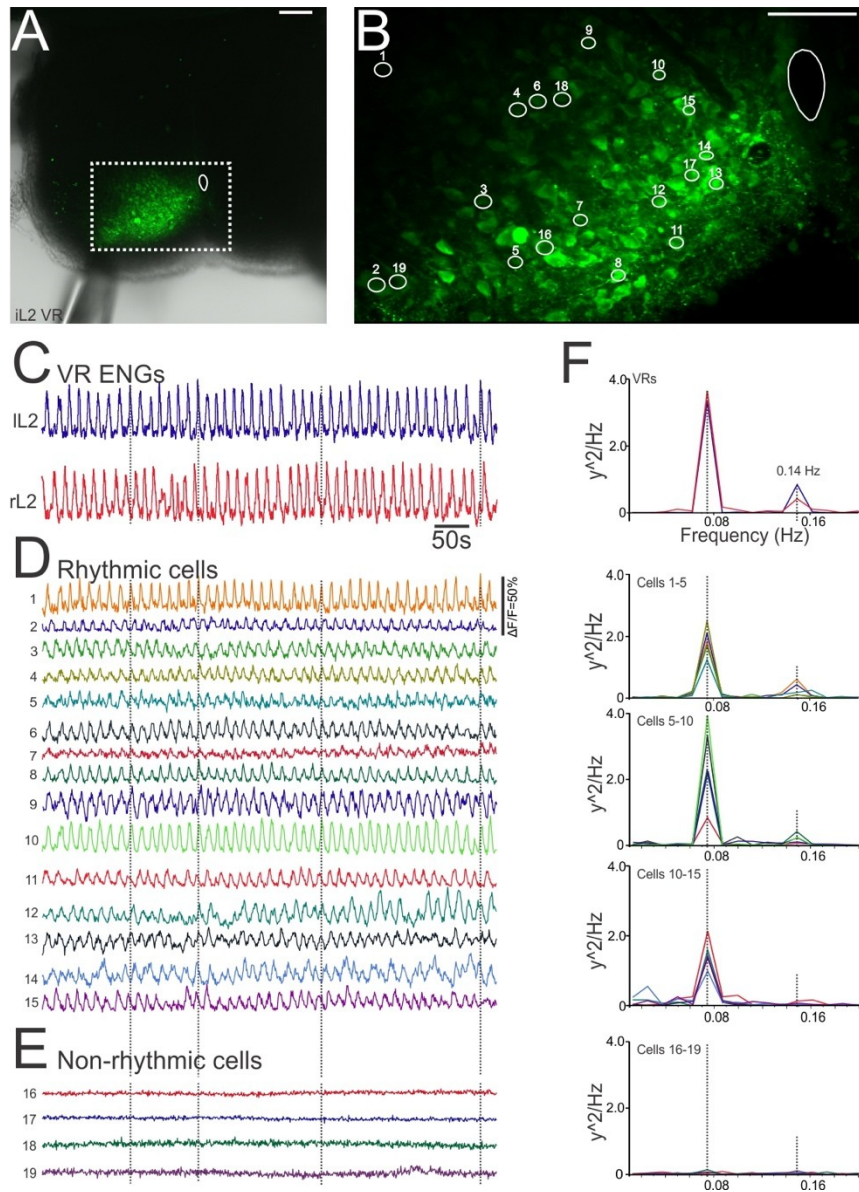
Figure 2.3: Imaging neuronal activity using the upright spinal cord preparation. A. Low magnification image of the sectioned surface of the spinal cord after injection of Cal-520AM into the L2 segment. **B.** Magnification of region within dashed box in panel A in which cells that have taken up the Ca^{2+} indicator appear green. White circles surround selected neurons which have their activity analyzed during fictive locomotion. In both panels A and B scale bar = 100 μm **C-E** ENG activity recorded in the left and right L2 ventral roots (lL2, rL2) (C) and Ca^{2+} activity (D, E) of the circled cells in panel B in response to bath application of 10 μm 5-HT and 10 μm dopamine. VRs (C) and cells 1-15 (D) oscillate in a phase locked manner (dashed lines indicate peak of the ENG burst in the lL2 VR) while those in panel E do not oscillate during fictive locomotion. Scale bar for time applies to all VR recordings and Ca^{2+} traces, ΔF/F scale bar applies to all Ca^{2+} traces. F. Spectral analysis indicates that the primary frequency of oscillation for the VRs and all 15 oscillatory cells is 0.074 Hz (indicated by dashed line).
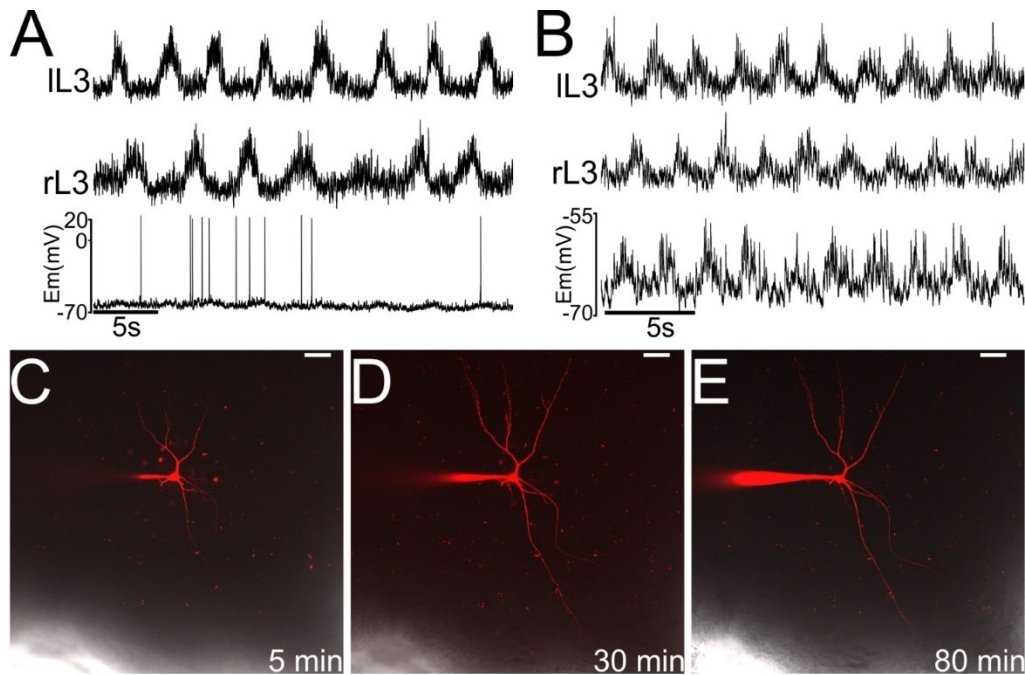
Figure 2.4. Electrophysiological and morphological analysis of neurons using the upright spinal cord preparation. A,B. Bath application of 5 μM NMDA and 10 μM 5-HT to an upright spinal cord sectioned at the L3 segment results in fictive locomotion marked by rhythmic alternation of right and left L3 ventral roots (rL3, lL3). Lower trace in panel **A** illustrates the activity of a cell in the rL3 segment. During fictive locomotion the membrane potential of this cell is rhythmically active in phase with the rL3 ventral root and typically fires action potentials in this phase. The lower trace in panel **B** depicts a cell is rhythmically active in phase with the lL3 VR that does not fire action potentials. **C-E.** A cell in the ventromedial aspect of the spinal cord 5, 30, and 80 minutes after breaking through the membrane with a recording pipette containing AlexaFluor594. The soma and primary processes are visible after 5 min (**C**) and more distal processes after 30 min (**D**). After this point (**E**) there is little difference in the extent to which the processes can be followed. Scale bar indicates 50 μm.

Chapter 3 -

WT1-expressing interneurons regulate left-right alternation during mammalian locomotor activity.

Haque F, Rancic V, Zhang W, Clugston R, Ballanyi K, Gosgnach S. (2018). WT1-Expressing Interneurons Regulate Left-Right Alternation during Mammalian Locomotor Activity. J Neurosci. 38:5666-5676.

Contributions

FH: experimental design, carried out electrophysiology and tracing experiments, data analysis

VR: experimental design, carried out electrophysiology experiments, data analysis

WZ: carried out immunohistochemical experiments

RC: carried out molecular experiments

KB: provided comments on manuscript

SG: experimental design, data analysis, wrote manuscript

Significance statement.

In this study we characterize WT1-expressing spinal interneurons in mice and demonstrate that they are commissurally projecting and inhibitory. Silencing of this neuronal population during a locomotor task results in a complete breakdown of left-right alternation while flexor-extensor alternation was not significantly affected. Axons of WT1 neurons are shown to terminate nearby commissural interneurons which coordinate motoneuron activity during locomotion, and presumably regulate their activity. Finally, the WT1 gene is shown to be present in the spinal cord of humans raising the possibility of functional homology between these species. This study not only identifies a key component of the locomotor circuitry but also begins to unravel the connectivity amongst the growing number of molecularly-defined interneurons that comprise this neural network.

3.1 Introduction.

The ventral region of the caudal spinal cord in mammals houses a neural circuit known as the locomotor central pattern generator (CPG) which is responsible for producing the basic pattern of rhythmic activity that underlies stepping (Kiehn 2016). Since the turn of the century significant advances have been made in our understanding of the structure and function of the locomotor CPG. This has been propelled by an experimental approach which enables populations of spinal interneurons to be identified and manipulated based on the transcription factors they express during development (Goulding 2009). Targeted inactivation of select interneuronal populations has allowed for the identification of those involved in a number of essential locomotor functions (Kiehn 2016).

Control of left-right alternation is perhaps the aspect of locomotion which has been best characterized. Coordination of motor activity on the left and right sides of the spinal cord has been shown to depend on excitatory and inhibitory commissural interneurons which project both intra- and intersegmental axons (Butt and Kiehn, 2003; Quinlan and Kiehn, 2007). Initial studies investigating the involvement of genetically-defined interneuronal populations demonstrated that left-right alternation is partially disrupted when Dbx1-expressing interneurons (i.e. the V0 population) are absent (Lanuza et al. 2004). Subsequently it was demonstrated that Dbx1-expressing $V0_D$ cells were responsible for coordinating left-right alternation via monosynaptic inhibition of contralateral motoneurons at slower locomotor speeds while Evx1-expressing $V0_V$ cells served this function, likely via a multisynaptic pathway, as locomotor speed increased (Talpalar et al. 2013). The discrete control of motor neurons on either side of the spinal cord is complex and it is now apparent that appropriate activity of these commissural interneurons is modulated by additional cell types including the ipsilaterally projecting V2a population which

are excitatory, express the transcription factor Chx10, receive input from putative rhythm generating cells (Dougherty et al. 2013), and synapse with the V0 population (Crone et al. 2008).

The dI6 interneurons, which express the homeobox transcription factor Lbx1 in the progenitor stages (Gross et al. 2002; Muller et al. 2002), are situated in the ventromedial spinal cord postnatally and have been divided into two genetically-distinct subsets based on the expression of either DMRT3 or WT1 (Vallstedt and Kullander 2013). The DMRT3-expressing subpopulation have been shown to be exclusively inhibitory, project axons to motoneurons on both sides of the spinal cord, and have been implicated in the development of ipsilateral and contralateral coordination (Andersson et al., 2012). Here we characterize the WT1-expressing subset of dI6 interneurons and investigate their role during locomotion. Our results indicate that these neurons are overwhelmingly inhibitory, project commissural axons which terminate in close proximity to both Evx1-expressing $V0_V$, and DMRT3-expressing dI6 neurons, and severe deficits in left-right alternation occur when they are selectively silenced during a locomotor task. Taken together these findings provide key insight into the network structure of the locomotor CPG by suggesting that WT1-expressing neurons control motor output on either side of the spinal cord by regulating the activity of commissural interneurons. Finally, our finding that WT1 is expressed in the adult human spinal cord indicates that expression of this gene is conserved in the CNS of the mouse and human. These neurons are thus the first genetically-defined interneuronal population involved in murine locomotion that have be mapped to the spinal cord in humans, raising the possibility that they play a similar role in regulating bipedal stepping.

3.2 Materials and methods.

Animals. All procedures were performed on mice of either sex in accordance with the Canadian Council on Animal Welfare and approved by the Animal Welfare Committee at the University of Alberta. Embryos were obtained via caesarian section from timed matings with the morning of the vaginal plug designated as E0.5.

The following mouse strains were used (all strains with stock numbers indicated are from The Jackson Laboratory): Wt1^{CreGFP} (#010911, RRID:IMSR_JAX:010911), Wt1^{CreER} (#010912, RRID:IMSR_JAX:010912), VGlut2^{Cre} (#028863RRID:IMSR_JAX:02886), ROSA26^{tdTomato} (#007909, RRID:IMSR_JAX:007909), R26-LSL-Gi-DREADD (#026219, RRID:IMSR_JAX:026219), GAD67^{GFP} (gift from Dr. Yuchio Yanagawa, Gunma University RRID:IMSR_RBRC09645).

Immunohistochemistry. Immunohistochemistry was performed as previously described (Griener et al. 2017). Briefly, frozen or wax serial sections of either whole embryos, postnatal mouse spinal cords, or human lumbar spinal cord were cut and incubated with primary antibodies overnight (4°C) followed by incubation with species specific secondary antibodies conjugated to Cy2, Cy3, or Cy5 for 4 hours at room temperature. After cover slipping, images were collected using a Leica TCS SP8 MP microscope running Leica Application Suite X software and figures were prepared with Adobe Photoshop and Corel Draw. Primary antibodies used were: WT1 (rabbit, 1:100, Santa Cruz, RRID:AB_632611), GFP (goat, 1:5000, gift from Eusera), Glycine (rat, 1:1000, Immunosolutions, RRID:AB_10013222), En1 (gift from Jessel lab, Columbia University- guinea pig, 1:1000), Chx10 (mouse, 1:200, Santa Cruz, RRID:AB_10842442), DMRT3 (goat, 1:100, Santa Cruz, RRID:AB_2091664), synaptotagmin

(rabbit, 1:200, Alomone Lab), Evx1 (mouse, 1:100, DSHB, , RRID:AB_2246711), NeuN (mouse, 1:500, Millipore, RRID:AB_177621).

Retrograde trans-synaptic labelling. Hindlimb extensor (gastrocnemius- GC) or flexor (tibialis anterior- TA) muscles in anesthetized P0 wildtype mice, were injected with 1-2 μL of PRV-152 viral stock (~6.68 x 108 infectious units per μL), a strain of pseudorabies virus which expresses GFP in all infected cells (Kerman et al. 2003). All animals were euthanized 40 or 46 hours after injection as these are times at which interneurons which are monosynaptically connected to motoneurons have been shown to be infected with the virus (Jovanovic et al., 2010). Spinal cords were dissected out and processed for immunohistochemistry as described above. The pattern and density of viral labelling in all spinal cords included in the dataset were similar to those previously reported (Jovanovic et al., 2010).

Electrophysiology. The *in vitro* upright spinal cord preparation was used to make whole cell patch clamp recordings from WT1-expressing interneurons. Briefly, neonatal WT1^{CreGFP} and WT1^{CreER};R26-LSL-Gi-DREADD pups were anesthetized, decapitated, and eviscerated. Spinal cords were dissected out in ice-cold oxygenated artificial cerebrospinal fluid (aCSF) containing (in mM) 120 NaCl, 3 KCl, 1.25 NaH$_2$PO$_4$, 26 NaHCO$_3$, 1.5 MgSO$_4$, 1.5 CaCl$_2$, 5 HEPES, 10 N-Acetyl- L-Cysteine and 10 L-Glucose. The dorsal side of the spinal cord was glued to a plastic support which was bent at an angle of 90 degrees at the upper-thoracic level. The specimen was then transferred to a vibratome and a transverse cut was made at a mid- lumbar segment. Care was taken throughout to ensure that the ventral roots remained intact. After a 30 minute recovery period in oxygenated aCSF the preparation (including the plastic support) was placed in a recording chamber located under the objective lens of an upright fluorescent microscope and

constantly perfused with oxygenated recording aCSF composed of (in mM) 111 NaCl, 3.08 KCl, 11 glucose, 25 NaHCO$_3$, 1.18 KH$_2$PO$_4$, 1.25 MgSO$_4$, 2.52 CaCl$_2$.

For whole cell recording patch electrodes (tip resistance: 5-7 MΩ) were filled with (in mM) 140 potassium gluconate, 1 NaCl, 0.5 CaCl$_2$, 2MgCl$_2$, 1ATP-Na$_2$, 10 HEPES, pH adjusted to 7.30. An infrared differential interference contrast (IR-DIC) and band pass (515-565 nm) filter was used to target GFP+ and mCitrane+ cells located along the extent of the cut surface of the spinal cord. Intracellular signals from all cells were amplified, digitized and acquired on a PC.

Fictive locomotion was induced in upright spinal cords, as well as intact spinal cords isolated from newborn WT1^{CreER};R26-LSL-Gi-DREADD, or wildtype littermates (which were simply isolated and pinned in a recording chamber) via addition of N-methyl-D-aspartate (NMDA, 5 μM) and 5-hydroxytryptamine creatine sulfate complex (5-HT, 5-15 μM) to the perfusate. In the intact spinal cord fictive locomotor activity was monitored via electroneurogram (ENG) recording acquired from bipolar suction electrodes positioned on one, two or three of the flexor-related (L1-L3) and extensor-related (L5) lumbar ventral roots. For the upright spinal cord preparation fictive locomotor activity was recorded from ventral roots at the level of the transverse cut- typically L3. The ENG signals were amplified, filtered, digitized and recorded on a PC. For fictive locomotor experiments on WT1^{CreER};R26-LSL-Gi-DREADD mice increasing concentrations (500nM, 10 μM, 100 μM) of clozapine N-oxide (CNO, Cayman Chemical, Ann Arbor, MI) were added to the perfusate after a minimum of 5 minutes of stable fictive locomotion. Each concentration was applied for 30 min and no measurements were made for at least 10 min after a new concentration was applied to allow sufficient time for the drug to penetrate the preparation. For patch clamp experiments CNO was applied after the resting membrane potential remained stable for 2 minutes. Since we were investigating the effect of

CNO on cells located just below the cut surface of the spinal cord each concentration was applied for 5 minutes before washing.

Retrograde dextran tracing. Newborn (P0) Wt1^{CreGFP} or wildtype mice were anesthetized and spinal cords were dissected out in oxygenated artificial cerebrospinal fluid (aCSF). A unilateral cut was made into the ventral spinal cord at the L2 segment and tetramethylrhodamine dextran (TMRD) crystals were inserted using insect pins. Spinal cords were then incubated in oxygenated aCSF for 16 -18 hours at room temperature. Following incubation, the tissue was fixed overnight with 4% PFA in 0.1 M PBS and processed for immunohistochemistry using antibodies to GFP (Wt1^{CreGFP} mouse) or WT1 (wildtype mouse), TMRD was visible without an antibody.

Data Analysis and Statistics. For immunohistochemical experiments all cell counts were carried out using the Cell Counter plugin in Image J (ImageJ, RRID:SCR_003070). All means are reported ± standard deviation (SD) and comparisons between means were made using t-tests, a one-way ANOVA, or Hotelling's paired test. For all statistical tests a p value ≤ 0.05 was used to determine statistical significance. In fictive locomotor experiments circular statistics (Zar, 1974) were used to probe the coupling strength between flexor and extensor related ventral roots or between the WT1 cell and the ventral roots. In order to generate polar plots 25 consecutive bursts in a given ventral root were selected, and their phase values were calculated in reference to each of the other ventral roots (for whole cell recordings phase values were calculated in reference to bursts recorded in the WT1 neuron). Mean phase values of 0.5 indicated the bursts being compared were completely out of phase (i.e. alternating), whereas mean phase values of 1 indicated the bursts were completely in phase (i.e. synchronous). r values, which provide a measure of the concentration of phase values around the mean, were also calculated. An r value

of 1 indicates all 25 phase values measured were identical, whereas an r value of 0 indicates the phase values were distributed randomly (Kjaerulff and Kiehn 1996). Hotelling's paired test was used to pool the data from all wildtype and all WT1[CreER];R26-LSL-Gi-DREADD mice and probe for significant differences between experimental conditions (Control, 10μM, 100μM, Wash).

qPCR. The mRNA expression level of WT1 in the adult human spinal cord was assessed using a pooled cDNA sample from 12 male/ female Caucasians, ages 18-56 (Clontech, Mountain View, CA). We also assessed the expression level of MNX1 as a marker of motoneurons (Ross et al. 1998), and used 18S as a reference gene. The following gene-specific primer sequences were used: WT1 forward: 5'-CGC ACG GTG TCT TCA GAG G-3', and reverse: 5'-CCT GGG TAA GCA CAC ATG AAG G-3' (amplicon = 118 bp); MNX1 forward: 5'-CTC ATG CTC ACC GAG ACC CA-3', and reverse: 5'-GCC CTT CTG TTT CTC CGC TT-3' (amplicon = 114 bp); 18S forward: 5'-CGG ACA GGA TTG ACA GAT TGA TAG C-3', and reverse: 5'-CGT TCG TTA TCG GAA TTA ACC AGA C-3' (amplicon = 107 bp). Quantitative PCR was performed using a QuantStudio 3 Real-time PCR system (ThermoFisher Scientific, Hampton, NH), with a SYBR Green I master mix, according to the manufacturer's protocol. The target gene expression ratio was calculated using the $2^{\Delta\Delta Ct}$ method. PCR products were run on a 1.2% agarose gel using standard methods to ensure the amplicon was of the predicted size.

3.3 Results.

WT1-expressing neurons are located in the ventromedial spinal cord.

Initial experiments were designed to map the development of WT1-expressing neurons in the mouse spinal cord and compare the number and location of these cells to the genetically-related DMRT3-expressing subpopulation of dI6 cells. In line with previous reports (Armstrong et al. 1993) expression of WT1 was first observed between E11 and E12 in the mouse (see

Figure 3.1A), shortly after expression of DMRT3, which can be seen at E10.5 (Andersson et al. 2012). By E13.5 WT1-expressing neurons began to migrate ventrally, and by E15.5 they had taken up their settling position in the ventromedial spinal cord where they remained postnatally (Figure 3.1A, n=3 spinal cords for E11.5, E13.5, E15.5, n=6 for P0). The position of all cells expressing DMRT3 and WT1 at P0 was analyzed in the lumbar segments of 6 spinal cords and plotted in reference to the central canal. DMRT3-expressing cells were distributed throughout the ventromedial spinal cord and most densely clustered in the dorsal aspect of this region around the level of the central canal, while the WT1-expressing cells were located more ventrally (Figure 3.1B). Analysis of the total number of cells along the extent of the lumbar spinal cord (Figure 3.1C) indicated that significantly fewer WT1+ cells were located in each 20 μm section when compared to the DMRT3+ population (WT1= 24.4 ± 5.8 cells, DMRT3= 34.8 ± 4.0 cells, df=33, t=6.18, p = 0.0013).

Interestingly, previous work has shown that the development and migration pattern of WT1-expressing neurons in the embryonic mouse spinal cord is recapitulated in the human embryo, and cells expressing WT1 can be seen in the ventromedial spinal cord of humans up to 74 d.p.c., a time point equivalent to E15 in the mouse (Armstrong et al. 1993). Since this study did not investigate postnatal tissue we were curious to determine whether WT1-expression in spinal interneurons was maintained at later developmental time points. Expression in both mouse and humans postnatally could lead to experiments which investigate whether these cells are functionally homologous in the two species. Initial experiments investigated whether WT1 was expressed in the mature mouse nervous system. For these experiments an antibody stain for WT1 and the neuronal marker NeuN was carried out in P28 wildtype mice, an age at which the nervous system has reached maturity (Finlay and Darlington, 1995), and also in 3 month old

mice- a time point at which the mouse can be considered to have reached adulthood. Inspection of 3 spinal cords at each of these time points indicated that WT1 neurons are present as WT1+/NeuN+ cells could be seen in the ventromedial aspect of all sections examined (mean$_{P28}$ 18.8 ± 4.3, mean$_{3month}$ 15.2 ± 3.9, Figure 3.1D). To investigate whether WT1 expression persists in the human spinal cord we performed quantitative PCR using a commercially-available pooled cDNA sample from spinal cords harvested from 12 adults aged 18 to 56. In addition to probing for WT1 we assessed the expression level of the human motor neuron marker MNX1 (Ross et al. 1998), and used 18S as a reference gene. Analysis indicated that both WT1 and MNX1 were expressed at similar levels relative to the reference gene (Fig. 1E) indicating that WT1 is expressed in the adult human spinal cord. Further support for this finding came from an antibody stain for WT1 in paraffin sections cut from the lumbar region of an adult human spinal cord (32 year old male) in which WT1+ labelling was present and could be seen primarily in the ventral region of all sections inspected (73.3% of all WT1 cells were located below the central canal, Figure 3.1F). While we were unable to confirm that these cells were neurons via antibody staining techniques, these findings along with the qPCR results suggests that WT1 cells are present in the human spinal cord and may reside in a similar location in both mouse and human.

WT1-expressing neurons are primarily inhibitory and project commissural axons.

To investigate the neurotransmitter phenotype of WT1-expressing interneurons we first stained transverse spinal cord sections cut from VGlut2^{Cre};ROSA26^{tdTomato} mice in which all excitatory cells expressed reporter protein, and looked for co-expression of WT1 and tdTomato. Excitatory WT1+ cells were extremely rare and comprised only 1.8% of the entire WT1+ population (2/111 WT1 cells, n=2 spinal cords, Figure 3.2A). Inhibitory WT1+ neurons were identified either by co-expression of WT1 and an antibody for glycine, or by co-expression of

WT1 and GFP in spinal cord sections cut from the GAD67^{GFP} mouse in which all GABAergic neurons express GFP. Results confirmed that this subset of dI6 cells is primarily inhibitory as 68.7% (66/96, n=3 spinal cords) of all WT1-expressing neurons co-expressed the GABAergic marker (Figure 3.2B) and 34.7% (32/92, n=3 spinal cords) of all WT1-expressing neurons stained positive for glycine (Figure 3.2C).

To broadly define the projection pattern of WT1+ axons backfill experiments were performed in which the fluorescent tracer tetra-methyl-rhodamine-dextran (TMRD) was applied to a cut region of the neonatal spinal cord (n=8) unilaterally which results in all processes passing through this region taking up the tracer and transporting it back to their soma (Figure 3.3A, 3.3B, Stokke et al. 2002). Following a 16-18 hour incubation period, transverse sectioning, and antibody staining for WT1, analysis of the spinal cords indicated that the mean number of WT1+/TMRD+ cells in each spinal cord located on the contralateral side of the spinal cord to the application site (mean$_{comm}$) was significantly greater than the mean number on the ipsilateral side (mean$_{ipsi}$) indicating that this population preferentially extends commissural axons (mean$_{comm}$=29.8 ± 9.7, mean$_{ipsi}$= 8.4 ± 4.31, df=14, t=4.07, p=0.0006, t-test, Figure 3.3C). There was no preference as to the mean number of WT1+/TMRD+ cells in each spinal cord located rostral (mean$_{rostral}$) or caudal (mean$_{caudal}$) to the application site (mean$_{rostral}$=21.4 ± 9.6, mean$_{caudal}$= 16.9 ± 7.8, df=14, t=0.87, p=0.20, t-test) with soma expressing TMRD labelled WT1+ neurons found up to 1800um (approximately 3 spinal segments) in both the rostral and caudal directions.

WT1-expressing neurons are rhythmically active during fictive locomotion.

Along with the DMRT3 subset of dI6 interneurons and the V0$_D$ population our initial findings indicate that the WT1 interneurons are the third molecularly-defined population of commissurally projecting, inhibitory interneurons in the mouse spinal cord. To determine

whether, similar to DMRT3+ and V0$_D$ interneurons, WT1-expressing neurons participate in locomotor activity we recorded from these cells during pharmacologically-induced fictive locomotion in the neonatal mouse spinal cord and investigated their activity in relation to flexor and extensor motor axons that innervate hindlimb muscles. For these experiments we utilized neonatal (P0-P2) WT1^{CreGFP} mice (Figure 3.4A). Analysis of the thoracolumbar spinal cords of 4 WT1^{CreGFP} mice indicated that while GFP labeled slightly more than half of all WT1-expressing spinal neurons (460/836), reporter protein expression is restricted to WT1-expressing cells as 99.1% (456/460) of GFP+ cells were WT1+ (Figure 3.4B). To record activity from GFP-expressing WT1 neurons during fictive locomotion the upright spinal cord preparation was used in which spinal cords from WT1^{CreGFP} mice were isolated, bent at a 90-degree angle so that the caudal end of the cord was facing upwards, and a transverse section was cut with a vibratome at a mid-lumbar segment. The preparation was then situated below the objective lens of a fluorescent microscope which allowed all GFP+ WT1 neurons along the cut surface to be visually identified for patch clamp recording (Figure 3.4C). Bath application of 5-HT (5μM) and NMDA (5-15μM) evoked rhythmic, alternating fictive locomotor activity which was recorded by extracellular electroneurogram (ENG) electrodes attached to one or two of the lumbar ventral roots on either side of the spinal cord, and GFP+ WT1 neurons were targeted for whole cell recording (Figure 3.4D). Activity from WT1-expressing interneurons was strikingly consistent with all 16 neurons from which we recorded exhibiting clear rhythmic oscillations relative to the ventral roots (Figure 3.4E) suggestive of involvement in locomotion. Eight of the 16 WT1+ cells were active in phase with ENG activity recorded from the ipsilateral ventral root in the same spinal segment, and the remaining eight oscillated in phase with the contralateral ventral root in the same spinal segment (Figure 3.4F).

Silencing of WT1+ spinal neurons disrupts left-right alternation during fictive locomotion.

To investigate the specific role WT1-expressing neurons play during locomotion we reversibly silenced this population and probed for deficits that are apparent in their absence. Given the expression of WT1 throughout the body (Armstrong et al. 1993), it was necessary to restrict the silencing of this population to the spinal cord since widespread ablation of WT1 cells results in early embryonic lethality. Ultimately we determined that the best approach was to use the R26-LSL-Gi-DREADD transgenic mouse in which an inhibitory DREADD (the mutant G protein-coupled receptor hM4Di) is present in all Cre expressing cells following recombination (Zhu et al. 2016). By performing experiments on spinal cords isolated from offspring of R26-LSL-Gi-DREADD x WT1^{CreER} matings we were able to inhibit the activity in WT1-expressing spinal neurons by adding the hM4Di receptor ligand clozapine-N-oxide (CNO) to the perfusate.

To confirm the DREADD system effectively inhibited WT1 neurons we isolated spinal cords from P0 WT1^{CreER};R26-LSL-Gi-DREADD mice and used the upright spinal cord preparation to record from mCitrane+ (co-expressed in all cells carrying the DREADD) neurons. Initial inspection revealed that these neurons were clearly visible under a fluorescent microscope and restricted to the ventromedial laminae (Figure 3.5A). Upon whole cell recording we applied an identical train of current steps before and after bath application of CNO. All three mCitrane+ cells from which we recorded were clearly inhibited in the presence of 500nM of CNO as a greater amount of current injection was required to evoke action potentials compared to the control condition and there was a mean reduction (to 43.7% ± 12.2% compared to the control condition) in the total number of action potentials evoked over the duration of the train of current steps which was partially reversed upon washout (to 72% ± 8.7% of control, Figure 3.5B). In contrast the mean number of action potentials evoked over the train of current steps in three

mCitrane- cells in the presence of 500nM of CNO was similar to control (97.7% ± 3.5%, 95.7% ± 2.4% after washout) and the amount of current injection required to evoke action potentials was unchanged (Figure 3.5B). Taken together this data allows us to conclude that CNO selectively inhibits cells expressing the DREADD.

Spinal cords from six P0-P2 wildtype and six WT1^{CreER};R26-LSL-Gi-DREADD mice were isolated and perfused with oxygenated artificial cerebrospinal fluid. Bath application of a cocktail of NMDA (5μM) and 5-HT (10μM) evoked fictive locomotion in each spinal cord which was recorded via ENG electrodes attached to three of the flexor-related or extensor-related ventral roots bilaterally. After recording a minimum of 5 minutes of stable fictive locomotor activity which would act as baseline, CNO was added to the perfusate at increasing concentrations (10 μM, 100 μM). A comparison of cycle period (CP- defined as the interval between the onset of burst n and burst n+1) indicated that there was no significant change in the frequency of locomotor outputs (df=5, F=0.85, p=0.49, one way ANOVA) between the control and CNO conditions in either the wildtype (CP$_{control}$= 2.7s ± 1.1s, SCP$_{CNO-100}$= 2.6s ± 0.7s) or WT1^{CreER}xR26-LSL-Gi-DREADD (CP$_{control}$= 3.1s ± 0.7s, CP$_{CNO-100}$= 3.2s ± 0.6s, n=6) mice.

Circular statistics were used to analyze the coordination of flexor and extensor related ventral root bursting during fictive locomotion. For each of the 6 wildtype and 6 WT1^{CreER}xR26-LSL-Gi-DREADD spinal cords we generated a polar plot in each condition (control, 10 μM CNO, 100 μM CNO, wash) which provided us with information on coupling strength between the ipsilateral and contralateral ventral roots (Kjaerulff and Kiehn, 1996). While Figure 3.5 displays data from a single wildtype (panels C-D) and a single WT1^{CreER}xR26-LSL-Gi-DREADD (panels E-H) spinal cord, Hotelling's paired test was used to pool the circular data from the 6 wildtype mice and the 6 mice expressing the DREADD and determine whether there

were significant differences in coupling strength between conditions. As expected, alternation could be seen between contralateral flexor (or contralateral extensor)-related (mean $r_{control}$= 0.94± 0.05, mean $r_{100-CNO}$= 0.89 ± 0.06) and ipsilateral flexor/extensor-related (mean $r_{control}$= 0.91± 0.04, mean $r_{100-CNO}$= 0.87 ± 0.10) ventral roots in wildtype mice (Figure 3.5C, 3.5D) and this was unaffected after application of 100 μM CNO (F_{contra}=0.13, p=0.89, F_{ipsi}=0.10, p=0.92, Figure 3.5C, 3.5D). Application of 10 μM CNO to spinal cords isolated from WT1^{CreER}xR26-LSL-Gi-DREADD mice resulted in disrupted alternation (F=6.4, p= 0.05, n=6, Figure 3.5E, 3.5F) between pairs of flexor-related (or pairs of extensor-related) ventral roots located on either side of the spinal cord when compared to control (mean $r_{control}$=.91±0.06, mean r_{10-CNO}=0.66±0.20). The fictive locomotor pattern in the presence of CNO was marked by alternation of ENG activity in extensor-related (or flexor-related) ventral roots on either side of the spinal cord which was regularly interrupted by periods of co-bursting (see * in Figure 3.5F-3.5H). Alternation between ipsilateral flexor and extensor ventral roots on the other hand, was not statistically altered ($r_{control}$=.93±0.02, r_{10-CNO}=0.91±0.05, $r_{100-CNO}$=0.87±0.06, r_{wash}=0.86±0.15, F=2.3, p=0.25, n=5, Figure 3.5E, 3.5F). Increasing the concentration of CNO (100 μM) resulted in further deterioration of contralateral alternation mean $r_{100-CNO}$=0.39±0.19 compared to the control condition (F=12.6, p=0.02, Figure 3.5G) in WT1^{CreER}xR26-LSL-Gi-DREADD mice, while alternation between ipsilateral flexor and extensor related ventral roots (mean $r_{100-CNO}$=0.87±0.06) remained statistically similar to the control condition (F=3.2, p= 0.18, Figure 3.5G). Following 30 min of washout of CNO (in aCSF containing baseline levels of 5-HT and NMDA) the activity of contralateral ventral roots became more tightly coupled, approached alternation (r_{wash}=0.81±0.11), and were not significantly different than the control condition (F=5.7, p=0.07, Figure 3.5H). Taken together these data indicate that inhibition of WT1-

expressing interneurons during a locomotor task results in a specific and severe breakdown of left-right alternation.

WT1 neurons terminate in close proximity to populations of commissural interneurons.

The two previously identified populations of commissurally projecting inhibitory interneurons (DMRT3+ dI6, and V0$_D$ neurons) have both been shown to make monosynaptic connections onto motoneurons (Lanuza et al. 2004; Andersson et al. 2012). To determine whether WT1-expressing neurons also regulate alternation of motor neurons in the spinal cord via a monosynaptic pathway we injected the retrograde transynaptic tracer pseudorabies virus 152 (PRV-152) into a hindlimb flexor (TA, n=4) or extensor (GC, n=4) muscle of eight P0 wildtype mice. Previous work has shown that this strain of PRV infects (and expresses GFP in) cells monosynaptically connected to hindlimb motoneurons 36-46 hours after intramuscular injection in neonatal mice (Jovanovic et al. 2010). Inspection of spinal cords harvested from all animals within this time window exhibited extensive GFP labeling of neurons in the ventral laminae ipsilateral to the injection as well as a modest number of cells (typically 5-15) in lamina VIII contralaterally. This pattern of staining is consistent with other studies which have used PRV (Lanuza et al. 2004; Zhang et al. 2008; Jovanovic et al. 2010) or rabies virus (Stepien et al. 2010) to identify interneurons that are monosynaptically connected to hindlimb motoneurons. The complete absence of GFP+ WT1-expressing neurons on either side of the spinal cord in any of the 8 mice indicates that this subset of dI6 cells is not monosynaptically connected to motoneurons (Figure 3.6A) and thus has a unique connectivity pattern when compared to the V0$_D$ and DMRT3+ subpopulations.

In an attempt to identify potential synaptic partners of WT1+ neurons we utilized offspring of WT1$^{\text{CreER}}$ x ROSA26$^{\text{tdtomato}}$ mice in which cell bodies and processes of WT1+ neurons

express the reporter protein tdTomato, and are visible (Figure 3.6C-3.6E). Transverse spinal cord sections were cut from these mice, and antibodies were used to identify four genetically-defined interneuronal populations that have been shown to be involved in locomotor activity: the ipsilaterally-projecting V2a (Chx10-expressing) and V1 (En1-expressing) cells as well as the contralaterally-projecting $V0_V$ neurons (Evx1-expressing) and the DMRT3+ dI6 cells. WT1-expressing neurons with axons terminating in close proximity to the soma of these cell populations were identified via co-localization of an antibody for synaptotagmin, which labels a Ca^{2+} sensor in presynaptic terminals, and tdTomato+ processes located on the "halo" surrounding a labeled nucleus (Figure 3.6B). Analysis of 4 WT1^{CreER};ROSA26^{tdtomato} spinal cords revealed that terminals from WT1 cells were absent on the soma of V2a cells (0/14 cells inspected, Figure 3.6C), and rarely observed on the soma of En1 cells (the soma of 2/14 En1 cells received terminals from WT1+ neurons, Figure 3.6D). In contrast WT1+ terminals were regularly found in close apposition to Evx1 (9/12 cells inspected, Figure 3.6E) and DMRT3 (16/20 cells inspected, Figure 3.6F) expressing cells suggestive of connectivity amongst these locomotor-related interneuronal populations.

3.4 Discussion

While the dorsal and ventral subsets of Dbx1-expressing V0 interneurons have been shown to be key regulators of left-right alternation during locomotion (Lanuza et al. 2004; Talpalar et al. 2013) it is becoming apparent that additional interneuronal populations are involved in this function either by direct contact onto motoneurons (Andersson et al. 2012), or via modulation of the V0 neurons (Crone et al. 2008). In this study we characterize the WT1-expressing subset of dI6 interneurons. Based on their neurotransmitter phenotype, axonal projection pattern, and the clear disruption of left-right alternation that occurs when they are selectively inhibited, we

provide evidence that WT1 interneurons are essential for appropriate left-right alternation during locomotion, likely via the regulation of other populations of commissural interneurons.

WT1 neurons are required for coordinated locomotor activity.

We were unable to assess the locomotor pattern of intact mice in the absence of WT1-expressing neurons since there is widespread expression of WT1 throughout the body (Armstrong et al. 1993) and manipulation of this gene results in early embryonic lethality. To circumvent this issue, the role of WT1-expressing neurons during locomotor activity was studied by performing fictive locomotor experiments in neonatal mice in which an inhibitory DREADD was expressed in WT1+ neurons which enabled selective and reversible silencing of these cells. This approach eliminated compensatory changes in network organization which may occur if the cells were to be ablated at earlier time points, and it also allowed us to analyze locomotor activity prior to application, and after washout, of CNO and use these epochs as control conditions for each mouse. In the presence of CNO the locomotor output from WT1^{CreER}xR26-LSL-Gi-DREADD mice was characterized by a significant disruption of contralateral coordination which became more severe with the application of an increased concentration of CNO and was reduced upon washout. Recently it has been demonstrated that systemically administered CNO can be metabolized to clozapine which binds to endogenous receptors and can have non-specific actions on neurons (Gomez et al. 2017). It is unlikely that this phenomenon is responsible for the locomotor phenotype seen in our study since CNO was directly applied to the spinal cord and had an effect over a short period of time whereas clozapine metabolism and effect typically takes 2-3 hours (Gomez et al. 2017). More importantly, electrophysiological recordings demonstrate a selective inhibition of cells carrying the DREADD in the presence of CNO.

Anatomical tracing experiments indicated that WT1-expressing cells do not contact motoneurons monosynaptically but regularly terminate in close proximity to the DMRT3 subset of dI6 neurons as well as Evx1-expressing V0 neurons, two populations shown to be involved in coordinating locomotor outputs. It is important to keep in mind that these experiments do not enable us to definitively conclude that these populations are synaptic partners however the presence of axon terminals from WT1 neurons on the soma surrounding Evx1 and DMRT3 nuclei combined with the fact that these terminals were seldom seen on soma surrounding En1 or Chx10 cells provide compelling evidence that these predominantly commissural populations may be interconnected. Taken together the results of these experiments provide novel insight into the manner in which populations of commissural interneurons may interact with one another. The only known synaptic contacts of the inhibitory DMRT3-expressing cells are motoneurons bilaterally (Andersson et al. 2012), while Evx1-expressing V0 neurons are excitatory (Talpalar et al. 2013) and presumed to activate interneurons on the contralateral side of the spinal cord which in turn inhibit local motoneurons (Shevtsova et al. 2015; Danner et al. 2017). Given our finding that the vast majority (>80%) of WT1+ neurons are inhibitory and a similar proportion project commissural axons we provide evidence that WT1+, DMRT3+, and Evx1+ cells are part of a microcircuit across the midline which is involved in regulating motoneuronal activity during locomotion.

WT1-expressing cells regulate the activity of commissural interneuron subtypes.

In our proposed circuit diagram of the locomotor CPG (Figure 3.7), we incorporate the WT1-expressing and DMRT3-expressing dI6 neurons into a previously devised wiring diagram that was assembled based on experimental and modeling data (Shevtsova et al. 2015). We suggest that WT1+ cells on the left side of the spinal cord project to, and inhibit, DMRT3+ dI6

and V0$_V$ cells on the right side of the spinal cord which in turn inhibit motor neurons on the left side either monosynaptically (DMRT3+) or di-synaptically (V0$_V$). In this arrangement activation of WT1-expressing neurons on the left side of the spinal cord release motoneurons on the left from contralateral inhibition via regulation of these two commissural interneuronal populations.

The circuitry proposed in Figure 3.7 can account for the locomotor defects observed during fictive locomotion when WT1-expressing neurons are inhibited. Specifically, since ablation of the DMRT3 neurons results in dissociation between activity in contralateral ventral roots (Andersson et al. 2012) we would expect inappropriate regulation of DMRT3-expressing neurons to have a similar effect. Conversely, we would not expect the V0$_V$ cells to be involved in left-right alternation in our experiments since it has been shown that the V0$_D$ subset are primarily responsible for appropriate left/right alternation at the slower fictive locomotor speeds evoked in these experiments while the V0$_V$ cells, which are required at higher frequencies, would presumably be inactive. While lack of a postnatal marker of the V0$_D$ population kept us from investigating their potential connectivity (as well as the connectivity of the locomotor-related V2b and V3 populations) with WT1-expressing neurons, it is possible that they also receive input from WT1+ cells which regulate activity in different subsets of the V0 population at different speeds. We must keep in mind that evidence suggesting connectivity between populations does not indicate exclusivity, and WT1+ neurons may contact several other cell populations (i.e. rhythm generating cells of the locomotor CPG) however we have left these connections out of our schematic as we currently have no supporting experimental evidence.

Given technical limitations inherent with large scale mapping of the spinal cord our knowledge regarding the connectivity amongst various populations of genetically defined interneurons shown to be involved in locomotion is limited, and the majority of the previously

described connections amongst components are based on deductive reasoning or computational modeling (dashed lines in Figure 3.7) as opposed to direct experimental evidence (solid lines in Figure 3.7). In fact, other than synapses on $V0_V$ cells from V2a interneurons, our demonstration of WT1+ terminals in close proximity to $V0_V$ and DMRT3+ cells is the only experimental evidence suggestive of synaptic connectivity amongst groups of genetically-defined interneurons that are active during locomotion. Based on the dearth of experimental evidence for connectivity amongst the genetically-defined interneuronal populations we believe that our tracing data marks a significant step forward in our understanding of the network structure of the locomotor CPG.

WT1-expression in the spinal cord is conserved between the mouse and human.

In this study we demonstrate that WT1 is expressed in the spinal cord of adult humans as well as mice. This builds on previous work showing that WT1 is expressed in spinal interneurons located in the ventromedial laminae of both mouse (E15) and human (74 d.p.c.) embryos (Armstrong et al. 1993). There is now substantial evidence (Dimitrijevic et al. 1998; Yang and Gorassini 2006; Dominici et al. 2011; Angeli et al. 2014; Guertin et al. 2014; Danner et al. 2015) that a locomotor CPG in the human spinal cord exists, and based on the role that WT1+ neurons play in coordinating left-right alternation in the mouse spinal cord it is tempting to suggest that they may also be a key component of the locomotor network in humans. While the generation of cell types in the CNS and their assembly into functional neural circuits in all species is achieved through precise regulation of spatiotemporal gene expression (Nord et al. 2015; Shibata et al. 2015), vast differences have been shown to exist between the function of genes that are expressed in both mice and humans (Liao and Zhang 2008), and functional homology of a gene can not be presumed (Silbereis et al. 2017) nevertheless WT1-expressing cells are the first genetically defined interneuronal population involved in murine locomotion that can be mapped

to the human spinal cord providing support that this experimental approach can potentially provide insight into the mechanisms of motor control in humans.

Conclusion

It is becoming clear that the circuitry responsible for coordination of motor pools across the midline requires precise modulation and regulation in order to switch seamlessly between the different gait patterns that predominate at various locomotor speeds (Bellardita and Kiehn, 2015). Here we begin to unravel the neural circuitry connecting these interneuronal populations to one another and demonstrate that the WT1-expressing subset of dI6 cells are an essential component of the locomotor network which appear to work in concert with several other cell types to precisely regulate motor neuronal activity during stepping. Despite potential species specific differences in gene function between the mouse and human our finding that WT1-cells exist in adult humans suggests that work in the mouse spinal cord may have relevance when studying motor control in more evolved species. Although we are cautious in suggesting a similar role for WT1-expressing neurons in bipedal locomotion, the fact that these cells are present in humans raises the possibility that their function can be investigated and, if found to be involved in motor control, they could potentially represent a target for therapeutic intervention after spinal cord injury.

REFERENCES

Andersson LS, Larhammar M, Memic F, Wootz H, Schwochow D, Rubin, CJ, Patra K, Arnason T, Wellbring L, Hjalm G, Imsland F, Petersen JL, McCue ME, Mickelson JR, Cothran G, Ahituv N, Roepstorff L, Mikko S, Vallstedt A, Lindgren G, Andersson, Kullander K. (2012) Mutations in DMRT3 affect locomotion in horses and spinal circuit function in mice. Nature. 488:642-646.

Angeli, CA, Edgerton, VR, Gerasimenko, YP, Harkema, SJ. (2014). Altering spinal cord excitability enables voluntary movements after chronic complete paralysis in humans. Brain 137:1394–409.

Armstrong JF, Pritchard-Jones K, Bickmore WA, Hastie ND, Bard JB. (1993). The expression of the Wilms' tumour gene, WT1, in the developing mammalian embryo. Mech Dev. 40:85-97.

Bellardita C, Kiehn O. (2015). Phenotypic characterization of speed-associated gait changes in mice reveals modular organization of locomotor networks. Curr Biol. 25:1426-1436.

Butt SJ, Kiehn O 2003. Functional identification of interneurons responsible for left-right coordination of hindlimbs in mammals. Neuron 38: 953-963.

Crone SA, Quinlan KA, Zagoraiou L, Droho S, Restrepo CE, Lundfald L, Endo T, Setlak J, Jessell TM, Kiehn O, Sharma K. (2008). Genetic ablation of V2a ipsilateral interneurons disrupts left-right locomotor coordination in mammalian spinal cord. Neuron. 60:70-83.

Danner, SM, Hofstoetter, US, Freundl, B, Binder, H, Mayr, W, Rattay, F, Minassian, K. (2015). Human spinal locomotor control is based on flexibly organized burst generators. Brain 138:577–588.

Danner SM, Shevtsova NA, Frigon A, Rybak IA. (2017). Computational modeling of spinal circuits controlling limb coordination and gaits in quadrupeds. eLife. pii:e31050.

Dimitrijevic, MR, Gerasimenko, Y, Pinter, MM. (1998). Evidence for a spinal central pattern generator in humans. Ann N Y Acad Sci 860:360–76.

Dougherty KJ, Zagoraiou L, Satoh D, Rozani I, Doobar S, Arber S, Jessell TM, Kiehn O. (2013) Locomotor rhythm generation linked to the output of spinal shox2 excitatory interneurons. Neuron. 80:920-933.

Dominici, N, Ivanenko, YP, Cappellini, G, d'Avella, A, Mondì, V, Cicchese, M, Fabiano, A, Silei, T, Di Paolo, A, Giannini, C, Poppele, RE, Lacquanti, F. (2011). Locomotor primitives in newborn babies and their development. Science 334:997–9.

Gomez JL, Bonaventura J, Lesniak W, Mathews WB, Sysa-Shah P, Rodriguez LA *et al* (2017). Chemogenetics revealed: DREADD occupancy and activation via converted clozapine. Science 357: 503–507.

Goulding, M 2009. Circuits controlling vertebrate locomotion: moving in a new direction. Nat. Rev. Neurosci. 10:507-518.

Goulding M, Bourane S, Garcia-Campmany L, Dalet A, Koch S. (2014). Inhibition down under: an update from the spinal cord. Curr Opin Neurobiol. 26 161-166.

Griener A, Zhang W, Kao H, Haque F, Gosgnach S. (2017). Anatomical and electrophysiological characterization of a population of dI6 interneurons in the neonatal mouse spinal cord. Neuroscience. 362:47-59.

Gross, MK, Dottori, M, Goulding, M (2002). Lbx1 specifies somatosensory association interneurons in the dorsal spinal cord. Neuron 34:535–549.

Guertin, PA. (2014). Preclinical evidence supporting the clinical development of central pattern generator-modulating therapies for chronic spinal cord-injured patients. Front Hum Neurosci 8:272.

Jovanovic K, Pastor AM, O'Donovan MJ. (2010). The use of PRV-Bartha to define premotor inputs to lumbar motoneurons in the neonatal spinal cord of the mouse. PLoS One. 5:e11743.

Kerman, I.A., Enquist, L.W., Watson, S.J., and Yates, B.J. (2003). Brainstem substrates of sympatho-motor circuitry identified using trans-synaptic tracing with pseudorabies virus recombinants. J. Neurosci. 23, 4657–4666.

Kiehn, O (2006). Locomotor circuits in the mammalian spinal cord. Ann. Rev. Neurosci. 29:279-306.

Kiehn O. (2016). Decoding the organization of spinal circuits that control locomotion. Nat Rev Neurosci. 17:224-238.

Kjaerulff, O., and Kiehn, O. (1996). Distribution of networks generat- ing and coordinating locomotor activity in the neonatal rat spinal cord in vitro: a lesion study. J. Neurosci. 16, 5777–5794.

Lanuza GM, Gosgnach S, Pierani A, Jessell TM, Goulding M 2004. Genetic identification of spinal interneurons that coordinate left-right locomotor activity necessary for walking movements. Neuron 42:375–386.

Liao BY, Zhang J. (2008). Null mutations in human and mouse orthologs frequently result in different phenotypes. Proc Natl Acad Sci USA 105:6987-6992.

Muller, T, Brohmann, H, Pierani, A, Heppenstall, AP, Lewin, GR, Jessell, TM, Birchmeier, C (2002). The homeodomain factor Lbx1 distinguishes two major programs of neuronal differentiation in the dorsal spinal cord. Neuron 34, 551–562.

Quinlan KA, Kiehn O. 2007. Segmental, synaptic actions of commissural interneurons in the mouse spinal cord. J. Neurosci 27:6521-6530.

Ross A. J., Ruiz-Perez V., Wang Y., Hagan D.-M., Scherer S., Lynch S. A., Lindsay S., Custard E., Belloni E., Wilson D. I., et al. (1998). A homeobox gene, HLXB9, is the major locus for dominantly inherited sacral agenesis. Nature 20, 358-361.

Shevtsova NA, Talpalar AE, Markin SN, Harris-Warrick RM, Kiehn O, Rybak IA. (2015). Organization of left-right coordination of neuronal activity in the mammalian spinal cord: Insights from computational modelling. J Physiol. 593:2403-2426.

Silbereis JC, Pochareddy S, Zhu Y, Li M, Sestan N. (2016). The Cellular and Molecular Landscapes of the Developing Human Central Nervous System. Neuron. 89:248-68.

Stepien AE, Tripodi M, Arber S. (2010) Monosynaptic rabies virus reveals premotor network organization and synaptic specificity of cholinergic partition cells. Neuron. 68:456-472

Stokke, M.F., Nissen, U.V., Glover, J.C. and Kiehn, O. (2002) Projection patterns of commissural interneurons in the lumbar spinal cord of the neonatal rat. J Comp Neurol. 446, 349-359.

Talpalar AE, Bouvier J, Borgius L, Fortin G, Pierani A, Kiehn O. 2013. Dual-mode operation of neuronal networks involved in left-right alternation. Nature. 500:85-88.

Vallstedt A, Kullander K. (2013). Dorsally derived spinal interneurons in locomotor circuits. Ann NY Acad Sci. 1279:32-42.

Yang, JF, Gorassini, M. (2006). Spinal and brain control of human walking: implications for retraining of walking. Neuroscientist 12:379–89.

Zar, J.H. (1974) Circular Distribution. In "Biostatistical Analysis", p310-327. Prentice Hall, Engelwood Cliffs, NJ.

Zhang Y, Narayan S, Geiman E, Lanuza GM, Velasquez T, Shanks B, Akay T, Dyck J, Pearson K, Gosgnach S, Fan CM, Goulding M. (2008) V3 spinal neurons establish a robust and balanced locomotor rhythm during walking. Neuron. 60:84-96.

Zhu H, Aryal DK, Olsen RH, Urban DJ, Swearingen A, Forbes S, Roth BL, Hochgeschwender, U. (2016). Cre-dependent DREADD (Designer Receptors Exclusively Activated by Designer Drugs) mice. Genesis. 54:439-446.
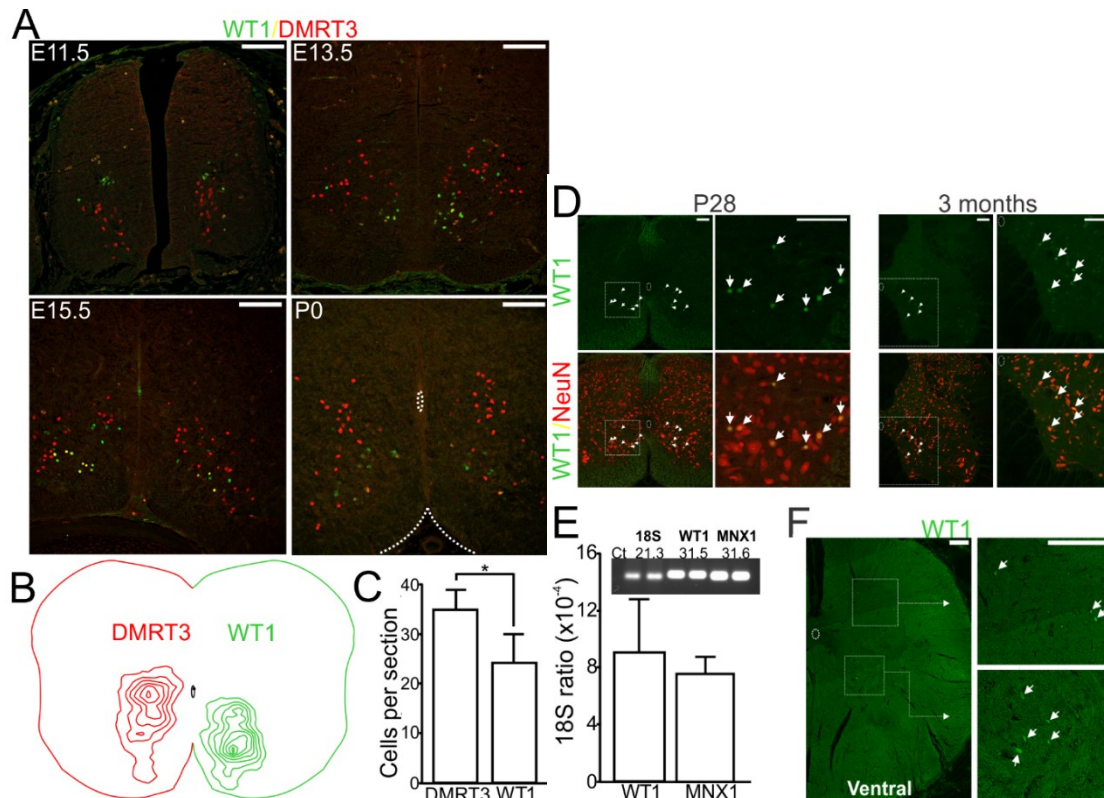
Figure 3.1. Development of WT1-expressing spinal interneurons. A. WT1-expressing interneurons (green) are first seen at E11.5, a time point at which dI6 neurons that express DMRT3 (red) have started to migrate ventromedially. Before birth WT1-expressing interneurons also migrate ventrally and are typically situated ventral to the central canal by P0. **B.** Topographical map illustrating the position of all dI6 cells belonging to the DMRT3+ (red) and WT1 (green) subsets (n=6 spinal cords). **C.** Bar chart indicating that the mean number of DMRT3+ cells (± SD) per 20µm thick spinal cord section is significantly greater than the mean number of WT1+ neurons (n=6 spinal cords, * denotes p=0.0013, t-test). **D.** Paraffin sections cut from the spinal cord of a P28, and 3 months old, mouse and stained with antibodies to WT1 and NeuN indicate that WT1 expression persists in spinal neurons to adulthood in the mouse. Region within the dashed box in the low magnification image is expanded to the right. **E.** Expression ratio of WT1 and MNX1 relative to 18S in the human spinal cord indicates that WT1 is expressed at a similar level as the motor neuronal marker. Inset: Representative image indicating agarose gel electrophoresis of qPCR amplicons and associated threshold cycle (Ct). For panels **C** and **E** data are represented as mean ± SD. **F.** 5µm thick section of lumbar spinal cord from a 32 year old male stained with an antibody to WT1 (green) demonstrates that WT1+ cells are present in the ventromedial as well as the dorsal spinal cord of humans (boxed regions are expanded to the right, white arrows indicating WT1+ cells). In all images scale bar = 100 µm.
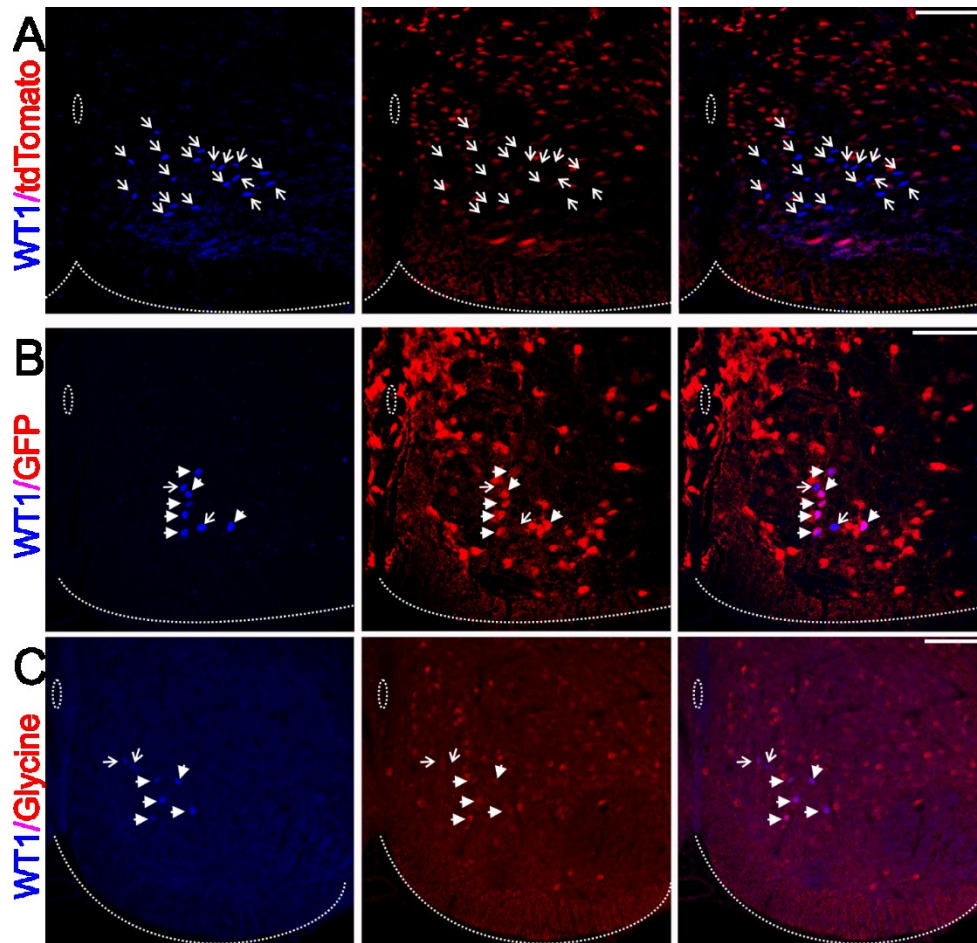
Figure 3.2. Neurotransmitter phenotype of WT1-expressing interneurons. **A-C.** Antibody stain for WT1 (blue) in **(A)** the VGlut2^{Cre}ROSA26^{tdTomato} mouse, **(B)** the GAD67^{GFP} mouse, and **(C)** together with an antibody for Glycine (scale bars = 100 µm). In all panels each WT1-expressing interneuron is indicated with an arrow. Filled arrowheads indicate those WT1+ cells which co-express the respective excitatory or inhibitory marker, open arrows indicate those WT1+ neurons which do not. While no WT1-expressing cells illustrated co-express the excitatory cell marker **(A)**, a significant proportion co-express the markers for GABAergic **(B)** or glycinergic cells **(C)**.
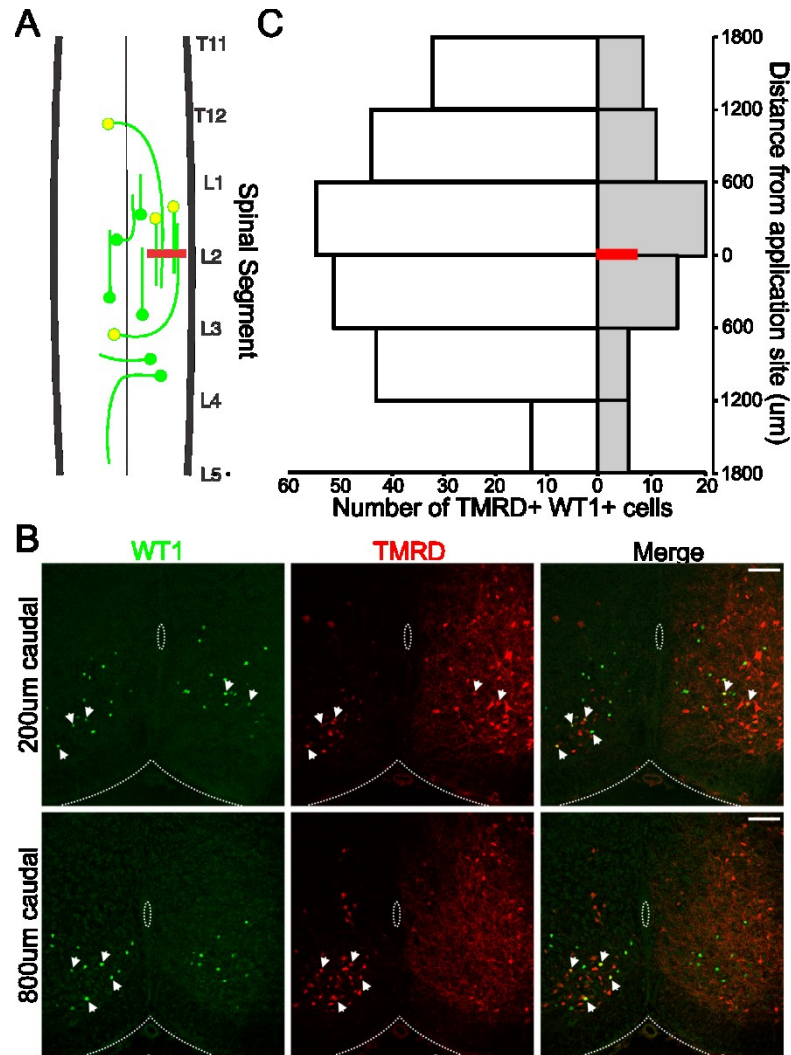
Figure 3.3. Axonal projection pattern of WT1-expressing neurons. A. Schematic of experimental setup in which the fluorescent tracer TMRD is applied to a cut region of the spinal cord unilaterally (red bar). All WT1 cells (green circles) cells passing their axons through this region will transport the tracer back to their cell bodies and also fluoresce red (yellow circles). **B.** 20 μm thick spinal cord section 18 hours after TMRD application 200 μm (upper images) and 800 μm (lower images) caudal to the application site and stained with an antibody to WT1 (scale bars = 100 μm). WT1+ cells (green) that have taken up the TMRD (red), indicated by the white arrows and can be seen in the merged image. **C.** Pooled data from 8 spinal cords indicates that the vast majority of WT1 cells project commissural axons (white bars) as opposed to ipsilateral axons (grey bars) and that a similar number of cells can be found rostral and caudal to the TMRD application site (red bar).
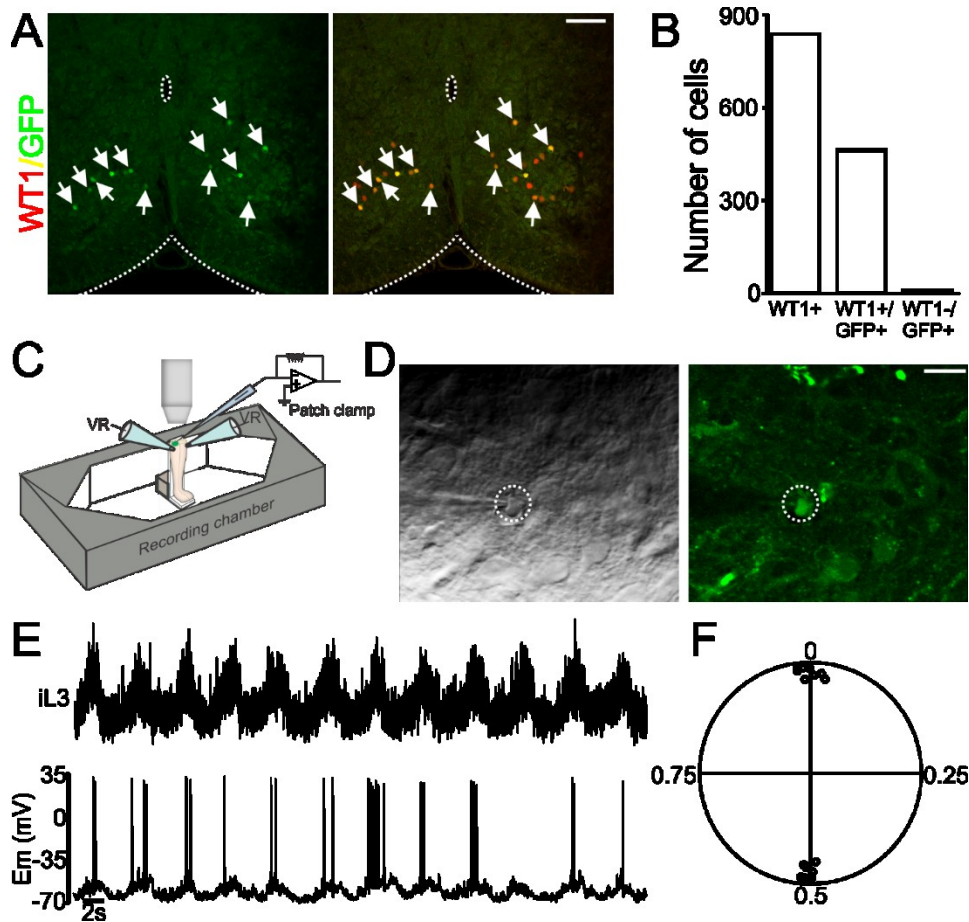
Figure 3.4. WT1-expressing neurons are rhythmically active during fictive locomotion. A. 20 μm thick section cut from a P0 WT1^{CreGFP} mouse and stained with antibodies to WT1 (red) and GFP (green). All GFP+ cells (indicated by arrows) are WT1+ (scale bar = 100 μm). **B**. Count of total number of WT1+ interneurons as well as total number of GFP+ cells which express WT1 indicate that this mouse strain is an accurate marker or WT1-expressing cells. **C.** Schematic of upright in vitro spinal cord preparation used to make patch clamp recordings from GFP+ interneurons as well as lumbar ventral roots (VR) during pharmacologically-induced fictive locomotion. **D.** Image of the surface of a spinal cord taken from a P0 WT1^{CreGFP} mouse and prepared for electrophysiological recording. GFP+/WT1 cell being recorded is circled in the image taken with a DIC (left) and GFP (right) filter (scale bar = 20 μm). **E.** During fictive locomotion GFP+, WT1-expressing neuron (lower trace) oscillates in phase with L3 ventral root located on the ipsilateral side of the spinal cord (iL3). **F.** Circular plot includes pooled data from 16 GFP+, WT1-expressing cells indicates that bursting in all cells are tightly coupled to fictive locomotor activity recorded in the local ventral root. Eight cells burst in phase with the local ventral root (those points located close to 0 in the circular plot), and 8 cells burst out of phase (those points located close to 0.5).
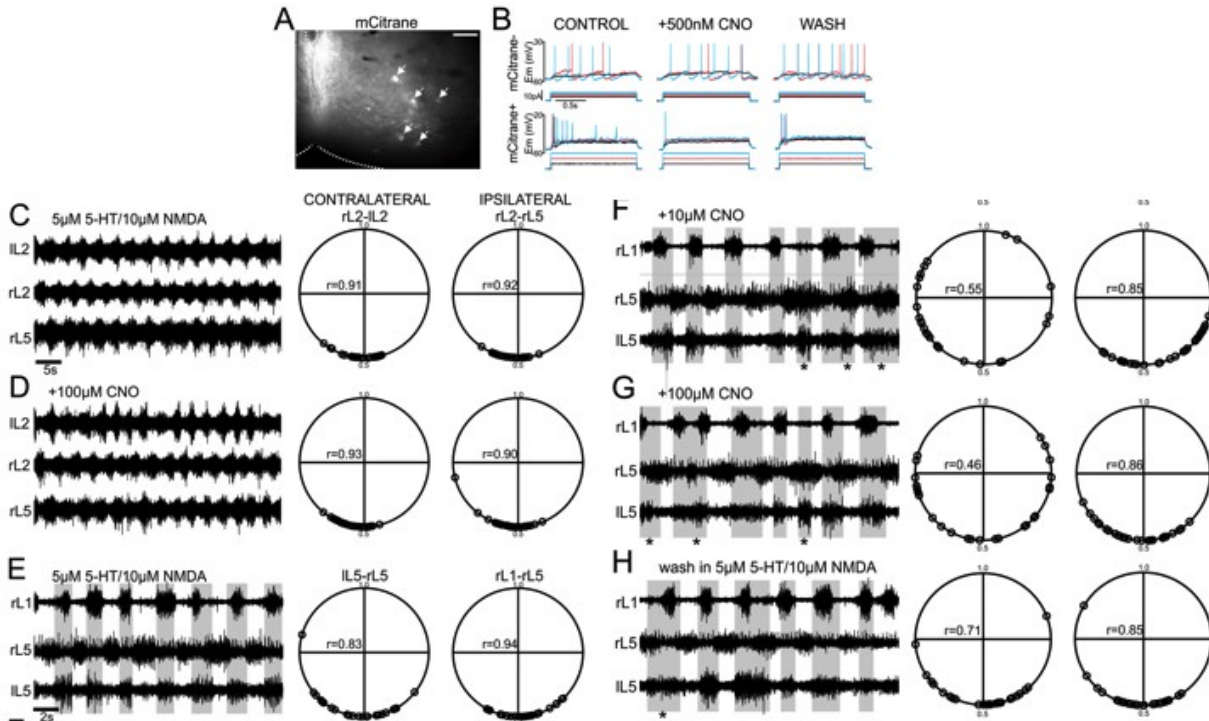
Figure 3.5. Left-right alternation is disrupted in the absence of WT1 cell function. A. Cre recombination results in expression of the DREADD as well as mCitrane (indicated by arrows) in the ventromedial laminae of an upright spinal cord preparation prepared from a P0 WT1^{CreER}xR26-LSL-Gi-DREADD mouse. Scale bar = 100 μm **B.** The response of a mCitrane-cell (no DREADD, upper traces), and mCitrane+ cell (DREADD receptor, lower traces) before CNO application, after application of 500nM CNO, and after washout. The cell containing the DREADD is inhibited and fires fewer action potentials in the presence of CNO while the cell without the DREADD is unaffected. **C, D.** ENG recordings illustrate pharmacologically induced fictive locomotion in a wildtype animal before (**C**) and after (**D**) addition of 100 μM of CNO to the bath. Polar plots illustrate that alternation between flexor (L2) and extensor (L5) related ventral roots is unaffected after CNO application. **E-H.** ENGs recorded from flexor (L1) and extensor (L5) related ventral roots of a spinal cord isolated from a WT1^{CreER}xR26-LSL-Gi-DREADD mouse following (**E**) bath application of 5-HT and NMDA, (**F**) addition of 10 μM of CNO, (**G**) addition of 100 μM of CNO, and (**H**) washout of CNO. Application of increasing concentrations of CNO to the bath disrupts alternation between contralateral roots marked by co-bursting in left and right L5 ventral roots (indicated by asterisks) and is partially restored after washout. Ipsilateral alternation of rL1-rL5 ventral roots is unaffected in the presence of CNO. Circular plots to the right of each panel illustrate coupling between ENG bursts in contralateral as well as ipsilateral ventral roots. Each polar plot illustrated includes analysis of 25 cycles for a single spinal cord in each condition.
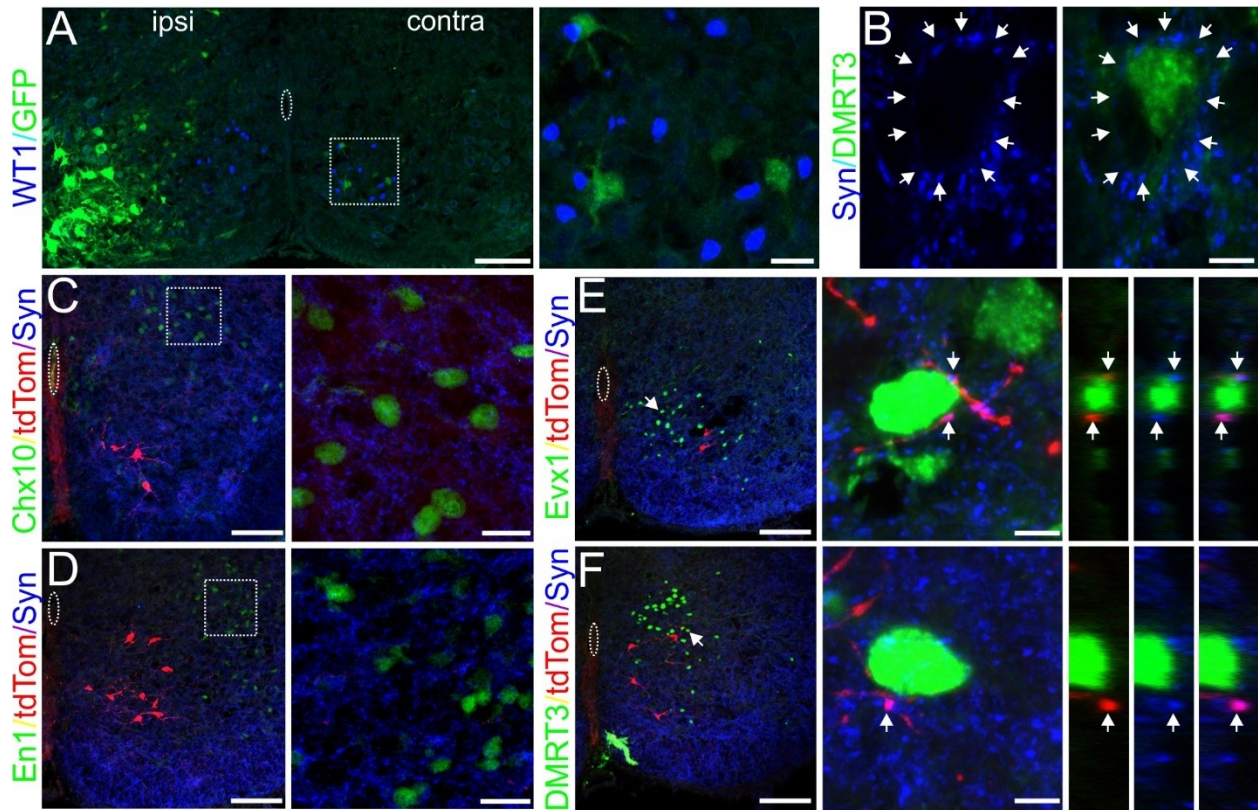
Figure 3.6. WT1-expressing neurons terminate in close proximity to populations of commissurally-projecting interneurons. A. 20μM thick section of a spinal cord 46h after PRV-152 injection into the GS muscle on the left side and stained with antibodies to GFP (green) and WT1 (blue). At this time point no WT1- expressing neurons on either side of the spinal cord have taken up the tracer. Contralateral region containing WT1-expressing cells (dashed box) is expanded to the right. **B.** In order to identify presumptive synapses on genetically defined interneuronal subtypes we inspected the synaptotagmin+ "halo" (indicated by white arrows) surrounding each labeled nuclei for WT1+/synaptotagmin+ terminals. **C-F.** 20 uM thick sections cut from a P0 WT1^{CreER}ROSA26^{tdTomato} spinal cord and stained with antibodies to tdTomato (red), the synaptic marker Synatotagmin (blue), as well as (green) a nuclear marker of V2a cells (Chx10- panel **C**), V1 cells (En1- panel **D**), V0$_V$ cells (Evx1- panel **E**), or DMRT3-expressing dI6 cells (panel **F**). WT1-expressing terminals (tdTomato+/Synaptotagmin+ processes) were rare or absent nearby Chx10 or En1 expressing cells but were commonly seen in close proximity to Evx1+ and DMRT3+ neurons. Dashed boxes in panels **C** and **D** are expanded to the right. In panels **E** and **F** the arrow in the low magnification image indicates the specific WT1 cell of interest in the panel to the right. In magnified images the arrows indicate presumptive WT1+ axon terminals. Double labelling of these processes is confirmed in orthogonal views to the right of panels **E** and **F**. Scale bars in all low magnification images indicate 100 μm. Scale bars in high magnification images in panels **A, C, D** indicate 20 μm, and 5 μm in panels **B, E, F**.
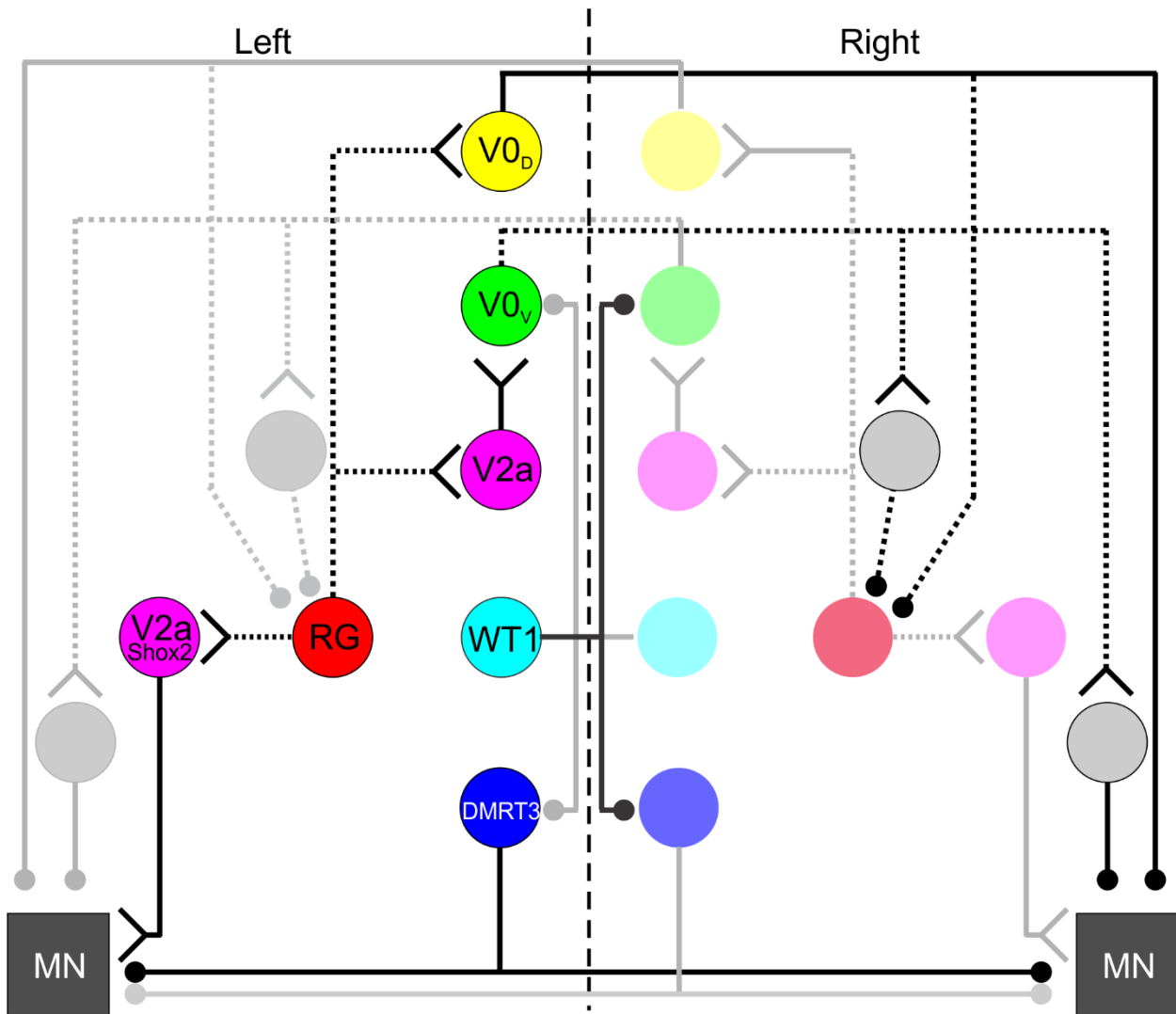
Figure 3.7. Incorporating the WT1-expressing neurons into the proposed circuitry of the locomotor CPG. Schematic is adapted from Shevtsova et al. 2015. Inhibitory synapses indicated by a filled circle, excitatory synapses indicated by (Y). Connectivity that has been directly demonstrated indicated with solid line, that which has been postulated indicated by dashed line.

Chapter 4 -

Mapping connectivity amongst interneuronal components of the locomotor CPG.

Farhia Haque and Simon Gosgnach (May 15, 2019)

Contributions

FH: experimental design, carried out tracing experiments, data analysis

SG: experimental design, wrote manuscript

4.1 Introduction

As animals forage for food, locomotion becomes key for their survival. For quadrupedal animals, this means that in addition to whole body stabilization, the timing and sequence of fore- and hind-limb muscle activation must be precisely controlled. Investigations into the specific mechanisms underlying hindlimb locomotion have demonstrated that this behavior is orchestrated by a highly specialized neural circuit, the locomotor central pattern generator (CPG), which is located in the spinal cord (see Kiehn 2016 for review). This neural network relies on the coordinated activity of interneurons located specifically within the ventral aspect of the lumbar spinal cord (Kiehn and Kjaerullf 1996) to generate the locomotor rhythm and maintain the alternating pattern of agonist and antagonistic hindlimb muscle activation. Recent work, incorporating molecular techniques to characterize spinal neurons, has demonstrated that spinal interneurons can be divided up into a handful of genetically defined ensembles (Goulding 2009 review). Based on the unique combination of transcription factors that each neuron expresses during embryonic development, they are broadly classified into V0, V1, V2, V3, or dI6 populations. Each of these "parent" populations then can be further subdivided into groups based on either intrinsic characteristics or the expression of additional transcription factors (Gosgnach et al. 2017 review).

While the functional role of each of these parent populations has been identified, we know very little about their intrinsic properties, the manner in which they are activated in response to command signals from higher centers in the intact animal, or the manner in which they are interconnected to one another. Characterization of these features is essential if we are to gain a better understanding of the network structure and mechanism of function of the locomotor

CPG, and use this knowledge to develop approaches aimed at the restoration of function in this neural network following spinal cord injury.

Given recent progress in the development of viral approaches to study connectivity within the nervous system (Luo 2018) we now possess the tools to investigate the manner in which these genetically-defined interneuronal populations are activated and interconnected. In this study we will focus on the WT1-expressing dI6 interneurons. Previous work from our laboratory has demonstrated that WT1-expressing neurons are inhibitory, project their axons both ipsilaterally and contralaterally and are involved in regulating appropriate left-right alternation via the control of Dmrt3- expressing dI6, and Evx1-expressing $V0_V$ neurons (Haque et al. 2018), two populations of spinal interneurons predicted to connect to motoneurons either mono- or di-synaptically. In this study we use a retrograde, transynaptic, viral tracing approach to identify upstream synaptic partners of WT1-expressing neurons. Results indicate that the WT1+ neurons receive monosynaptic input from spinal interneurons belonging to the DMRT3-expressing subpopulation of dI6 cells located in both the lumbar and cervical spinal cord, as well as regions of the reticular formation which have been implicated in the initiation of locomotor activity in the spinal cord (Caggiano et al. 2018 and Josset et al. 2018). Collectively, these data provide support for our hypothesis that WT1$^+$ and Dmrt3$^+$ cells form a microcircuit which controls motoneuronal activity during locomotion, and also indicate that WT1$^+$ cell activity may be modulated directly by descending propriospinal neurons as well as those in brainstem locomotor centres that are involved in initiating and modulating activity in the locomotor CPG.

4.2 Materials and methods.

Animals. All procedures were performed on postnatal day 0 – postnatal day 7 (P0-P7) mice of either sex in accordance with the Canadian Council on Animal Welfare and approved by the Animal Welfare Committee at the University of Alberta. The following mouse strains were used (all strains with stock numbers indicated are from The Jackson Laboratory): WT1^{CreGFP} (#010911, RRID:IMSR_JAX: 010911), VGlut2^{Cre} (#028863, RRID:IMSR_JAX:028863), ROSA26^{tdTomato} (#007909, RRID:IMSR_JAX:007909). Wt1^{CreGFP} mice express GFP reporter protein in WT1-expressing spinal neurons (see Haque et al. 2018). Crossing the VGlut2^{Cre} strain with the ROSA26^{tdtomato} strain results in VGlut2^{Cre}ROSA26^{TdTomato} offspring in which glutamatergic neurons express the reporter protein.

Stereotaxic surgeries for viral injection. VGlut2^{Cre}ROSA26^{Tdtomato} or WT1^{CreGFP} transgenic mice (P3-P5) were anesthetized with isoflurane (4% in 95% O$_2$/ 5% CO$_2$) for the duration of the surgical procedure. After surgical plane was reached, a laminectomy was performed to expose the L3/L4 spinal segments. PRV-introvert-GFP (150 nL, gift from Friedman lab, Rockefeller University, NY) was loaded into a glass pipette (~10-30 μm tip diameter) and attached to a microsyringe which was connected to a picospritzer (Dagan Corporation, Minneapolis, MN). PRV-introvert-GFP has an inverted thymidine kinase and GFP between two inverted loxP sites (Pomeranz et al. 2017). Thus, in mice infected with PRV-Introvert-GFP, viral propagation, which is mediated by thymidine kinase, and GFP expression, are both dependent on Cre recombination. The pipette was situated to the left of the midline of the exposed surface of the spinal cord and driven 300-400 μm from the dorsal surface using a stereotaxic frame. Based on anatomical analysis of the P3-P5 spinal cord, this placed the pipette tip in the ventral aspect of the spinal cord. The picospritzer was then used to eject the virus (15-

35 ms pulses at 40 p.s.i.). In some cases, fluorobeads were included in the pipette to assess the injection site post hoc. After viral injections, the pipette was left in place for at least 2 min before slow retraction. After the pipette was removed, the overlying skin was closed with superglue and pups were returned to their home cage where they remained until the tissues were harvested.

Perfusion. In order to analyze the speed at which the PRV-introvert-GFP travels across synapses in the CNS, and to identify infected neurons, brainstems/ spinal cords were extracted 10, 15, 24, 30, 48 and/ or 64 h post injection. At the appropriate time, pups were transcardially perfused with 0.1 M PBS followed by 4% PFA/PBS, quickly eviscerated, and brainstems/ spinal cords were dissected out, fixed overnight in 4% PFA/PBS, and cryoprotected in a 30% sucrose/PBS solution. The tissues were then placed in Tissue-Tek O.C.T. compound to make cryomoulds and 20 μm 30 μm thick transverse cryostat sections brainstem were collected on slides. Antibody staining was either carried out immediately or the slides were stored at -80°C.

Immunohistochemistry. Immunohistochemistry was performed as previously described (Griener et al., 2017). Briefly, slides containing sections of postnatal mouse spinal cords/ brainstems were incubated with primary antibodies overnight (4°C) followed by incubation with species-specific secondary antibodies conjugated to Cy2, Cy3, or Cy5 for 4 h at room temperature. After coverslipping, images were collected using a Leica TCS SP8 MP microscope running Leica Application Suite X software, and figures were prepared with Adobe Photoshop and Corel Draw. Primary antibodies used were as follows: WT1 (rabbit, 1:100, Santa Cruz Biotechnology, RRID:AB_632611), GFP (goat, 1:5000, gift from Eusera), En1 (gift from Jessel laboratory, Columbia University, guinea pig, 1:1000), Chx10 (mouse, 1:200, Santa Cruz Biotechnology, RRID:AB_10842442), DMRT3 (goat, 1:100, Santa Cruz Biotechnology,

RRID:AB_2091664), Evx1 (mouse, 1:100, DSHB, RRID:AB_2246711), and NeuN (mouse, 1:500, Millipore, RRID:AB_177621).

4.3 Results.

In order to trace upstream synaptic partners of WT1 neurons a retrograde virus, PRV-Introvert-GFP was injected into the spinal cords of WT1^{CreGFP} mice. Propagation of both the virus and GFP expression are dependent on Cre recombination (Pomeranz et al. 2017). First, to confirm that the virus was in fact Cre-dependent, we injected PRV-Introvert-GFP into the lumbar spinal cord of P3-P5 wild type and VGlut2^{Cre}ROSA26^{tdTomato} mice. Inspection of tissue harvested from wildtype animals 24 h after intraspinal injection, and incubated with antibodies to GFP, resulted in no GFP expression in the spinal cord (Figure 4.1 top panel), indicating that there is no PRV-Introvert-GFP expression in mice that do not express the Cre recombinase. Fluobeads added to the virus confirmed that the injection site was localized to the ventral spinal cord (Figure 4.1A-C). In contrast, spinal cords harvested from VGlut2^{Cre}ROSA26^{tdTomato} mice at 15 h post injection showed viral expression in a handful cells, while by 24 h there was GFP expression in majority of the glutamtergic neurons (Cre expressing neurons) in the lumbar segment (Figure 4.1E-F) confirming that expression of Cre recombinase is required for viral transport.

The next goal was to determine the speed of transport of the virus, in order to identify those neurons that monosynaptically contact Cre-expressing cells which are infected at the injection site. To this end PRV-Introvert-GFP was injected into the lumbar enlargement (L3-L4) of P3-P5 VGlut2^{Cre}ROSA26^{TdTomato} mice. Although our ultimate goal was to map contacts onto WT1-expressing neurons, the VGlut2^{Cre}ROSA26^{TdTomato} mouse strain was initially used since it

contains many more Cre expressing neurons than the WT1[CreGFP] strain (Haque et al 2018), and thus allows us to better visualize the infection and explore the spread of Cre-dependent virus. In 3 VGlut2[Cre]ROSA26[TdTomato] spinal cords a mean of 86±20.8 tdTomato-expressing (i.e. glutamatergic) cells were identified per hemisection in the lumbar segments. Spinal cords were harvested 10, 15, 24, 30, 48 and 64 hours after PRV-Introvert-GFP injection and immunohistochemistry for GFP was carried out (Figure 4.1D-I). Ten hours after injection there was no GFP expression in the lumbar region (n=2 spinal cords, Figure 4.1D). The first GFP+ neurons were visible 15 h (Figure 4.1E) after injection and they were restricted to the region immediately surrounding the injection site (mean 5.1 ± 2 .4 GFP cells per 20 μm section; n=3 spinal cords). Since the primary viral infection should encompass most of the glutamatergic neurons in the ventral horn of L3-L4 segment, we increased the incubation time and extracted the tissue 24 h post injection. At this time point GFP expression was limited to the L3/L4 spinal cord segment (n=3) and on average 38.2 ± 10.7 cells expressed the virus (Figure 4.1F). At 30 and 48 h post injection, the GFP expression had spread not only to neurons within the L3/L4 segment (Figure 4.1 G-H) but also to the cervical segments of the spinal cord (Figure 4.2 A-B) and various nuclei in the brainstem (Figure 4.2 C-F). It was previously shown that reticulospinal neuron from pons and medulla and long projections from the cervical spinal segment terminate in the lumbar segment where motor-related interneurons and motor neurons reside (Ruder et al. 2016). Hence, the presence of virus in the cervical segments 30h post injection suggests that at this time point the virus has crossed one synapse. Since PRV-Introvert-GFP is not monosynaptically restricted, we drew inference about higher order connectivity by analyzing the retrograde spread over time. The spread of virus from 24 h to 30 h led us to believe that the

primary infection occurs by 24 h and the infection crosses a synapse by 30 h post injection and two synapses by 48 h.

We followed this timeline and injected PRV-Introvert-GFP directly in L2/L3 spinal segment of WT1^{CreGFP} mice. Spinal cords from these mice were harvested and immunostained for GFP 24 h and 30 h after the injection. Since both the virus and the transgenic mouse strain express GFP, we looked at cell morphology to differentiate between GFP expressing WT1 cells and GFP expressed by PRV-Introvert-GFP. The WT1^{CreGFP} mice has a knock-in allele that expresses an enhanced green fluorescent protein-Cre recombinase fusion protein under the WT1 promoter element and has been shown to express GFP in approximately half of all WT1-expressing neurons (Haque et al. 2018). Since WT1 is a nuclear transcription factor, the GFP expression is restricted to the nucleus. Whereas the virus expresses GFP in both the processes and cytoplasm of infected cells. The differences in GFP expression can be distinguished under high magnification (Figure 4.3 A-C) and allows us to identify infected WT1-expressing cells. Spinal cord harvested 24 h post PRV-Introvert-GFP injection were immunostained with GFP and WT1 antibodies and we found that 3.3 ± 2.0 WT1+ neurons (n=4 spinal cords) had been infected by the virus around the L3 spinal segment where the virus was injected (Figure 4.3 A). In these spinal cords we also observed viral expression in a smaller population (1.7 ± 0.8 neurons) that did not express WT1.

The next step was to determine the genetic identity of these spinal interneurons that contact WT1 neurons in the lumbar spinal cord as they are likely to comprise the upstream synaptic partners of the WT1 population. Spinal cord sections were cut from the lumbar, and cervical spinal cord as well as the brainstem 30 h after injection of PRV-Introvert-GFP in an

additional 5 spinal cords. In addition to staining for GFP, antibodies against Evx1, En1, Chx10, and DMRT3 were used to label V0$_V$, V1, V2a, and a subset of the dI6 interneuronal populations respectively. At 30 h post injection, we found a mean of 5.4 ± 3.9 GFP+ cells per 20 μm hemi-section (n=5) throughout the lower thoracic to lumbar (T10-L5) segments of the spinal cord. Throughout the same segments, our antibodies labelled on average 25.5 ± 6.1 Evx1, 10.2 ± 4.2 Chx10, 22.0 ± 6.9 En1, and 25.4 ± 13.2 DMRT3 neurons per hemi-section. In these spinal cords we found no co-labelling of the virus with En1 (Figure 4.3 D-F) or Chx10 (Figure 4.3 G-I) neurons, and we found only one viral infected cells that was Evx1+ (Figure 4.3 M-O). Interestingly, of the 398 GFP+ neurons we identified within the lumbar segments of all spinal cords, 382 were also positive for DMRT3 (Figure 4.3 J-L). Given the consistency of this data it provides strong evidence that the DMRT3-expressing subset of dI6 neurons provides substantial input on the the WT1-expressing neurons.

Propriospinal neurons that project to and connect various segments of the spinal cord are important for relaying supraspinal signals (Cowley et al 2008, 2010), postural control, and interlimb coordination (Alstermark et al. 1987; Ballion et al. 2001; Pocratsky et al. 2014; Ruder et al. 2016; Flynn et al. 2017). Long descending propriospinal neurons, located in the cervical and upper thoracic spinal segment, that project their axons to the lumbar enlargement are important for interlimb coordination (reviewed in Cowley et al. 2010). In order to determine whether these neurons provide input onto WT1 cells we examined sections cut from the cervical and upper thoracic segments (~C2-T2) of the same 5 mice as in the previous experiment in which PRV-Introvert-GFP had been injected into L2/L3 segments and spinal cords were harvested after 30 hours. We identified a mean of 1.8 ± 0.9 (n=5) viral infected neurons per hemi-section and observed these GFP+ cells distributed on either side of the spinal cord. To

identify the developmental genetic class of these neurons we again stained these sections with antibodies to transcription factors Evx1, En1, Chx10, and DMRT3 in the cervical segments. We saw no co-expression of the virus with En1 (Figure 4.4 A-C), Chx10 (Figure 4.4 D-F), or Evx1 (Figure 4.4 J-L) in any of the sections from the C2-T2 segments. Interestingly however, we identified in total 20 of the 23 viral infected neurons identified in these segments also expressed DMRT3 (Figure 4.4 G-I) indicating that long descending propriospinal input onto WT1 neurons in the lumbar spinal cord originates from DMRT3-expressing neurons.

The reticulospinal system that sends descending tracts from the pontine and medullary reticular formation are important in conveying command signals for locomotor initiation (Shefchyk et al. 1984; Drew and Rossignol 1984; Capelli et al. 2017) however the targets of these reticulospinal neurons in the lumbar spinal cord have yet to be identified. To determine whether WT1 neurons received input from these regions we simply investigated whether viral infected neurons could be identified in the pontine and medullary reticular formation 30 hours after injection of PRV-Introvert-GFP into the lumbar spinal cord of WT1^{CreGFP} mice. For these experiments serial brainstem sections were taken at 90 μm intervals, nuclei were identified based on the distribution of ChAT immunoreactivity (Armstrong et al. 1983; Tago et al. 1989), and general brain architecture that was compared with the Allen mouse brain atlas. GFP-expressing neurons were only found in the medullary reticular formation ventral part (MdV) (n=3 brainstems; 8±3 GFP+ cells per section) and in gigantocellular reticular nucleus ventral part (GiV) (n=3 brainstems; 4±2 cells- Figure 4.5 A-D) indicating that the WT1-expressing neurons do receive input from locomotor related brainstem sites.

4.4 Discussion.

In order to understand how locomotor activity is generated and modulated we must be able to identify the interneuronal components of the locomotor CPG, determine the intrinsic physiological properties of these interneurons, as well as the manner in which they are interconnected to one another and activated by descending systems that initiate stepping. Previous work indicates that WT1-expressing cells are derived from the dI6 interneuronal population which migrates to the ventral spinal cord during the later stages of development and takes up position in lamina VII/VIII postnatally (Goulding 2009). These neurons are primarily inhibitory, project commissural axons, and are involved in regulating left-right alternation during locomotion, likely via interactions with the Evx1 expressing $V0_V$ neurons and the DMRT3 expressing subset of dI6 neurons (Haque et al. 2018). In this study we provide further insight into the network structure of the locomotor CPG by identifying sources of synaptic input onto the WT1-expressing population. Tracing experiments demonstrate that these neurons receive extensive, likely monosynaptic, input from DMRT3-expressing interneurons located in the lumbar and cervical segments of the spinal cord, in addition to input from brainstem sites involved in locomotor initiation.

It is important to keep in mind that there are other sources of input to WT1-expressing neurons that were not revealed in this study. While a surprisingly small percentage of cells in the lumbar spinal cord (4%) were infected with the virus but did not express DMRT3, this number rose to 14% in the cervical spinal cord. These neurons were not able to be identified with antibodies to transcription factors expressed postnatally by the $V0_V$ (Evx1), V1 (En1), or V2a

(Chx10) populations however this does not rule out connectivity between these populations and the WT1-expressing neurons since these antibodies do not exhaustively label each population.

In spite of this, given the overwhelming number of viral infected neurons that expressed DMRT3, it is clear that there is a substantial degree of communication between the two subsets of dI6 neurons. Mutations in the DMRT3 gene in horses is required to perform alternate gait (pacing or four-beat ambling), and thus suggests that DMRT3-expressing neurons have a critical role for left/right alternation and also for coordinated movement of the fore- and hind-limbs (Andersson et al. 2014). Connectivity between DMRT3-, and WT1-expressing neurons in the lumbar spinal cord fits with our previous prediction that these two populations, along with the V0 interneurons, form a microcircuit across the midline that is responsible for coordinating motoneurons on either side of the spinal cord (Haque et al. 2018) and ensuring left-right alternation during stepping. In addition, our data demonstrating that DMRT3+ neurons in the cervical spinal cord project to WT1-expressing neurons in the lumbar segments raises the possibility that these subpopulations of dI6 neurons communicate in order to coordinate fore- and hind-limb movements during stepping, circuitry that has been shown to be key for balance in in both bipeds and quadrupeds animals (Dietz 2002) and implicated in sensorimotor integration, as well as functional recovery following spinal cord injury (Flynn et al. 2017).

An unexpected finding in this study was the connectivity between locomotor-related centres in the brainstem and WT1-expressing neurons in the spinal cord. Viral expression was seen in the MdV and GiV, two nuclei that comprise the reticular formation, receive input from the mesencephalic locomotor region, (Capelli et al. 2017), and initiate activity in the locomotor CPG. In spite of these projections it is extremely unlikely that WT1 neurons in the lumbar spinal

cord are involved in locomotor initiation since this is a function carried out by glutamatergic neurons (Hagglund et al. 2010), and less than 2% of WT1-expressing neurons fit this description. Our data does raise the possibility that, rather than simply initiating activity in the locomotor CPG these brainstem sites provide ongoing modulation of the interneuronal components of this neural network, circuitry that would be functionally relevant when quadrupedal animals switch between gaits from walking to trotting to galloping, each of which requires a unique synergy of hindlimb muscles on either side of the spinal cord (Bellardita and Kiehn, 2015).

Summary

The incorporation of molecular genetic techniques has enabled a number of genetically-defined interneuron populations to be identified and their specific function during locomotion to be defined. In addition, the specific brainstem regions that interface with the locomotor CPG and are involved in starting and stopping (Josset et al 2018, Capelli et al 2017; Caggiano et al 2018) locomotor activity have been determined. In spite of this, there is limited knowledge regarding the connectivity of these neurons within the neural network which controls stepping. In fact, other than connectivity between Shox2-expressing interneurons and V0 cells (Dougherty et al. 2013), there is little information detailing synaptic connectivity amongst the genetically-defined populations and the manner in which they work together to generate the various gaits used to locomote at various speeds. This study, together with previous work from our lab (Haque et al. 2018), has begun to fill this gap by identified the upstream and downstream synaptic partners of WT1-expressing neurons and demonstrating that this connectivity pattern is consistent with their involvement of coordinating left-right alternation during stepping.

REFERENCES

Alstermark B, Lundberg A, Pinter M, and Sasaki S. (1987) Subpopulations and functions of long C3–C5 propriospinal neurons. *Brain Res* 404: 395–400.

Andersson LS, Larhammar M, Memic F, Wootz H, Schwochow D, Rubin CJ, Patra K, Arnason T, Wellbring L, Hjälm G, Imsland F, Petersen JL, McCue ME, Mickelson JR, Cothran G, Ahituv N, Roepstorff L, Mikko S, Vallstedt A, Lindgren G, Andersson L, Kullander K. (2012) Mutations in DMRT3 affect locomotion in horses and spinal circuit function in mice. *Nature.* 488(7413):642-6.

Armstrong DM., Saper CB., Levey AI., Wainer BH., and Terry RD. (1983) Distribution of cholinergic neurons in rat brain: Demonstrated by the immunocytochemical localization of choline acetyltransferase. *Jouranl of Comparative Neurology.* 216(1):53-68.

Ballion B., Morin D., and Viala D. (2001) Forelimb locomotor generators and quadrupedal locomotion in the neonatal rat. Eur. *J. Neurosci.* 14, 1727–1738.

Bellardita C, Kiehn O. (2015) Phenotypic characterization of speed-associated gait changes in mice reveals modular organization of locomotor networks. *Curr Biol.* 1;25(11):1426-36.

Caggiano V.,Leiras R., Goñi-Erro H., Masini D., Bellardita C., Bouvier J., Caldeira V., Fisone G., Kiehn O. (2018) Midbrain circuits that set locomotor speed and gait selection. *Nature.* 553: 455-460

Capelli, P., Pivetta, C., Esposito, M.S., and Arber, S. (2017). Locomotor speed control circuits in the caudal brainstem. *Nature* 551, 373–377.

Cowley KC, Zaporazhets E, Schmidt BJ. (2008) Propriospinal neurons are sufficient for bulbospinal transmission of the locomotor command signal in the neonatal rat spinal cord. *J Physiol* 586: 1623–1635.

Cowley KC, Zaporazhets E, Schmidt BJ. (2010) Propriospinal transmission of the locomotor command signal in the neonatal rat. *Ann NY Acad Sci* 1198: 42–53.

Dietz V. (2002) Do human bipeds use quadrupedal coordination? *Trends in Neuroscience.* 25(9):462-7.

Drew T, Rossignol S. (1984) Phase-dependent responses evoked in limb muscles by stimulation of medullary reticular formation during locomotion in thalamic cats. *J Neurophysiol.* 52(4):653-75.

Dougherty KJ, Zagoraiou L, Satoh D, Rozani I, Doobar S, Arber S, Jessell TM, Kiehn O. (2013) Locomotor rhythm generation linked to the output of spinal shox2 excitatory interneurons. *Neuron.* 80(4):920-33.

Flynn JR, Conn VL, Boyle KA, Hughes DI, Watanabe M, Velasquez T, Goulding MD, Callister RJ and Graham BA (2017) Anatomical and Molecular Properties of Long Descending Propriospinal Neurons in Mice. *Front. Neuroanat.* 11:5.

Gosgnach S, Bikoff JB, Dougherty KJ, El Manira A, Lanuza GM, Zhang Y. (2017) Delineating the Diversity of Spinal Interneurons in Locomotor Circuits. *The Journal of Neuroscience.* 37(45), pp.10835–10841.

Goulding, M. (2009). Circuits controlling vertebrate locomotion: moving in a new direction. *Nat.*

Rev. Neurosci. 10, 507–518.

Griener A, Zhang W, Kao H, Haque F, Gosgnach S. (2017) Anatomical and electrophysiological characterization of a population of dI6 interneurons in the neonatal mouse spinal cord. *Neuroscience.* 362:47-59

Hägglund M, Borgius L, Dougherty KJ, Kiehn O. (2010) Activation of groups of excitatory neurons in the mammalian spinal cord or hindbrain evokes locomotion. *Nat Neurosci.* 2010 Feb;13(2):246-52.

Haque F, Rancic V, Zhang W, Clugston R, Ballanyi K, Gosgnach S. (2018) WT1-expressing interneurons regulate left-right alternation during mammalian locomotor activity. *J Neurosci.* 38:5666–5676.

Josset N., Roussel M., Lemieux M., Lafrance-Zougba D., Rastqar A. and Bretzner F. (2018) Distinct contributions of mesencephalic locomotor region nuclei to locomotor control in the freely behaving mouse. *Curr. Biol.* 28: 884-901

Jovanovic K, Angel M. Pastor AM, and O'Donovan MJ. (2010) The Use of PRV-Bartha to Define Premotor Inputs to Lumbar Motoneurons in the Neonatal Spinal Cord of the Mouse. *PLoS One.* 5(7): e11743.

Kiehn, O. (2016) Decoding the organization of spinal circuits that control locomotion. *Nature Reviews Neuroscience.* 17(4): 224-38.

Kjaerulff O. and Kiehn O. (1996) Distribution of networks generating and coordinating locomotor activity in the neonatal rat spinal cord in vitro: a lesion study. *J Neurosci.* 16(18):

5777-94.

Luo L., Callaway E.M., Svoboda K., 2018. Genetic Dissection of Neural Circuits: A Decade of Progress. *Neuron.* 98(2): 256-281.

Pocratsky AM, Burke DA, Morehouse JR, Beare JE, Riegler A, Tsoulfas P, States GJR, Whittemore SR, Magnuson DSK. (2017) Reversible silencing of lumbar spinal interneurons unmasks a task-specific network for securing hindlimb alternation. *Nat Commun.* 8(1):1963.

Pomeranz LE, Ekstrand MI, Latcha KN, Smith GA, Enquist LW, and Friedman JM. (2017) Gene expression profiling with Cre-conditional pseudorabies virus reveals a subset of midbrain neurons that participate in reward circuitry. *J. Neurosci.* 37 pp. 4128-4144.

Ruder L, Takeoka A, and Arber S. (2016) Long-Distance Descending Spinal Neurons Ensure Quadrupedal Locomotor Stability. *Neuron.* 92, 1063-1078.

Shefchyk SJ, Jell RM, and Jordan LM. (1984) Reversible cooling of the brainstem reveals areas required for mesencephalic locomotor region evoked treadmill locomotion. *Experimental Brain Research.* 56(2):257-62.

Tago H, McGeer PL, McGeer EG, Akiyama H, and Hersh LB. (1989) Distribution of choline acetyltransferase immunopositive structures in the rat brainstem. *Brain Research.* 495, 2, (271).
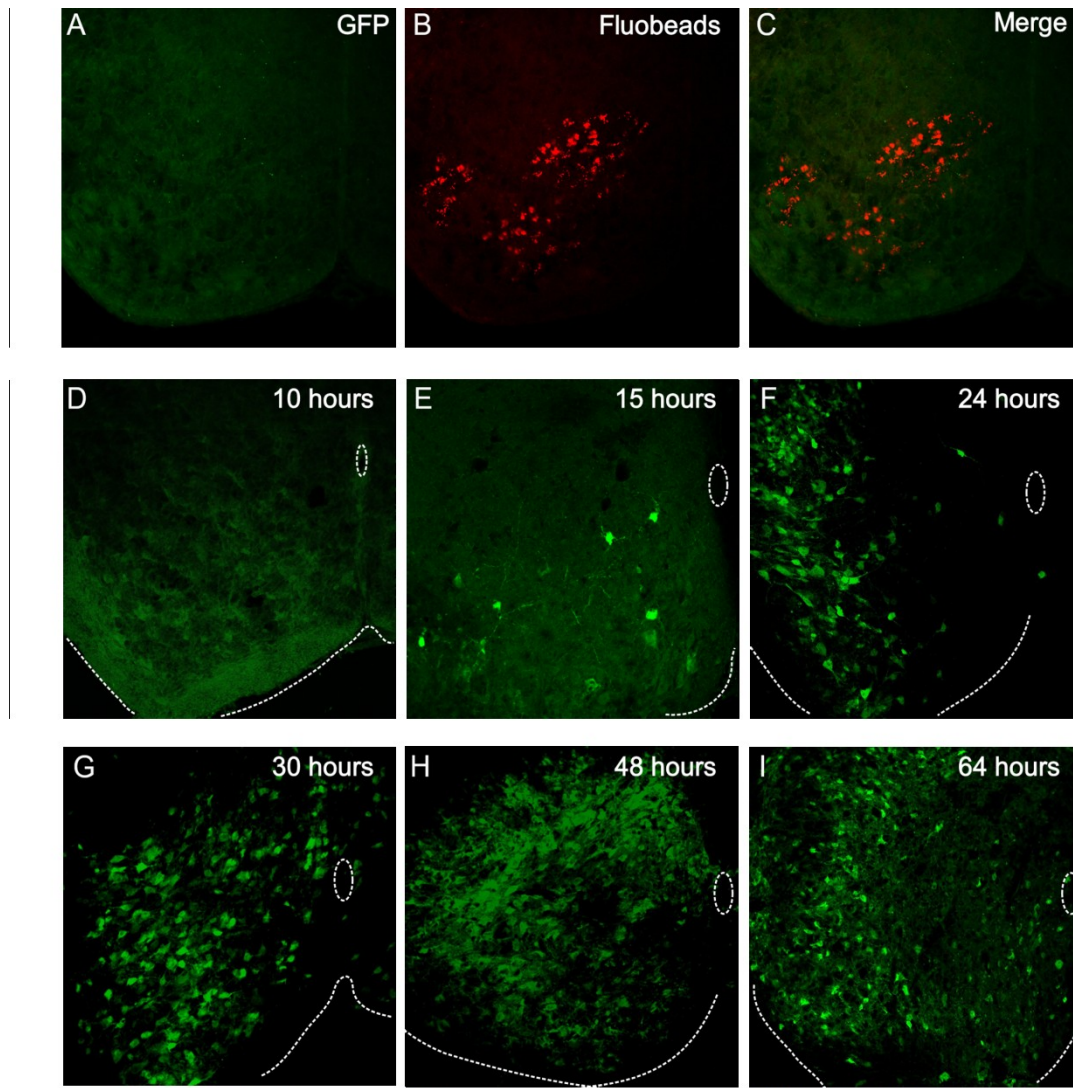
Figure 4.1. Injection and spread of PRV-Introvert-GFP in the neonatal mouse spinal cord. **(A-C)** Spinal cord from wild type animal was harvested 24 hours after injection of PRV-Introvert-GFP into the lumbar spinal cord. In the absence of the Cre recombinase no infected cells (green) can be seen. Confirmation that the injection was localized to the lumbar spinal cord comes from cells in this region that have taken up Fluobeads (red), which were included in the injection pipette. **(D-I)** Lumbar spinal cord sections from VGlut2^{Cre}ROSA26^{tdTomato} spinal cords harvested at various time points after injection. The first viral infected cells (green) can be identified 15 hours after injection, by 48 hours most cells in the ventral spinal cord are infected.
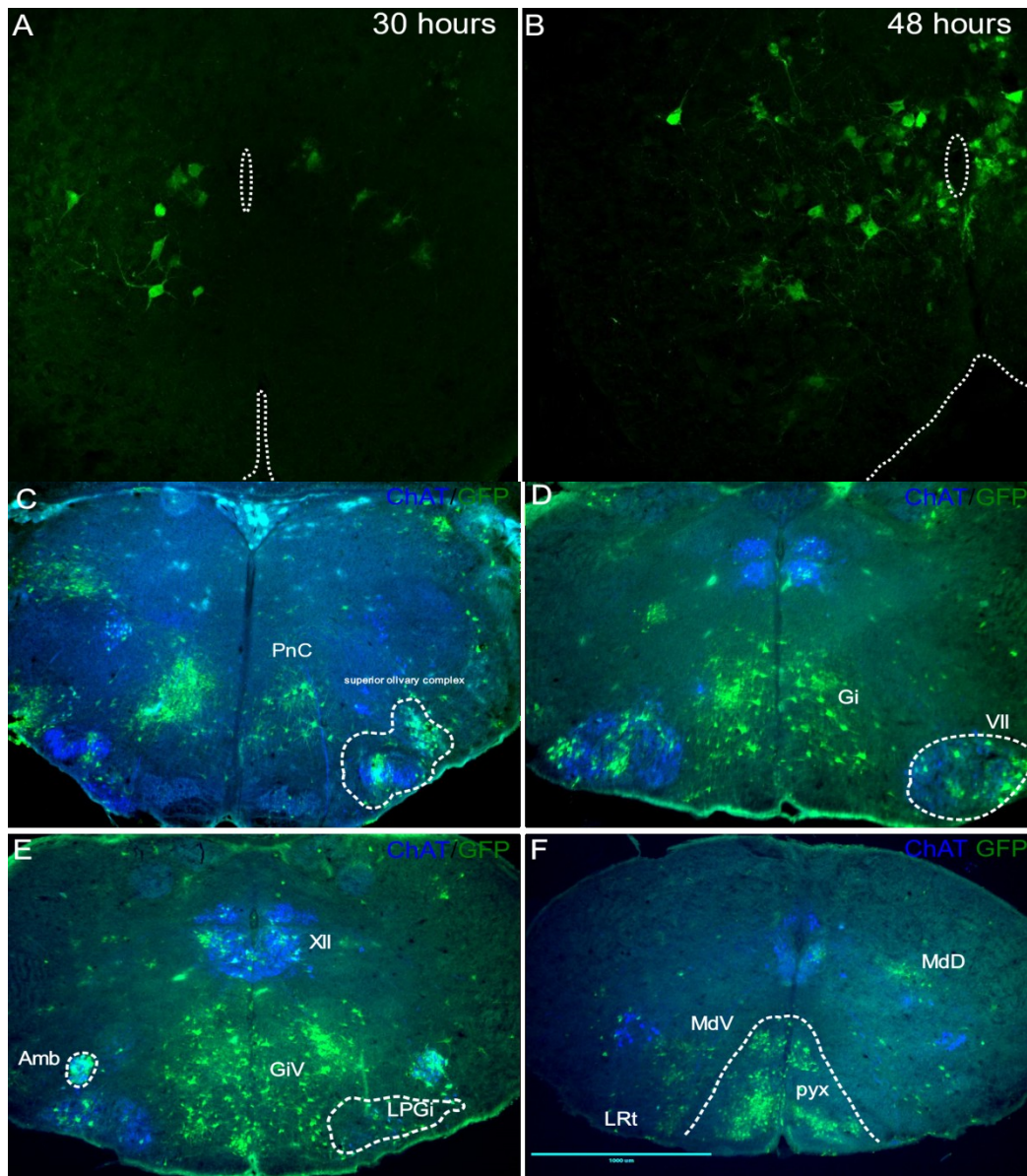
Figure 4.2 Infection of descending cells that project to glutamatergic neurons in the lumbar spinal cord. A-B. Sections cut from the cervical spinal cord 30 (**A**) and 48 (**B**) hours after PRV-Introvert-GFP injection into the lumbar spinal cord of a VGlut2^{Cre}ROSA26^{tdTomato} mouse indicate that cells surrounding the central canal (dashed circle) have been infected with the virus, and express GFP (green) at these timepoints, with a greater number of cells expressing GFP after 48 hours. **C-F.** Sections cut from rostral (C), medial (D, E), and caudal (F) brainstem 48 hours after PRV-Introvert-GFP injection into the VGlut2^{Cre}ROSA26^{tdTomato} mouse indicates that cells in several nuclei are infected with the virus (green cells) and project to the lumbar spinal cord. Sections are also stained with an antibody to ChAT (blue) to identify nuclei for orientation. PnC-pontine reticular nucleus; Gi- gigantocellular reticular nucleus; VII- facial nucleus; XII-hypoglossal nucleus; Amb- nucleus ambiguous; LPGi- lateral paragigantocellular nucleus; MdV/MdD- medullary reticular formation ventral/dorsal part; pyx- pyramidal decussation.
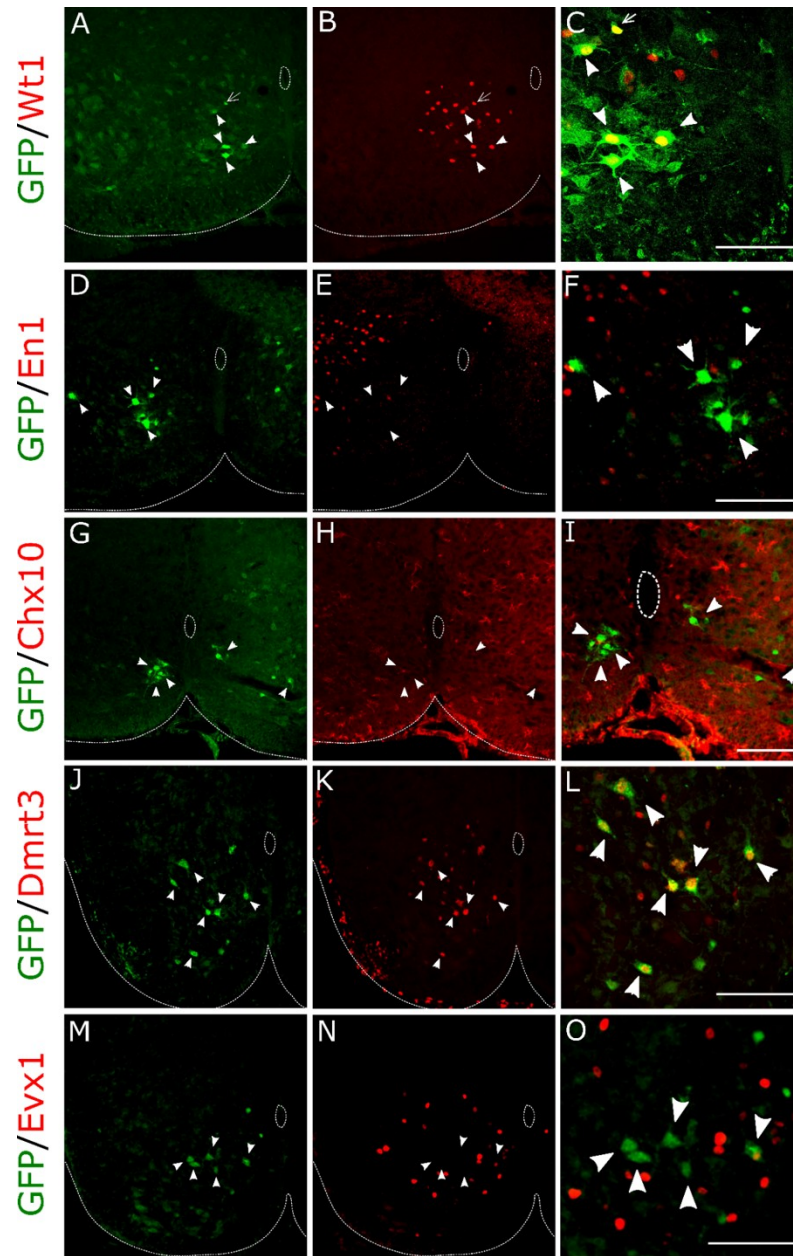
Figure 4.3. Expression of PRV-Introvert-GFP in the lumbar spinal segment of WT1^{CreGFP} mice. (A-C) Expression of the virus 26 hrs post injection indicates that the virus is selectively expressed in WT1 cells (closed arrows). Virus derived GFP is expressed in the cell body of Wt1 cells (closed arrow) whereas GFP expressed as a reporter protein in WT1 cells of WT1^{CreGFP} mice is restricted to the nucleus (open arrows). Sections cut from the lumbar spinal cord 30 h post intraspinal virus injection and labelled with GFP and antibodies to En1 **(D-F)**, Chx10 **(G-I)**, DMRT3 **(J-L)**, and Evx1 **(M-O)** shows that the viral expression was limited to DMRT3 expressing neurons in the lumbar segments. Panels C, F, I, L, O are magnifications of the regions containing the GFP+ cells (arrowheads) in the panels to the left. Scale bar, 100 μm.
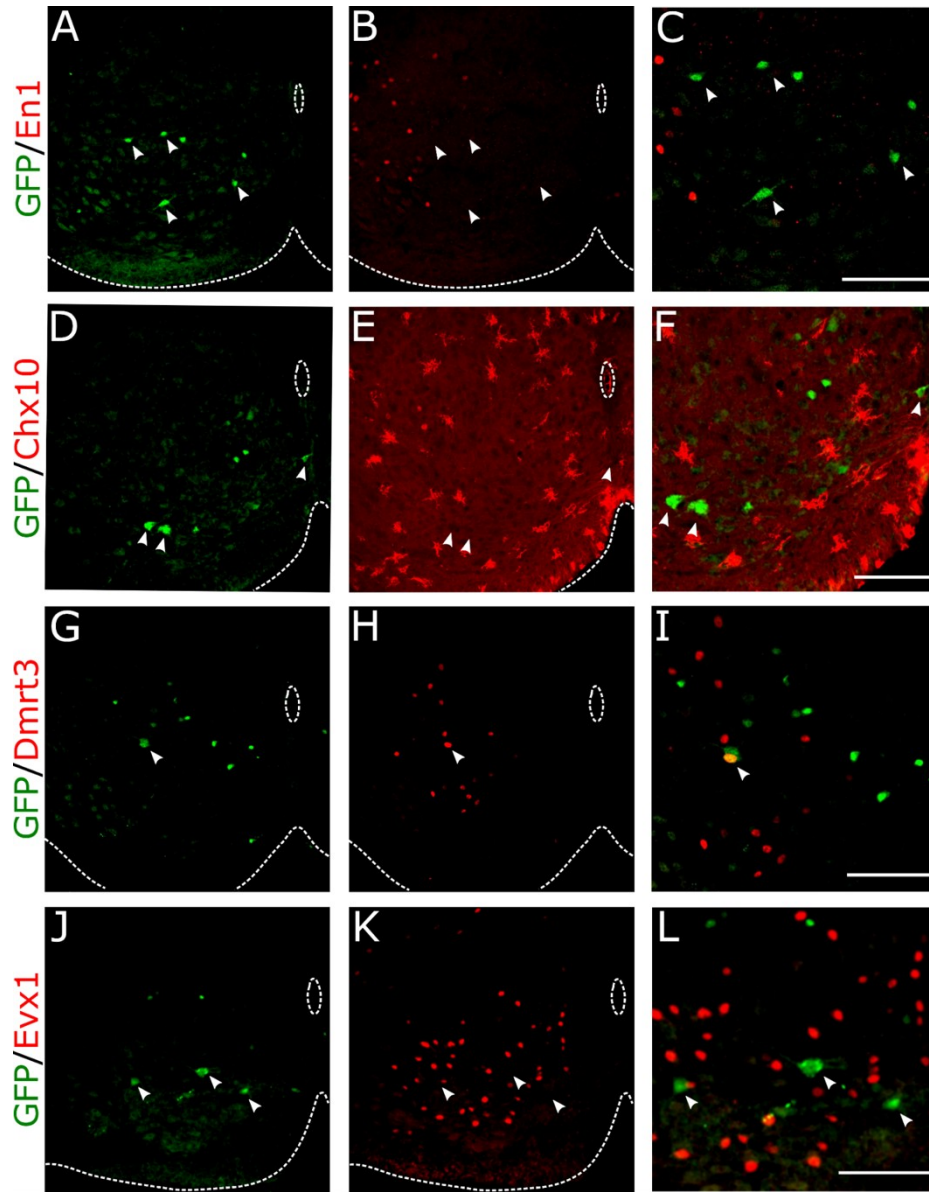
Figure 4.4. Expression of PRV-Introvert-GFP in the cervical segments of Wt1^{CreGFP} mice. Sections cut from the cervical spinal cord of WT1^{CreGFP} mice 30 h after PRV-Introvert-GFP injection into the lumbar spinal cord. Sections are stained with antibodies to En1 **(A-C)**, Chx10 **(D-F)**, DMRT3 **(G-I)**, and Evx1 **(J-L)** to identify propriospinal neurons that project to WT1 expressing cells in the lumbar spinal cord. Of these populations only the DMRT3+ cells in the cervical spinal cord were seen to take up the virus. Panels to the right are magnifications of the regions containing the GFP+ cells (arrowheads) in the panels to the left. Scale bar, 100 μm.
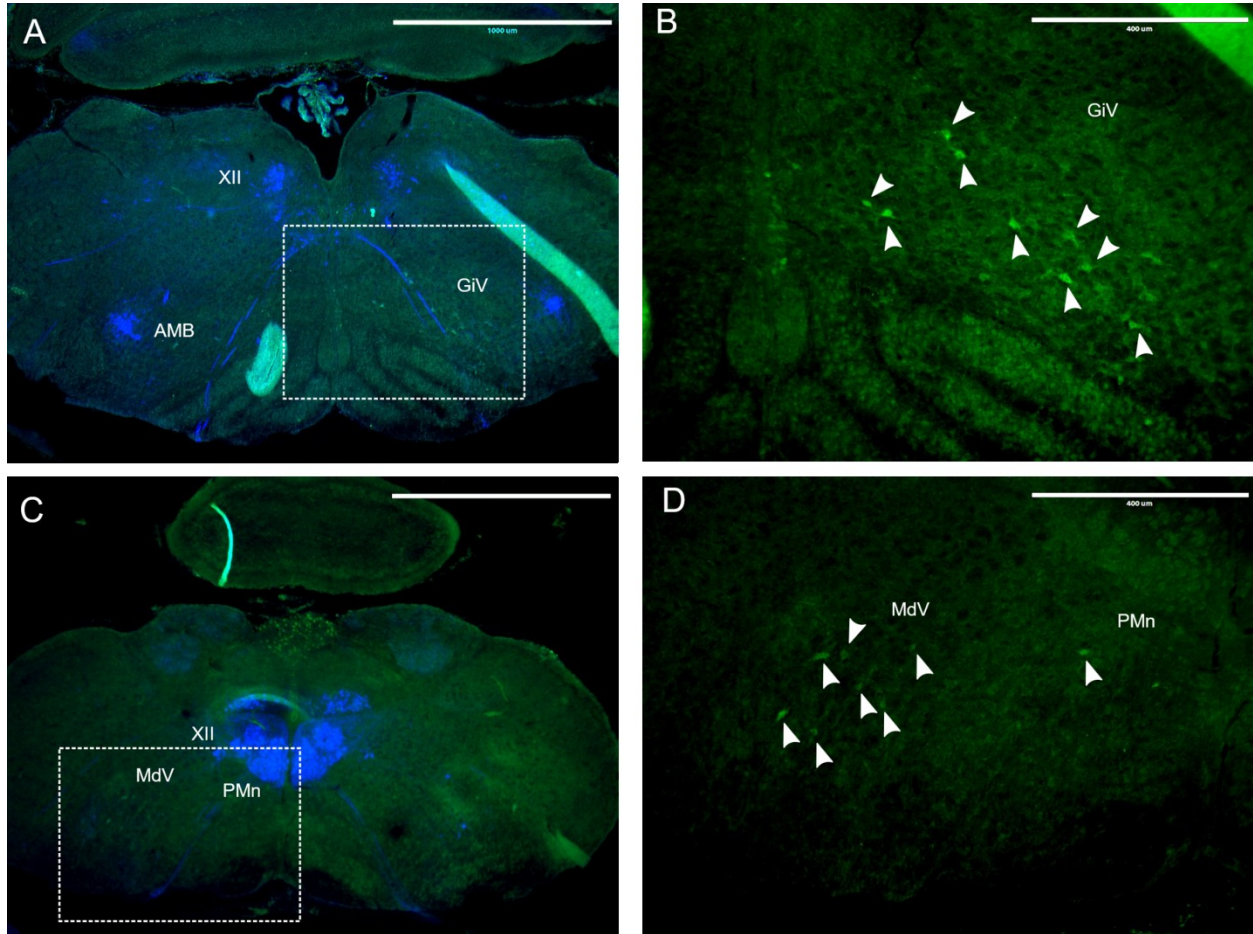
Figure 4.5. Identification of nuclei in the caudal brainstem that project to WT1+ neurons in the lumbar spinal cord. A-D. Transverse section cut from the brainstem 30 h after injection of PRV-Introvert-GFP into the lumbar spinal cord of a WT1^{CreGFP} mouse. Viral infected cells (green) can be seen in the GiV (A-B) and MdV nucleus (C-D). ChAT immunostaining (blue) was performed to identify motor nuclei (hypoglossal nucleus; XII and nucleus ambiguous; amb) for orientation (shown in the low magnification images only). Scale bar 1000 μm (A,C); 400 μm (B,D).

Chapter 5 – General Discussions and Conclusions

Over the course of the past 150 years, our understanding of locomotor control has developed significantly. Much of the work investigating the structure and function of the locomotor CPG has relied on electrophysiological and anatomical approaches to identify component interneurons that make up this neural circuit. Due to the relative simplicity of the nervous system in lower vertebrates, this experimental approach has provided a great deal of information on the neural mechanisms underlying locomotion in the lamprey (Grillner 2003), and Xenopus tadpole (Roberts et al. 1990); however insight into the mammalian locomotor CPG has historically been modest due to the vast number, and heterogeneity, of neurons in the CNS. In the past 20 years, widespread use of molecular genetic techniques has led to a better understanding of the manner in which spinal interneurons develop. This has, in turn, resulted in the division of mammalian spinal interneurons into a manageable number of genetically defined populations (Tanabe and Jessell, 1996). This approach has enabled neuronal populations with a similar genetic lineage to be labeled and studied individually in order to characterize their morphology, anatomical properties, and activity during a locomotor task. Furthermore, each population can be silenced or ablated in order to identify their specific role during stepping. The incorporation of this experimental approach has proven to be a significant milestone for the study of locomotor control as it has provided the first reliable method for consistently identifying component interneurons of the mammalian locomotor CPG. The focus of this thesis has been to use this approach to comprehensively characterize one population of genetically defined interneurons, the WT1-expressing dI6 cells, and determine whether they are involved in shaping locomotor outputs.

5.1 The in vitro upright spinal cord preparation.

In order to understand how the component neurons of the locomotor CPG work in

concert to generate stepping, it is necessary to identify the interneuronal components of this neural circuit and characterize their anatomical and electrophysiological properties. Typically, this has been achieved by recording from single neurons during locomotor activity, identifying those that are rhythmically active, and then determining their key intrinsic properties. Anatomical features of relevant neurons can be identified by inclusion of an intracellular tracer (i.e. Neurobiotin/AlexaFluor) in the recording pipette, and performing post hoc morphological analysis. Historically these experiments have been carried out using the isolated spinal cord (or brainstem/spinal cord) fictive locomotor preparation (Kudo and Yamada 1987; Smith and Feldman 1987) as this allows access to spinal interneurons with a recording pipette. Unfortunately, given the requirement that several segments of the spinal cord must remain intact for fictive locomotor activity to be generated, recordings from locomotor-related neurons have been made using a "blind" approach, which greatly reduces the chance of making a substantial number of recordings from a functionally homogeneous population of interneurons. In order to address this issue, and allow access to genetically-labeled interneuronal populations, several groups have modified the in vitro preparation to facilitate visualized recordings. These modifications have typically involved sectioning the spinal cord in order to reveal specific areas of interest. While it has been demonstrated that the ventral spinal cord must remain intact for fictive locomotor activity to be produced, removal of the dorsal half of the spinal cord does not impact the quality of fictive locomotion, and enables neurons close to the central canal to be targeted for anatomical/electrophysiological characterization during a locomotor task. This preparation has been used to characterize certain members of the Hb9 (Hinckley et al. 2005; Wilson et al. 2007), dI6 (Dyck and Gosgnach 2009), and V2a (Zhong et al. 2010; Dougherty et al., 2013) interneuronal populations, however it does not allow access to any neurons located

below the ventral lip of the central canal- a region which houses the vast majority of interneurons which participate in locomotor activity (Kjaerullf and Kiehn 1996).

To address this limitation, we developed an upright preparation of the spinal cord that allows us to visualize the entire transverse surface. By optimizing this preparation, we are able to make visually-guided, whole cell patch clamp recordings from neurons located across the transverse plane, including those in laminae VII and VIII. Importantly, we also integrated calcium imaging into this preparation which enables the identification of neurons across the transverse plane that are rhythmically active during drug evoked fictive locomotion. Using calcium indicators to monitor neuronal activity greatly improves "throughput" of these experiments since it allows us to focus our characterization solely on those neurons which are locomotor-related. By using this imaging approach in mouse strains that have genetically defined neuronal populations "tagged" with fluorescent proteins we can determine the proportion of each population that are rhythmically active during locomotion, and selectively investigate the anatomical and electrophysiological properties of these specific neurons. This is crucial since it has become apparent that not all members of a genetically-defined population are rhythmically active during locomotion. While the electrophysiological activity of the V1, V2b, and V3 interneuronal populations during locomotion have not been assessed, whole cell recordings from the dI6 (Dyck et al. 2012), V2a (Zhong et al. 2010) and Shox2 (Dougherty et al. 2013) populations have indicated that only a subset of each (53%, 44%, and 67% respectively) are rhythmically active during fictive locomotion, while the remainder are either silent or tonically active. Thus, when considering the electrophysiological features and synaptic connectivity of any of the interneuronal populations the upright spinal cord preparation is well suited to identify those properties that are unique to locomotor-related neurons.

5.2 The role of WT1-expressing interneurons during locomotion.

The transcription factor WT1 is expressed in a subset of the dI6 interneuronal population, and partially overlaps with expression of DMRT3 (Goulding 2009). The primary goal of this thesis was to characterize WT1-expressing neurons and determine whether they play a specific role in shaping locomotor outputs in mammals. Our data indicate that this population of interneurons, which is located in laminae VII and VIII of the postnatal spinal cord, is exclusively inhibitory, and primarily extends commissural axons. Using the upright preparation that we developed (Chapter 2 of the thesis), we were able to record from this population of interneurons and define their activity during fictive locomotion. All WT1-expressing neurons from which we recorded were rhythmically active during pharmacologically induced fictive locomotion, and were tightly correlated with rhythmic ventral root (i.e. motoneuronal) activity. Compared to many of the other genetically-defined populations of interneurons there are relatively few WT1 cells in the spinal cord, despite this fact we show that they play an essential role in securing left-right alternation during stepping as synchronous bursts in flexor and/or extensor related ventral roots is apparent when synaptic transmission from WT1-expressing neurons is blocked. Based solely on their similar transcriptional profile to the V0 population previous work (Lanuza et al. 2004) hypothesized that the dI6 population plays a role in left-right alternation during stepping. The data presented in this thesis a) provides experimental evidence supporting this hypothesis, b) demonstrates the specific subset of the dI6 population involved, and c) provides insight into the mechanism by which this function is carried out.

5.3 Connectivity amongst interneuronal components of the locomotor CPG.

We are approaching 20 years since the first published work incorporating a molecular genetic approach to identify, and functionally characterize, interneuronal components of the

locomotor CPG. While this approach has resulted in a tremendous amount of new data regarding the identity of components of this neural network, we still know little regarding the manner in which these populations are interconnected, or activated by locomotor initiating regions in the midbrain and brainstem. This information is required if we hope to understand how this neural circuit operates, and eventually devise therapies targeted at restoring function after spinal cord injury.

Thus far a number of studies have investigated connectivity using intramuscular injection of the retrograde trans-synaptic tracer pseudorabies (i.e. PRV-152) in order to identify interneuronal populations that contact hindlimb motoneurons. While it is certainly valuable to identify last order interneurons that project to hindlimb motoneurons, it is essential to keep in mind that these experiments do not indicate exclusivity, and that these last order interneurons are also likely to project to other interneuronal populations. Largely due to the lack of an effective assay, relatively little connectivity has been revealed amongst the genetically-defined interneuronal populations, however studies that have incorporated an anterograde approach to investigate the distribution of axon terminals of a given interneuronal population have led to the identification of input to multiple regions, or onto multiple cell types, within the spinal cord (See Table 1.1). Given the vast diversity within each "parent" genetically-defined population these findings are not surprising. While the diversity within each population makes studies into the connectivity of the locomotor CPG more technically demanding, recent progress in the development of viral tracing approaches (reviewed in Luo et al. 2018) suggests that a great deal of data may be generated in the next decade.

The current state of knowledge regarding connectivity of the locomotor CPG is illustrated in Figure 5.1. Each contact is numbered, and a brief description of the function of the cell

population and its connectivity follows. The V0 interneurons which play a role in left-right alternation do so by projecting to multiple targets on the contralateral side of the spinal cord. While connectivity to motoneurons was demonstrated via intramuscular PRV-152 injection (Lanuza et al. 2004), subsequent studies indicated that this pattern is likely only displayed by the $V0_D$ subset as $V0_v$ neurons are disynaptically connected to contralateral motoneurons (Figure 5.1, connections 1 and 2- Griener et al. 2015). Based on the function of $V0_v$ during locomotion, and their excitatory neurotransmitter phenotype (Talpalar et al. 2013), it is assumed that the unidentified interneurons, to which they project, are inhibitory. In preliminary experiments which were completed while carrying out my thesis I investigated the specific genetically-defined population(s) receiving input from V0 interneurons. Using an identical approach to that outlined in Chapter 3 of this thesis I mapped the synaptic terminals of tdTomato expressing neurons in the Dbx1^{Cre}ROSA26^{tdTomato} mouse (which expresses the reporter protein tdTomato in all V0 neurons) and demonstrated that they could be found in close proximity to members of the V1 (Figure 5.2A) and V2a (Figure 5.2B) populations as well as both the WT1- (Figure 5.2C) and DMRT3- (Figure 5.2D) expressing subsets of dI6 cells. Since we were unable to restrict our study to rhythmically-active V0 interneurons there is currently no way to determine which of these pathways may be specifically involved in left-right alternation, however the data highlights the diverse axonal projection pattern that can be possessed by each population.

The V1 population, which is important for regulating locomotor speed, have been shown to project to ipsilateral motoneurons (Figure 5.1, connection 3) however it is unclear whether this projection pattern holds for the entire V1 population, or just the specific subsets which differentiate into RCs and Ia inhibitory interneurons (Saueressig et al. 1999; Sapir et al. 2004). Similarly, V2b neurons, which work together with V1 neurons to coordinate flexor/extensor

alternation, are thought to exert their effect via projections to ipsilateral motoneurons (Figure 5.1, connection 4- Zhang et al. 2014). The Chx10-expressing V2a cells have been shown to regulate left right alternation via excitatory input onto ipsilateral $V0_v$ interneurons (Figure 5.1, connection 5- Crone et al. 2008) while a second subset of V2a neurons, which express Shox2, project directly to motoneurons (Figure 5.1, connection 7- Dougherty et al. 2013). V3 interneurons, which are involved in locomotor stability, have recently been divided into a medial and lateral subpopulation based on their position in the spinal cord (Chopek et al. 2018). The medially located V3s are interconnected with each other and project to lateral V3 interneurons. The lateral V3s project to ipsilateral motoneurons and simultaneously send descending projections to other spinal segments on the contralateral side of the spinal cord (Figure 5.1, connection 6- Chopek et al. 2018).

Finally, regarding the dI6 population, the DMRT3-expressing subset have previously been shown to project monosynaptically to ipsilateral and contralateral motoneurons (Figure 5.1, connection 8- Andersson et al. 2012; Perry et al. 2018) while data presented in this thesis indicates that the WT1-expressing subset project onto DMRT3 and Evx1+ $V0_v$ (Figure 5.1, connection 9) cells, two subtypes also involved in regulating left-right alternation, and receive monosynaptic input primarily from DMRT3-expressing interneurons within the lumbar and cervical segments of the spinal cord (Figure 5.1, 10).

In addition to intraspinal connectivity we also identified connectivity between brainstem sites and WT1-expressing interneurons in the lumbar spinal cord. If we consider that the neurons within the CPG are organized according to the two-layer model, which dictates that neurons involved in forming the motor pattern of locomotion receive projection from a group of neurons responsible for generating the motor rhythm, it is surprising that WT1 neurons receive

monosynaptic input from the caudal brainstem nuclei MdV and GiV. However, as it was shown that neurons in the MdV mediates forelimb grasping (Esposito et al. 2014), and because we found that the WT1 neurons receive synaptic input from MdV as well as DMRT3 neurons in the cervical spinal segment (where forelimb CPG resides), the WT1 neurons may be part of forelimb-hindlimb coordination in quadrupedal animals. Based on the projection of WT1 neurons onto $V0_V$ and DMRT3 neurons, when the WT1 neurons are recruited during overground locomotion, it could potentially modulate the activity of motoneurons via DMRT3 mediated disynaptic pathway or $V0_V$ mediated oligosynaptic pathway. In the disynaptic pathway, the WT1 neurons will exert an inhibitory effect on DMRT3 neurons which would otherwise inhibit the motoneurons thus resulting in the excitation of the motoneurons. In the oligosynaptic pathway the WT1 neurons will inhibit the $V0_V$ neurons which in turn removes excitation from an unknown class of inhibitory that projects to motoneurons and thus resulting in the inhibition of the motoneurons. Because we postulate that the WT1 neurons can both excite or inhibit the activity of motoneurons given the specific pathway it takes, this could potentially explain our finding that inhibiting WT1 neurons result in moderate disruption in left right alternation.

5.4 Limitations of this study

Over the past decade, as the molecular tools used to analyze the locomotor CPG have been refined, additional genetic markers have been identified which has resulted in the division of each of the V0-V3 interneuronal populations into two or more of subsets (Gosgnach et al. 2017). The extent of diversity within each "parent" population varies. As an example, the V0 population can be divided into the Dbx1-expressing $V0_D$ neurons and the Evx1-expressing $V0_V$ neurons, while the V1 population can be divided up into 19 genetically distinct subsets (Bikoff et al. 2016). At this point, it seems as if the extent of diversity within each parent population is

limited simply by the tools used for investigation- the more detailed the investigation the greater number of subsets that can be found. When considering the V1 population it has been shown that each genetically distinct subset has distinct physiological characteristics, and occupies a distinct position in the ventral spinal cord (Bikoff et al. 2016). These findings limit the conclusions we can draw when interpreting our data characterizing the WT1-expressing neurons as it is likely that additional diversity may exist within this population.

In addition, although isolated spinal cord preparation has been indispensable for the electrophysiological and anatomical characterization of the interneuronal populations that are involved in locomotor activity, fictive locomotion captured in reduced isolated spinal cord preparation does not truly reflect the complexity of gait in a freely moving animal. Hence the function of each interneuronal population, including the WT1-neurons, needs to be tested *in vivo* in order to truly determine the role that these interneuronal populations play during stepping. Again, the development of viral approaches to deliver various reporter proteins and molecules capable of activating/inactivating specific cell populations (Luo et al. 2018), together with the finer grain molecular dissection of each interneuronal population has the potential to address this issue, and determine whether the function of a given cell population in a fictive locomotor preparation accurately reflects their role during overground stepping.

Finally, In this project we probed the function of the WT1 interneuronal population using DREADDs (designer receptors exclusively activated by designer drugs), a powerful new technique in behavioural studies for modulating the activity of targeted neuronal subpopulation by activating synthetically derived receptors using synthetic ligands (Roth 2016). Neurons expressing the DREADD can be activated or inhibited by administering an exogenous ligand, CNO. Although CNO itself is a biologically inert substance (Roth et al. 1994), it can be back

metabolized to clozapine which can readily cross the blood brain barrier where it interacts with numerous endogenous receptors such as 5-HT, or dopamine (Jann et al. 1994; MacLaren et al. 2016; Gomez et al. 2017). Clozapine acts as an antagonist at these receptors sites and can have a myriad of downstream effects. However, these limitations do not affect the interpretation of our results where we used CNO to selectively inhibit the activity in our WT1 neurons expressing the DREADD receptor since we are using an in vitro spinal cord preparation where the CNO is bath applied for a short period of time and thus chances of CNO metabolizing to clozapine is virtually none. Furthermore, our control experiments indicate that that CNO has no substantial effect on the fictive locomotor pattern.

5.5 Future directions.

Work presented in this thesis characterizes the WT1-expresing interneurons, describes their function, and provides insight into the synaptic connectivity that may be attributed to that function. As the dI6 population can be divided into at least three subsets (WT1+, DMRT3+ and WT1+DMRT3+) the logical next step would be to identify the functional role of neurons that co-express the two transcription factors and determine if they have a complementary role to the WT1-expressing, and DMRT3-expressing neurons.

Given that we have found the WT1+ cells to receive monosynaptic input from caudal brainstem nuclei involved in locomotor control – the GiV and the MdV, it will be interesting to identify the role of this pathway in shaping the motor output. Reticular neurons in the Gi and MdV have been shown by others to project to forelimb motoneurons and monosynaptic input from the MdV to motoneurons in the cervical spinal cord is particularly important for manipulation of the forelimbs (Esposito et al. 2014). Our data indicating that WT1-expressing neurons receive synaptic input from DMRT3 neurons located in the cervical segments and also

from GiV and MdV could be an indication that this pathway is important for hindlimb-forelimb coordination. Future work to test this hypothesis could involve injection of a retrograde virus expressing inhibitory rhodopsin (i.e. archaerhodopsin- Arch) into the spinal cord such that it is taken up by WT1+ and transports Arch to all monosynaptically connected neurons. Optogenetics can then be used to silence this specific neural pathway, identify the changes in locomotor pattern in freely behaving animals, and determine whether the WT1-expressing neurons play additional roles in shaping locomotor outputs.

REFERENCES

Armbruster BN, Li X, Pausch MH, Herlitze S, Roth BL. Evolving the lock to fit the key to create a family of G protein-coupled receptors potently activated by an inert ligand. Proc Natl Acad Sci USA. 2007; 104(12):5163-8.

Andersson LS, Larhammar M, Memic F, Wootz H, Schwochow D, Rubin CJ, Patra K, Arnason T, Wellbring L, Hjälm G, Imsland F, Petersen JL, McCue ME, Mickelson JR, Cothran G, Ahituv N, Roepstorff L, Mikko S, Vallstedt A, Lindgren G, Andersson L, Kullander K. (2012) Mutations in DMRT3 affect locomotion in horses and spinal circuit function in mice. *Nature.* 488(7413):642-6.

Bikoff JB, Gabitto MI, Rivard AF, Drobac E, Machado TA, Miri A, Brenner-Morton S, Famojure E, Diaz C, Alvarez FJ, Mentis GZ, and Jessell TM. (2016) Spinal inhibitory interneuron diversity delineates variant motor microcircuits. *Cell.* 165(1): 207-219.

Chopek JW, Nascimento F, Beato M, Brownstone RM, Zhang Y. (2018) Sub-populations of Spinal V3 Interneurons Form Focal Modules of Layered Pre-motor Microcircuits. *Cell Reports.* 25(1):146-156

Crone SA, Quinlan KA, Zagoraiou L, Droho S, Restrepo CE, Lundfald L, Endo T, Setlak J, Jessell TM, Kiehn O, Sharma K. (2008). Genetic ablation of V2a ipsilateral interneurons disrupts left-right locomotor coordination in mammalian spinal cord. *Neuron.* 60:70-83.

Dougherty KJ, Zagoraiou L, Satoh D, Rozani I, Doobar S, Arber S, Jessell TM, Kiehn O. (2013). Locomotor rhythm generation linked to the output of spinal shox2 excitatory interneurons. *Neuron.* 80:920-933.

Dyck J and Gosgnach S (2009) Whole cell recordings from visualized neurons in inner laminae of the functionally intact spinal cord. *J Neurophysiol.* 102:590-597.

Dyck J, Lanuza GM, Gosgnach S. (2012) Functional characterization of dI6 interneurons in the neonatal mouse spinal cord. *J Neurophysiol.* 107(12):3256-66.

Esposito MS, Capelli P, Arber S. (2014) Brainstem nucleus MdV mediates skilled forelimb motor tasks. *Nature.* 508(7496):351-6.

Gomez JL, Bonaventura J, Lesniak W, Mathews WB, Sysa-Shah P, Rodriguez LA et al (2017). Chemogenetics revealed: DREADD occupancy and activation via converted clozapine. Science 357: 503–507.

Gosgnach, S. et al., 2017. Delineating the Diversity of Spinal Interneurons in Locomotor Circuits. *The Journal of Neuroscience*, 37(45), pp.10835–10841.

Goulding, M., 2009. Circuits controlling vertebrate locomotion: Moving in a new direction. *Nature Reviews Neuroscience.* 10(7):507-18.

Griener A, Zhang W, Kao H, Wagner C, Gosgnach S (2015) Probing diversity within subpopulations of locomotor-related V0 interneurons. *Dev Neurobiol.* 75(11):1189-203.

Grillner, S., 2003. The motor infrastructure: from ion channels to neuronal networks. *Nature Review Neuroscience.* 4(7): 573-86.

Hinckley CA, Hartley R, Wu L,Todd A, Ziskind-Conhaim L (2005) Locomotor-like rhythms in a

   genetically distinct cluster of interneurons in the mammalian spinal cord. *J. Neurophysiology*.

   93:1439–49.

Jann MW, Lam YW, Chang WH. (1994) Rapid formation of clozapine in guinea-pigs and man

   following clozapine-N-oxide administration. Arch. Int. Pharmacodyn. Ther. 328: 243-250.

Kjaerulff, O., and Kiehn, O. (1996). Distribution of networks generat- ing and coordinating

   locomotor activity in the neonatal rat spinal cord in vitro: a lesion study. *J. Neurosci.* 16,

   5777–5794.

Kudo N, Yamada T (1987) N-methyl-D-aspartate induced locomotor activity in a spinal cord

   hind limb muscle preparation of the newborn studied in vitro. *Neuroscience Letter.* 75:43–48.

Lanuza, G.M. et al., 2004. Genetic identification of spinal interneurons that coordinate left-right

   locomotor activity necessary for walking movements. *Neuron.* 42(3):375-86.

Luo L., Callaway E.M., Svoboda K., 2018. Genetic Dissection of Neural Circuits: A Decade of

   Progress. *Neuron.* 98(2): 256-281.

MacLaren DA, Browne RW, Shaw JK, Krishnan Radhakrishnan S, Khare P et al (2016).

   Clozapine N-oxide administration produces behavioral effects in Long-Evans rats:

   implications for designing DREADD experiments. eNeuro 3. pii: ENEURO.0219-16.2016.

Perry S, Larhammar M, Vieillard J, Nagaraja C, Hilscher MM, Tafreshiha A, Rofo F, Caixeta

   FV, Kullander K. (2019) Characterization of Dmrt3-Derived Neurons Suggest a Role within

   Locomotor Circuits. *J Neurosci.* 39(10):1771-1782.

Roberts A. (1990) How does a neurons system produce behavior? A case study in neurobiology. Science Progress. 74, 31-51.

Roth BL. (2016) DREADDs for Neuroscientists. Neuron. 89(4), p683-694.

Roth BL, Craigo SC, Choudhary MS, Uluer A, Monsma Jr, FJ, Shen Y, Meltzer HY, Sibley DR. (1994) Binding of typical and atypical antipsychotic agents to 5-hydroxytryptamine-6 and 5-hydroxytryptamine-7 receptors. J. Pharmacol. Exp. Ther. 268: 1403-1410.

Sapir T, Geiman EJ, Wang Z, Velasquez T, Mitsui S, Yoshihara Y, Frank E, Alvarez FJ, Goulding M. (2004) Pax6 and Engrailed 1 regulate two distinct aspects of Renshaw cell development. J. Neurosci. 24:1255–1264.

Saueressig H., Burrill J., Goulding M. (1999) Engrailed-1 and netrin-1 regulate axon pathfinding by association interneurons that project to motor neurons. *Development*. 126: 4201-4212.

Smith JC, Feldman JL (1987) In vitro brainstem-spinal cord preparations for study of motor systems for mammalian respiration and locomotion. *J Neuroscience Methods*. 21:321–333.

Talpalar AE, Bouvier J, Borgius L, Fortin G, Pierani A, Kiehn O (2013). Dual-mode operation of neuronal networks involved in left-right alternation. *Nature*. 500:85-88.

Tanabe Y, Jessell TM. (1996) Diversity and pattern in the developing spinal cord. *Science*. 274(5290):1115-23.

Wilson J, Dombeck D, Diaz-Rios M, Harris-Warrick R, Brownstone R (2007) Two-photon
calcium imaging of network activity in XFP-expressing neurons in the mouse. *J Neurophys*
97:3118-25.

Zhang J, Lanuza GM, Britz O, Wang Z, Siembab VC, Zhang Y, Velasquez T, Alvarez FJ, Frank
E, Goulding M. (2014) V1 and v2b interneurons secure the alternating flexor-extensor motor
activity mice require for limbed locomotion. *Neuron*. 82(1):138-50.

Zhong G., Droho S., Crone S.A., Dietz S., Kwan A.C., Webb W.W., Sharma K., and Harris
Warrick R.M. (2010) Electrophysiological Characterization of V2a Interneurons and Their
Locomotor-Related Activity in the Neonatal Mouse Spinal Cord. *The Journal of
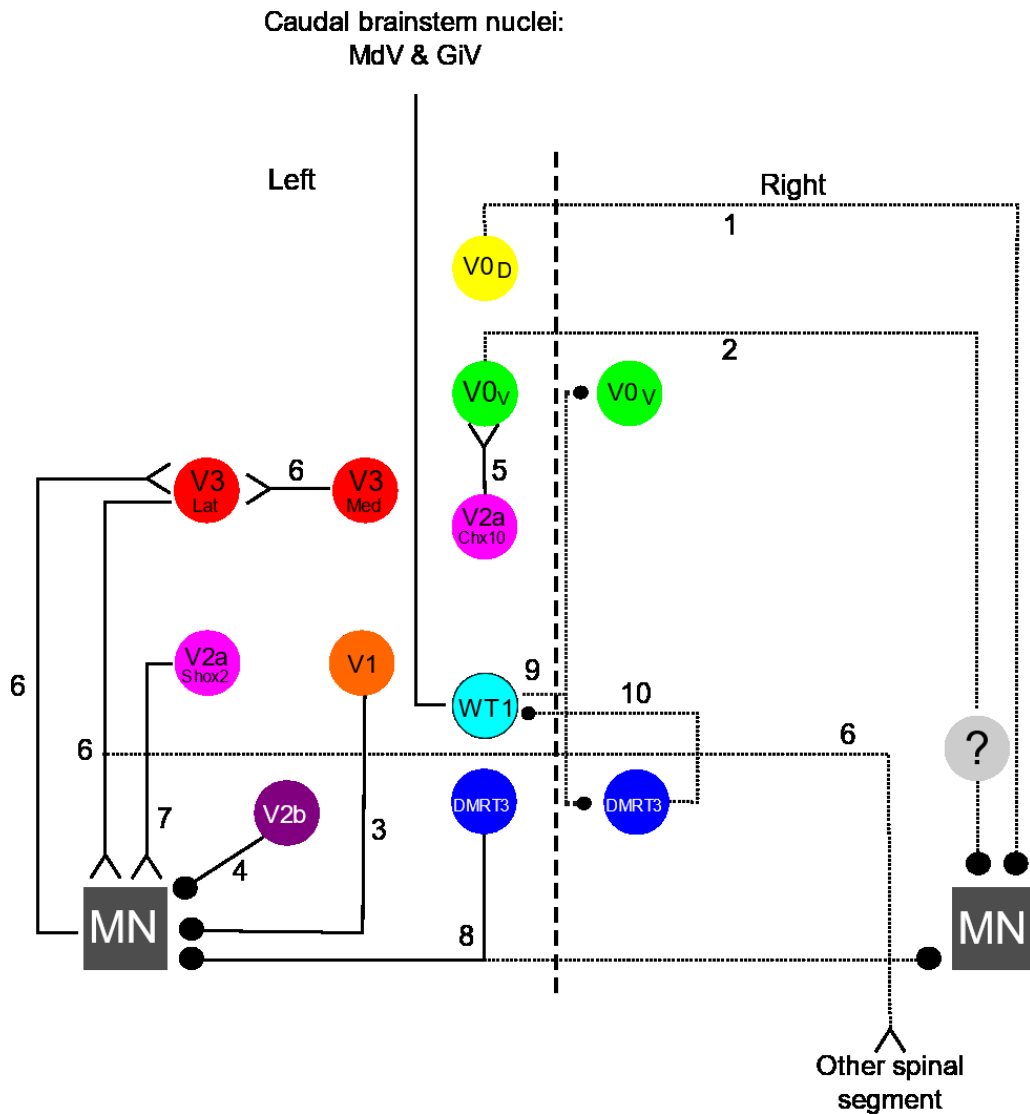Neuroscience*. 30(1):170 –182.

Figure 5.1. Connectivity of spinal neurons within the circuitry for locomotor CPG. Synaptic connectivity shown to exist amongst component interneurons of the locomotor CPG. Inhibitory synapses indicated by a filled circle at the termination point, excitatory synapses indicated by (Y). Ipsilateral projections are indicated by solid lines and contralateral projections by dashed lines. Each "connection" is numbered and details are provided in the General Discussion.
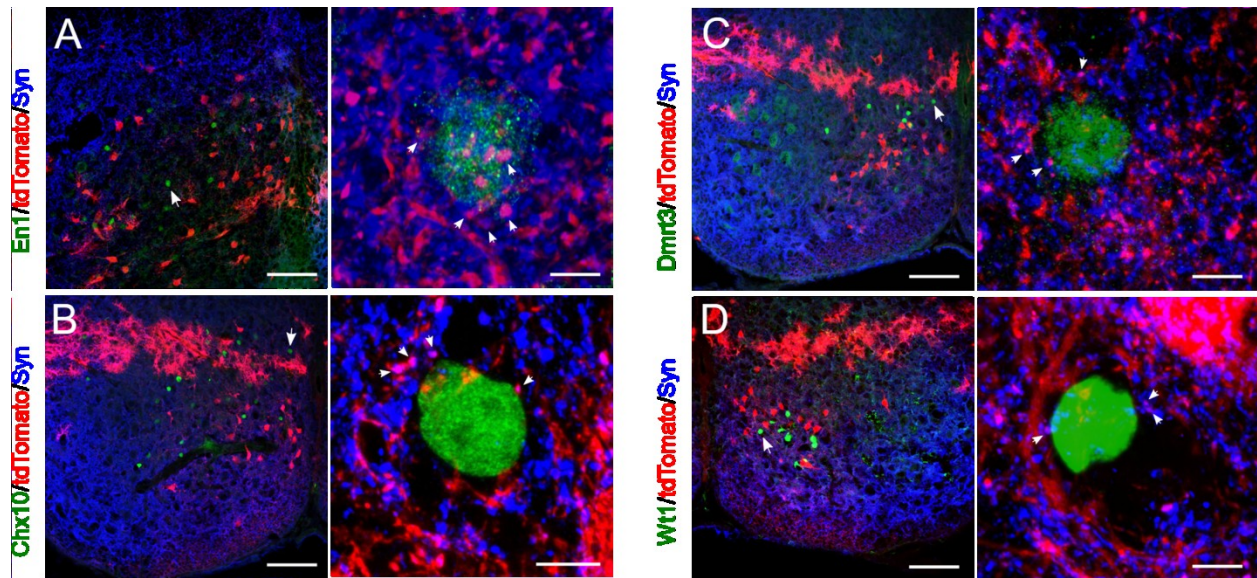
Figure 5.2. Connectivity of V0 interneurons onto other genetically defined interneuronal populations.

(A-D). 20 uM thick sections cut from a P0 Dbx1^{Cre}ROSA26^{tdTomato} spinal cord (n=2) and stained with antibodies to tdTomato (red), the synaptic marker Synatotagmin (blue), as well as En1, Chx10, DMRT3 or WT1 (green cells in A-D). In order to identify presumptive synapses from V0 neurons onto genetically defined interneuronal subtypes we inspected the "halo" surrounding each labeled nuclei for tdTomato+/synaptotagmin+ terminals. These terminals (indicated by arrows in the high magnification panels to the right) were commonly seen in close proximity to each of the four cell types. Scale bar in all low magnification images indicates 100 μm and in high magnification image 5 μm.

COMPREHENSIVE BIBLIOGRAPHY

Afelt, Z. (1970) Reflex activity in chronic spinal cats. Acta Neurobiol. 30:129-144.

Al-Mosawie, A., Wilson, J.M. and Brownstone, R.M., (2007) Heterogeneity of V2-derived interneurons in the adult mouse spinal cord. European Journal of Neuroscience. 26(11):3003-15.

Alstermark B, Lundberg A, Pinter M, and Sasaki S. (1987) Subpopulations and functions of long C3–C5 propriospinal neurons. *Brain Res* 404: 395–400.

Alvarez FJ, Jonas PC, Sapir T, Hartley R, Berrocal MC, Geiman EJ, Todd AJ, Goulding M. (2005) Postnatal phenotype and localization of spinal cord V1 derived interneurons. J Comp Neurol. 493(2):177-92.

Anden NE, Lundberg A, E Rosengren LV. 1963. The effect of DOPA on spinal reflexes from the FRA (flexor reflex afferents). 229, pp.654–655.

Anden, N.E., Carlsson, A., Hillarp, N.A., and Magnusson T. (1964) 5-Hydroxytryptamine release by nerve stimulation of the spinal cord. Life Sci. 3: 473-478.

Anden, N.E., Carlsson, A., Hillarp, N.A., and Magnusson T. (1965) Noradrenaline release by nerve stimulation of the spinal cord. Life Sci. 4: 129-132.

Andersson LS, Larhammar M, Memic F, Wootz H, Schwochow D, Rubin CJ, Patra K, Arnason T, Wellbring L, Hjälm G, Imsland F, Petersen JL, McCue ME, Mickelson JR, Cothran G, Ahituv N, Roepstorff L, Mikko S, Vallstedt A, Lindgren G, Andersson L, Kullander K. (2012) Mutations in DMRT3 affect locomotion in horses and spinal circuit function in mice. *Nature.* 488(7413):642-6.

Angeli, CA, Edgerton, VR, Gerasimenko, YP, Harkema, SJ. (2014). Altering spinal cord excitability enables voluntary movements after chronic complete paralysis in humans. Brain 137:1394–409.

Antri M, Mellen N, Cazalets JR. (2011). Functional organization of locomotor interneurons in the ventral lumbar spinal cord of the newborn rat. PLoS One 6:e20529.

Armbruster BN, Li X, Pausch MH, Herlitze S, Roth BL. Evolving the lock to fit the key to create a family of G protein-coupled receptors potently activated by an inert ligand. Proc Natl Acad Sci USA. 2007; 104(12):5163-8.

Armstrong JF, Pritchard-Jones K, Bickmore WA, Hastie ND, Bard JB. (1993). The expression of the Wilms' tumour gene, WT1, in the developing mammalian embryo. Mech Dev. 40:85-97.

Armstrong DM., Saper CB., Levey AI., Wainer BH., and Terry RD. (1983) Distribution of cholinergic neurons in rat brain: Demonstrated by the immunocytochemical localization of choline acetyltransferase. *Jouranl of Comparative Neurology*. 216(1):53-68.

Ballion B., Morin D., and Viala D. (2001) Forelimb locomotor generators and quadrupedal locomotion in the neonatal rat. Eur. *J. Neurosci.* 14, 1727–1738.

Barbeau, H. and Rossignol, S. (1991) Initiation and modulation of the locomotor pattern in the adult chronic spinal cat by noradrenergic, serotonergic and dopaminergic drugs. Brain Research. 546(2):250-60.

Barbeau, H. and Rossignol, S. (1990) The effects of serotonergic drugs on the locomotor pattern and on cutaneous reflexes of the adult chronic spinal cat. Brain Research.

Bellardita C, Kiehn O. (2015). Phenotypic characterization of speed-associated gait changes in mice reveals modular organization of locomotor networks. Curr Biol. 25:1426-1436.

Bikoff JB, Gabitto MI, Rivard AF, Drobac E, Machado TA, Miri A, Brenner-Morton S, Famojure E, Diaz C, Alvarez FJ, Mentis GZ, Jessell TM. (2016). Spinal Inhibitory Interneuron Diversity Delineates Variant Motor Microcircuits. Cell. 165:207-219.

Bernau NA, Puzdrowki RL, Leonard RB (1991) Identification of the midbrain locomotor region and its relation to descending locomotor pathways in the Atlantic stingray,Dasyatis sabina. Brain Res 557:83–94.

Briscoe J, Pierani A, Jessell TM, and Ericson J. (2000) A homeodomain protein code specifies progenitor cell identity and neuronal fate in the ventral neural tube. Cell. 101(4):435-45.

Britz, O. Zhang J, Grossmann KS, Dyck J, Kim JC, Dymecki S, Gosgnach S, Goulding M. (2015) A genetically defined asymmetry underlies the inhibitory control of flexor-extensor locomotor movements. eLife, pp.1–22.

Brown, T.G. (1911) The intrinsic factors in the act of progression in mammals. Proc. R. Soc. B, 84, pp. 308-319

Brown, T.G. (1912) The Factors in Rhythmic Activity of the Nervous System. Royal Society Publishing.

Brown, TG. (1913) The phenomenon of "narcosis progression" in mammals. Proc. R. Soc. B 86, 140–164.

Brown, T.G. (1914) On the nature of the fundamental activity of the nervous centres; together with an analysis of the conditioning of rhythmic activity in progression, and a theory of the evolution of function in the nervous system. Physiology, 48(1), pp.18–46.

Buchanan JT, Grillner S. (1987) Newly identified 'glutamate interneurons' and their role in

locomotion in the lamprey spinal cord. Science, 236, pp. 312-314

Buchanan JT, Grillner, S. (1988) A new class of small inhibitory interneurones in the lamprey

spinal cord. Brain Res., 438, pp. 404-407

Butt SJ, Kiehn O 2003. Functional identification of interneurons responsible for left-right

coordination of hindlimbs in mammals. Neuron 38: 953-963.

Caggiano V.,Leiras R., Goñi-Erro H., Masini D., Bellardita C., Bouvier J., Caldeira V., Fisone

G., Kiehn O. (2018) Midbrain circuits that set locomotor speed and gait selection. *Nature*.

553: 455-460

Caldeira V, Dougherty KJ, Borgius L, Kiehn O. (2017) Spinal Hb9::Cre-derived excitatory

interneurons contribute to rhythm generation in the mouse. Scientific Reports. 7:41369.

Cangiano, L., Wallen, P. and Grillner, S. (2002) Role of apamin-sensitive KCa channels for

reticulospinal synaptic transmission to motoneuron and for the afterhyperpolarization. J.

Neurophysiol. 88, 289–299.

Cangiano L, Grillner S. (2003) Fast and slow locomotor burst generation in the hemi-spinal cord

of the lamprey. J. Neurophysiol. 89(6):2931–42.

Cangiano L, Grillner S. (2005) Mechanisms of rhythm generation in a spinal locomotor network

deprived of crossed connections: the lamprey hemicord. J. Neurosci. 25(4):923–35.

Capelli, P., Pivetta, C., Esposito, M.S., and Arber, S. (2017). Locomotor speed control circuits in

the caudal brainstem. *Nature* 551, 373–377.

Cazalets, J.R., Sqalli-Houssaini, Y. and Clarac, F., (1992). Activation of the central pattern generators for locomotion by serotonin and excitatory amino acids in neonatal rat. J. Physiol., 455:187-204.

Chopek JW, Nascimento F, Beato M, Brownstone RM, Zhang Y. (2018) Sub-populations of Spinal V3 Interneurons Form Focal Modules of Layered Pre-motor Microcircuits. Cell Reports. 25(1):146-156.

Christie KJ, Whelan PJ. (2005). Monoaminergic establishment of rostrocaudal gradients of rhythmicity in the neonatal mouse spinal cord. J Neurophysiol. 94:1554-1564.

Clarac F, 2005. The history of reflexes. Part 2: from Sherrington to 2004. IBRO Neuro History

Cowley KC and Schmidt BJ. (1994). A comparison of motor patterns induced by N-methyl-D-aspartate, acetylcholine and serotonin in the in vitro neonatal rat spinal cord. Neurosci Lett. 171:147-150.

Cowley KC and Schmidt BJ. (1995) Effects of inhibitory amino acid antagonists on reciprocal inhibitory interactions during rhythmic motor activity in the in vitro neonatal rat spinal cord. J Neurophysiol. 74(3):1109-17.

Cowley KC and Schmidt BJ. (1997) Regional distribution of the locomotor pattern-generating network in the neonatal rat spinal cord. Journal of neurophysiology. 77(1):247-59.

Cowley KC, Zaporazhets E, Schmidt BJ. (2008) Propriospinal neurons are sufficient for bulbospinal transmission of the locomotor command signal in the neonatal rat spinal cord. *J Physiol* 586: 1623–1635.

Cowley KC, Zaporazhets E, Schmidt BJ. (2010) Propriospinal transmission of the locomotor command signal in the neonatal rat. *Ann NY Acad Sci* 1198: 42–53.

Crone SA, Quinlan KA, Zagoraiou L, Droho S, Restrepo CE, Lundfald L, Endo T, Setlak J, Jessell TM, Kiehn O, Sharma K. (2008). Genetic ablation of V2a ipsilateral interneurons disrupts left-right locomotor coordination in mammalian spinal cord. Neuron. 60:70-83.

Crone SA, Zhong G, Harris-Warrick R, Sharma K. (2009) In Mice Lacking V2a Interneurons, Gait Depends on Speed of Locomotion. Journal of Neuroscience. 29(21):7098-109.

Dai X, Noga BR, Douglas JR, Jordan LM. (2005). Localization of spinal neurons activated during locomotion using the c-fos immunohistochemical method. J Neurophysiol. 93:3442-3452.

Danner, SM, Hofstoetter, US, Freundl, B, Binder, H, Mayr, W, Rattay, F, Minassian, K. (2015). Human spinal locomotor control is based on flexibly organized burst generators. Brain 138:577–588.

Danner SM, Shevtsova NA, Frigon A, Rybak IA. (2017). Computational modeling of spinal circuits controlling limb coordination and gaits in quadrupeds. eLife. pii:e31050.

Dhalstrom A. & Fuxe K. (1964) Evidence for the existence of monoamine neurons in the central nervous system - I. Demonstration of monoamines in the cell bodies of brainstem neurons. Acta physiologica Scandinavica. 232:1-55.

Dietz V. (2002) Do human bipeds use quadrupedal coordination? *Trends in Neuroscience.* 25(9):462-7.

Dimitrijevic, MR, Gerasimenko, Y, Pinter, MM. (1998). Evidence for a spinal central pattern generator in humans. Ann N Y Acad Sci 860:360–76.

Dominici, N, Ivanenko, YP, Cappellini, G, d'Avella, A, Mondì, V, Cicchese, M, Fabiano, A, Silei, T, Di Paolo, A, Giannini, C, Poppele, RE, Lacquanti, F. (2011). Locomotor primitives in newborn babies and their development. Science 334:997–9.

Dougherty KJ, Zagoraiou L, Satoh D, Rozani I, Doobar S, Arber S, Jessell TM, Kiehn O. (2013). Locomotor rhythm generation linked to the output of spinal shox2 excitatory interneurons. Neuron. 80:920-933.

Drew T, Rossignol S. (1984) Phase-dependent responses evoked in limb muscles by stimulation of medullary reticular formation during locomotion in thalamic cats. *J Neurophysiol.* 52(4):653-75.

Dubuc R, Brocard F, Antri M, Fénelon K, Gariépy JF, Smetana R, Ménard A, Le Ray D, Viana Di Prisco G, Pearlstein É, Sirota MG, Derjean D, St-Pierre M, Zielinski B, Auclair F, Veilleux D (2008) Initiation of locomotion in lampreys. Brain Res Rev 57:172–182.

Dyck J and Gosgnach S (2009) Whole cell recordings from visualized neurons in inner laminae of the functionally intact spinal cord. *J Neurophysiol.* 102:590-597.

Dyck J, Lanuza GM, Gosgnach S. (2012) Functional characterization of dI6 interneurons in the neonatal mouse spinal cord. *J Neurophysiol.* 107(12):3256-66.

Eidelberg E, Yu J (1981) Effects of corticospinal lesions upon treadmill locomotion by cats. Exp brain Res 43:101–103.

El Manira A, Tegner J, Grillner S. (1994) Calcium-dependent potassium channels play a critical role for burst termination in the locomotor network in lamprey. J. Neurophysiol. 72, 1852–1861.

Engberg I. & Lundberg A. (1969) An Electromyographic Analysis of Muscular Activity in the Hindlimb of the Cat during Unrestrained Locomotion. Acta Physiologica Scandinavica. 75(4):614-30.

Esposito MS, Capelli P, Arber S. (2014) Brainstem nucleus MdV mediates skilled forelimb motor tasks. *Nature.* 508(7496):351-6.

Flynn JR, Conn VL, Boyle KA, Hughes DI, Watanabe M, Velasquez T, Goulding MD, Callister RJ and Graham BA (2017) Anatomical and Molecular Properties of Long Descending Propriospinal Neurons in Mice. *Front. Neuroanat.* 11:5.

Gatto G, Smith KM, Ross SE, Goulding M. (2019). Neuronal diversity in the somatosensory system: bridging the gap between cell type and function. Curr Opin Neurobiol. 56:167-174.

Getting PA. (1989). Emerging principles governing the operation of neural networks. Annu. Rev. Neurosci. 12:185–204.

Gomez JL, Bonaventura J, Lesniak W, Mathews WB, Sysa-Shah P, Rodriguez LA *et al* (2017). Chemogenetics revealed: DREADD occupancy and activation via converted clozapine. Science 357: 503–507.

Gordon IT, Whelan PJ. (2006). Monoaminergic control of cauda-equina-evoked locomotion in the neonatal mouse spinal cord. J Neurophysiol. 96:3122-3129.

Gosgnach S, Lanuza GM, Butt SJ, Saueressig H, Zhang Y, Velasquez T, Riethmacher D, Callaway EM, Kiehn O, Goulding M. (2006) V1 spinal neurons regulate the speed of vertebrate locomotor outputs. Nature. 440(7081):215-9.

Gosgnach S, Bikoff JB, Dougherty KJ, El Manira A, Lanuza GM, Zhang Y. (2017) Delineating the Diversity of Spinal Interneurons in Locomotor Circuits. *The Journal of Neuroscience*. 37(45), pp.10835–10841.

Goulding, M., (2009) Circuits controlling vertebrate locomotion: Moving in a new direction. Nature Reviews Neuroscience. 10(7):507-18.

Goulding M, Bourane S, Garcia-Campmany L, Dalet A, Koch S. (2014). Inhibition downunder: an update from the spinal cord. Curr Opin Neurobiol. 26 161-166.

Griener A, Zhang W, Kao H, Wagner C, Gosgnach S (2015) Probing diversity within subpopulations of locomotor-related V0 interneurons. *Dev Neurobiol*. 75(11):1189-203.

Griener A, Zhang W, Kao H, Haque F, Gosgnach S. (2017). Anatomical and electrophysiological characterization of a population of dI6 interneurons in the neonatal mouse spinal cord. Neuroscience. 362:47-59.

Grillner, S., (1981) Control of Locomotion in Bipeds, Tetrapods, and Fish. In M. V. In: Brookhart JM, ed. Comprehensive Physiology. Bethesda.

Grillner, S., (2003) The motor infrastruction: from ion channels to neuronal networks. Nature Review Neuroscience. 4(7): 573-86.

Grillner, S., Buchanan, J.T. & Lansner, A., (1988) Simulation of the segmental burst generating

network for locomotion in lamprey. Neuroscience Letters. 89(1):31-5.

Grillner, S., Hongo, T. & Lund, S., (1968) The origin of descending fibres monosynaptically activating spinoreticular neurones. Brain Research. 10(2):259-62.

Grillner S, Jessell TM (2009). Measured motion: searching for simplicity in spinal locomotor networks. Curr. Opin. Neurobiol. 19:572-586.

Grillner, S., Wallén, P., Hill, R., Cangiano, L., & El Manira, A. (2001). Ion channels of importance for the locomotor pattern generation in the lamprey brainstem-spinal cord. The Journal of physiology. 533(Pt 1), 23–30.

Grillner, S. and Zangger, P. (1975) How detailed is the central pattern generation for locomotion? Brain Research.

Grillner, S. and Zangger, P. (1979) On the central generation of locomotion in the low spinal cat. Exp. Brain Res. 34: 241-261.

Gross, MK, Dottori, M, Goulding, M (2002). Lbx1 specifies somatosensory association interneurons in the dorsal spinal cord. Neuron 34:535–549.

Guertin, PA. (2014). Preclinical evidence supporting the clinical development of central pattern generator-modulating therapies for chronic spinal cord-injured patients. Front Hum Neurosci

Ha NT, Dougherty KJ. (2018). Spinal Shox2 interneuron interconnectivity related to function and development. Elife. 31 pii: e42519.

Hägglund, M., Borgius, L., Dougherty, K.J., Kiehn, O. (2010) Activation of groups of excitatory neurons in the mammalian spinal cord or hindbrain evokes locomotion. Nature

Neuroscience. 13(2): 246-52.

Hägglund M, Dougherty K.J., Borgius L., Itohara S., Iwasato T. and Kiehn O. (2013) Optogenetic dissection reveals multiple rhythmogenic modules underlying locomotion. Proc. Natl Acad. Sci. 110:11589–11594.

Haque F, Rancic V, Zhang W, Clugston R, Ballanyi K, Gosgnach S. (2018). WT1-Expressing Interneurons Regulate Left-Right Alternation during Mammalian Locomotor Activity. J Neurosci. 38:5666-5676.

Hinckley CA, Hartley R, Wu L, Todd A, Ziskind-Conhaim L. (2005) Locomotor-Like Rhythms in a Genetically Distinct Cluster of Interneurons in the Mammalian Spinal Cord. Journal of Neurophysiology.

Jann MW, Lam YW, Chang WH. (1994) Rapid formation of clozapine in guinea-pigs and man following clozapine-N-oxide administration. Arch. Int. Pharmacodyn. Ther. 328: 243-250.

Jankowska E, Fu TC, & Lundberg, A. (1975) Reciprocal Ia inhibition during the late reflexes evoked from the flexor reflex affrents after DOPA. Brain Research. 85(1):99-102.

Jankowska E, Jukes MG, Lund S, Lundberg A. (1967a) The Effect of DOPA on the Spinal Cord 5. Reciprocal organization of pathways transmitting excitatory action to alpha motoneurones of flexors and extensors. Acta Physiologica Scandinavica. 70(3):369-88.

Jankowska E, Jukes MG, Lund S, Lundberg A. (1967b) The Effect of DOPA on the Spinal Cord 6. Half- centre organization of interneurones transmitting effects from the flexor reflex afferents. Acta Physiologica Scandinavica. 70(3):389-402.

Jasmin L, Gogas KR, Ahlgren SC, Levine JD, Basbaum AI. (1994). Walking evokes a distinctive pattern of Fos-like immunoreactivity in the caudal brainstem and spinal cord of the rat. Neuroscience. 58:275-286.

Jean-Xavier C, Perreault MC. (2018). Influence of Brain Stem on Axial and Hindlimb Spinal Locomotor Rhythm Generating Circuits of the Neonatal Mouse. Front Neurosci. 12:53.

Josset N., Roussel M., Lemieux M., Lafrance-Zougba D., Rastqar A. and Bretzner F. (2018) Distinct contributions of mesencephalic locomotor region nuclei to locomotor control in the freely behaving mouse. *Curr. Biol.* 28: 884-901.

Jovanovic K, Pastor AM, O'Donovan MJ. (2010). The use of PRV-Bartha to define premotor inputs to lumbar motoneurons in the neonatal spinal cord of the mouse. PLoS One. 5:e11743.

Jovanovic K, Angel M. Pastor AM, and O'Donovan MJ. (2010) The Use of PRV-Bartha to Define Premotor Inputs to Lumbar Motoneurons in the Neonatal Spinal Cord of the Mouse. *PLoS One*. 5(7): e11743.

Kerman, I.A., Enquist, L.W., Watson, S.J., and Yates, B.J. (2003). Brainstem substrates of sympatho-motor circuitry identified using trans-synaptic tracing with pseudorabies virus recombinants. J. Neurosci. 23, 4657–4666.

Kiehn, O (2006). Locomotor circuits in the mammalian spinal cord. Ann. Rev. Neurosci. 29:279-306.

Kiehn O. (2016). Decoding the organization of spinal circuits that control locomotion. Nat Rev Neurosci. 17:224-238.

Kiehn O, Johnson BR, Raastad M. (1996). Plateau properties in mammalian spinal interneurons during transmitter-induced locomotor activity. Neuroscience. 75:263-273.

Kjaerulff O, Barajon I, Kiehn O. (1994). Sulphorhodamine-labelled cells in the neonatal rat spinal cord following chemically induced locomotor activity in vitro. J Physiol. 478 :265-273.

Kjaerulff, O. & Kiehn, O., (1996) Distribution of networks generating and coordinating locomotor activity in the neonatal rat spinal cord in vitro: a lesion study. J Neurosci. 16(18):5777-94.

Koch SC, Acton D, Goulding M. (2018). Spinal circuits for touch, pain, and itch. Annu Rev Physiol. 80: 189-217.

Kudo N, Yamada T. (1987). N-methyl-D,L-aspartate-induced locomotor activity in a spinal cord-hindlimb muscles preparation of the newborn rat studied in vitro. Neurosci Lett. 75(1):43-48.

Kwan AC, Dietz SB, Webb WW, Harris-Warrick RM. (2009). Activity of Hb9 interneurons during fictive locomotion in mouse spinal cord. J Neurosci. 29:11601-11613.

Kudo N, Yamada T. (1987). N-methyl-D,L-aspartate-induced locomotor activity in a spinal cord-hindlimb muscles preparation of the newborn rat studied in vitro. Neurosci Lett. 75(1):43-48.

Lanuza GM, Gosgnach S, Pierani A, Jessell TM, Goulding M. (2004) Genetic identification of spinal interneurons that coordinate left-right locomotor activity necessary for walking movements. Neuron. 42(3):375-86.

Lev-Tov A, O'Donovan MJ. (1995). Calcium imaging of motoneuron activity in the en-bloc spinal cord preparation of the neonatal rat. J Neurophysiol. 74:1324-1334.

Li J, Zhang J, Wang M, Pan J, Chen X, Liao X. (2017). Functional imaging of neuronal activity of auditory cortex by using Cal-520 in anesthetized and awake mice. Biomed Opt Express. 8:2599-2610.

Liao BY, Zhang J. (2008). Null mutations in human and mouse orthologs frequently result in different phenotypes. Proc Natl Acad Sci USA 105:6987-6992.

Liu J., Jordan LM. (2005) Stimulation of the parapyramidal region of the neonatal rat brainstem produces locomotor-like activity involving spinal 5-HT7 and 5-HT2A receptors. J.Neurophysiol. 94:1392–404.

Lock JT, Parker I, Smith IF. (2015). A comparison of fluorescent Ca^{2+} indicators for imaging local Ca^{2+} signals in cultured cells. Cell Calcium. 58:638-648.

Lundfald L, Restrepo CE, Butt SJ, Peng CY, Droho S, Endo T, Zeilhofer HU, Sharma K, Kiehn O. (2007) Phenotype of V2-derived interneurons and their relationship to the axon guidance molecule EphA4 in the developing mouse spinal cord. European Journal of Neuroscience. 26(11):2989-3002.

Luo L., Callaway E.M., Svoboda K., 2018. Genetic Dissection of Neural Circuits: A Decade of

Progress. *Neuron.* 98(2): 256-281.

MacLaren DA, Browne RW, Shaw JK, Krishnan Radhakrishnan S, Khare P et al (2016). Clozapine N-oxide administration produces behavioral effects in Long-Evans rats: implications for designing DREADD experiments. eNeuro 3. pii: ENEURO.0219-16.2016.

Madriaga MA, McPhee LC Chersa T, Christie KJ, Whelan PJ. (2004). Modulation of locomotor activity by multiple 5-HT and dopaminergic receptor subtypes in the neonatal mouse spinal cord. J. Neurophysiol. 92:1566-1576.

Magnuson DS, Lovett R, Coffee C, Gray R, Han Y (2005) Functional consequences of lumbar spinal cord contusion injuries in the adult rat. J. Neurotrauma 22:529–43

McClellan A.D., (1984) Descending control and sensory gating of 'fictive' swimming and turning responses elicited in an in vitro preparation of the lamprey brainstem/spinal cord. 302(1): 151-162.

McCrea DA, & Rybak IA. (2008) Organization of mammalian locomotor rhythm and pattern generation. Brain Research Reviews. 57(1):134-46.

Moran-Rivard L., Kagawa T., Saueressig H., Gross MK., Burrill J., and Goulding M. (2001) Evx1 is a postmitotic determinant of v0 interneuron identity in the spinal cord. *Neuron.* 29(2):385-99.

Muller, T, Brohmann, H, Pierani, A, Heppenstall, AP, Lewin, GR, Jessell, TM, Birchmeier, C (2002). The homeodomain factor Lbx1 distinguishes two major programs of neuronal differentiation in the dorsal spinal cord. Neuron 34, 551–562.

Perry S, Larhammar M, Vieillard J, Nagaraja C, Hilscher MM, Tafreshiha A, Rofo F, Caixeta FV, Kullander K. (2019) Characterization of Dmrt3-Derived Neurons Suggest a Role within Locomotor Circuits. *J Neurosci.* 39(10):1771-1782.

Philipson, M. (1905) L'autonomie et la centralisation dans le systeme nerveux dex animaux. Trav. Lab. Physiol. Inst. Solvay, Bruxelles 7, Part 2: 1-208.

Pierani A, Moran-Rivard L, Sunshine MJ, Littman DR, Goulding M, Jessell TM. (2001) Control of interneuron fate in the developing spinal cord by the progenitor homeodomain protein Dbx1. Neuron. 29(2):367-84.

Pocratsky AM, Burke DA, Morehouse JR, Beare JE, Riegler A, Tsoulfas P, States GJR, Whittemore SR, Magnuson DSK. (2017) Reversible silencing of lumbar spinal interneurons unmasks a task-specific network for securing hindlimb alternation. *Nat Commun.* 8(1):1963.

Pomeranz LE, Ekstrand MI, Latcha KN, Smith GA, Enquist LW, and Friedman JM. (2017) Gene expression profiling with Cre-conditional pseudorabies virus reveals a subset of midbrain neurons that participate in reward circuitry. *J. Neurosci.* 37 pp. 4128-4144.

Quinlan KA, Kiehn O. 2007. Segmental, synaptic actions of commissural interneurons in the mouse spinal cord. J. Neurosci 27:6521-6530.

Roberts A. (1990) How does a neurons system produce behavior? A case study in neurobiology. Science Progress. 74, 31-51.

Robertson RM, & Pearson KG, (1985.) Neural circuits in the flight system of the locust. Journal of Neurophysiology. 53(1):110-28.

Ross A. J., Ruiz-Perez V., Wang Y., Hagan D.-M., Scherer S., Lynch S. A., Lindsay S., Custard E., Belloni E., Wilson D. I., et al. (1998). A homeobox gene, HLXB9, is the major locus for dominantly inherited sacral agenesis. Nature 20, 358-361.

Roth BL. (2016) DREADDs for Neuroscientists. Neuron. 89(4), p683-694.

Roth BL, Craigo SC, Choudhary MS, Uluer A, Monsma Jr, FJ, Shen Y, Meltzer HY, Sibley DR. (1994) Binding of typical and atypical antipsychotic agents to 5-hydroxytryptamine-6 and 5-hydroxytryptamine-7 receptors. J. Pharmacol. Exp. Ther. 268: 1403-1410.

Rovainen, C.M., Dill, D.A. Counts of axons in electron microscopic sections of ventral roots in lampreys. J. Comp. Neurol., 225 (1984), pp. 433-440

Rovainen, C.M. Synaptic interactions of identified nerve cells in the spinal cord of the sea lamprey. J. Comp. Neurol., 154 (1974), pp. 189-206.

Ruder L, Takeoka A, and Arber S. (2016) Long-Distance Descending Spinal Neurons Ensure Quadrupedal Locomotor Stability. *Neuron.* 92, 1063-1078.

Sapir T, Geiman EJ, Wang Z, Velasquez T, Mitsui S, Yoshihara Y, Frank E, Alvarez FJ, Goulding M. (2004) Pax6 and Engrailed 1 regulate two distinct aspects of Renshaw cell development. J. Neurosci. 24:1255–1264.

Saueressig H., Burrill J., Goulding M. (1999) Engrailed-1 and netrin-1 regulate axon pathfinding by association interneurons that project to motor neurons. *Development.* 126: 4201-4212.

Shefchyk SJ, Jell RM, and Jordan LM. (1984) Reversible cooling of the brainstem reveals areas required for mesencephalic locomotor region evoked treadmill locomotion. *Experimental*

Brain Research. 56(2):257-62.

Sherrington, CS. (1910) Flexion- reflex of the limb, crossed extension- reflex, and reflex stepping and standing. The Journal of Physiology, 40(1–2), pp.28–121.

Shevtsova NA, Talpalar AE, Markin SN, Harris-Warrick RM, Kiehn O, Rybak IA. (2015). Organization of left-right coordination of neuronal activity in the mammalian spinal cord: Insights from computational modelling. J Physiol. 593:2403-2426.

Shik ML, Severin FV & Orlovskii GN, (1966) Control of walking and running by means of electric stimulation of the midbrain. Biofizika. 26(5):549.

Silbereis JC, Pochareddy S, Zhu Y, Li M, Sestan N. (2016). The Cellular and Molecular Landscapes of the Developing Human Central Nervous System. Neuron. 89:248-68.

Sirota MG, and Shik ML, (1973) The cat locomotion elicited through the electrode implanted in the midbrain. Sechenom Physiol. J. USSR 59: 1314-1321.

Skinner RD, Garcia-Rill E (1984) The mesencephalic locomotor region (MLR) in the rat. Brain Res 323:385–389.

Smith JC, Feldman JL. (1987). In vitro brainstem-spinal cord preparations for study of motor systems for mammalian respiration and locomotion. J Neurosci Methods. 1987 21:321-333.

Stepien AE, Tripodi M, Arber S. (2010) Monosynaptic rabies virus reveals premotor network organization and synaptic specificity of cholinergic partition cells. Neuron. 68:456-472.

Stokke, M.F., Nissen, U.V., Glover, J.C. and Kiehn, O. (2002) Projection patterns of commissural interneurons in the lumbar spinal cord of the neonatal rat. J Comp Neurol. 446, 349-359.

Szokol K, Perreault MC. (2009). Imaging synaptically mediated responses produced by brainstem inputs onto identified spinal neurons in the neonatal mouse. J Neurosci Methods. 180:1-8.

Tada M, Takeuchi A, Hashizume M, Kitamura K, Kano M. (2014). A highly sensitive fluorescent indicator dye for calcium imaging of neural activity in vitro and in vivo. Eur J Neurosci. 39:1720-1728.

Tago H, McGeer PL, McGeer EG, Akiyama H, and Hersh LB. (1989) Distribution of choline acetyltransferase immunopositive structures in the rat brainstem. *Brain Research*. 495, 2, (271).

Talpalar AE, Bouvier J, Borgius L, Fortin G, Pierani A, Kiehn O. (2013) Dual-mode operation of neuronal networks involved in left-right alternation. Nature. 500:85-88.

Tanabe Y, Jessell TM. (1996) Diversity and pattern in the developing spinal cord. Science. 274(5290):1115-23.

Vallstedt A, Kullander K. (2013). Dorsally derived spinal interneurons in locomotor circuits. Ann NY Acad Sci. 1279:32-42.

Wallén, P., Hess, D., El Manira, A. & Grillner, S. (2002) A slow non-Ca2+-dependent afterhyperpolarization in lamprey neurons. Soc. Neurosci. Abstr. 28, 46.9.

Wallén, P. & Grillner, S. (1987) N-methyl-D-aspartate receptor-induced, inherent oscillatory

   activity in neurons active during fictive locomotion in the lamprey. J. Neurosci. 7, 2745–

   2755.

Wallén P. & Williams TL. (1984) Fictive locomotion in the lamprey spinal cord in vitro

   compared with swimming in the intact and spinal animal. The Journal of Physiology.

   347:225-39.

Wilson JM, Hartley R, Maxwell DJ, Todd AJ, Lieberam I, Kaltschmidt JA, Yoshida Y, Jessell

   TM, Brownstone RM. (2005) Conditional Rhythmicity of Ventral Spinal Interneurons

   Defined by Expression of the Hb9 Homeodomain Protein. Journal of Neuroscience.

   25(24):5710-9.

Wilson J, Dombeck D, Diaz-Rios M, Harris-Warrick R, Brownstone R (2007) Two-photon

   calcium imaging of network activity in XFP-expressing neurons in the mouse. J Neurophys

   97:3118-25.

Yang, JF, Gorassini, M. (2006). Spinal and brain control of human walking: implications for

   retraining of walking. Neuroscientist 12:379–89.

Zagoraiou, L. Akay T, Martin JF, Brownstone RM, Jessell TM, Miles GB. (2009) A Cluster of

   Cholinergic Premotor Interneurons Modulates Mouse Locomotor Activity. Neuron.

   64(5):645-62.

Zar, J.H. Circular Distribution. In "Biostatistical Analysis", p310-327. Prentice Hall, Engelwood

   Cliffs, NJ. 1974.

Zhang J, Lanuza GM, Britz O, Wang Z, Siembab VC, Zhang Y, Velasquez T, Alvarez FJ, Frank E, Goulding M. (2014). V1 and v2b interneurons secure the alternating flexor-extensor motor activity mice require for limbed locomotion. Neuron. 82:138-150.

Zhang Y, Narayan S, Geiman E, Lanuza GM, Velasquez T, Shanks B, Akay T, Dyck J, Pearson K, Gosgnach S, Fan CM, Goulding M (2008). V3 spinal neurons establish a robust and balanced locomotor rhythm during walking. Neuron 60:84-96

Zhong G, Droho S, Crone SA, Dietz S, Kwan AC, Webb WW, Sharma K, Harris-Warrick RM. (2010). Electrophysiological characterization of V2a interneurons and their locomotor-related activity in the neonatal mouse spinal cord. J Neurosci.30:170-182.

Zhu H, Aryal DK, Olsen RH, Urban DJ, Swearingen A, Forbes S, Roth BL, Hochgeschwender, U. (2016). Cre-dependent DREADD (Designer Receptors Exclusively Activated by Designer Drugs) mice. Genesis. 54:439-446.